

**New anti-infective compounds against
*Staphylococcus aureus***

Dissertation

der Mathematisch-Naturwissenschaftlichen Fakultät
der Eberhard Karls Universität Tübingen
zur Erlangung des Grades eines
Doktors der Naturwissenschaften
(Dr. rer. nat.)

vorgelegt von
Aparna Viswanathan Ammanath
aus Thrissur Kerala/ Indien

Tübingen
2022

Gedruckt mit Genehmigung der Mathematisch-Naturwissenschaftlichen Fakultät der
Eberhard Karls Universität Tübingen.

Tag der mündlichen Qualifikation:	14.12.2022
Dekan:	Prof. Dr. Thilo Stehle
1. Berichterstatter/-in:	Prof. Dr. Friedrich Götz
2. Berichterstatter/-in:	Prof. Dr. Andreas Peschel

Table of contents

Preparatory statement	6
Abstract	7
Zusammenfassung	9
General Introduction	11
<i>Staphylococcus aureus</i> and its intracellular survival	12
Lipoproteins	13
Biosynthesis of Lipoproteins	13
Functions of bacterial lipoproteins.....	15
Lpl, A Special Class of Lpp in <i>S.aureus</i> , contributes to Invasion and virulence	17
Lpl protein triggers host cell invasion via activation of Hsp90 receptor	18
<i>Galleria mellonella</i> larvae as an infection model	19
Plant derived antimicrobials	21
Rhodomirtone	22
Polycyclic polyprenylated acylphloroglucinols (PPAPs)	24
Objectives	26
Materials	30
Chemicals and media.....	30
Consumables/ Standard labware	32
Technical equipment.....	33
Mammalian cell lines.....	34
Bacterial strains	35
Methods.....	35
Bacterial strains, growth conditions and antibiotics.....	35
Peptide synthesis.....	35
Antibiotic susceptibility testing.....	35
Invasion studies in HaCaT and N/TERT-1 cells	36
CD14 ⁺ monocyte isolation.....	36
Phagocytosis assay	37
Bacterial Growth kinetics.....	37
Peptide - Hsp90 α interaction studies with immunoblotting	37
F-actin formation	38
Cytotoxicity studies	38
Larval studies.....	38
<i>Ex vivo</i> killing assay of <i>Galleria mellonella</i> larvae	39

Hemolysin activity	39
Mouse studies.....	39
Immune stimulation.....	40
Bioinformatics analysis.....	40
Statistical analysis.....	41
Ethical Statement.....	41
Results.....	43
L15 reduces USA300 invasion into keratinocytes	44
L15 and L13 directly interacts with Hsp90 α	46
L15- Hsp90 α interaction reduces F-actin levels in keratinocytes	47
L15 and L13 are non-toxic to cells <i>in vitro</i>	48
L15/L13 rescues larvae from <i>S. aureus</i> infection	49
Mice studies	52
Multiple sequence alignment.....	53
L15/L13 couldn't rescue larvae from <i>E.coli</i> and <i>P. aeruginosa</i> infection	55
L15 didn't cause any immune stimulation in human PBMCs.....	56
Pretreatment with L15 and L13 reduced the phagocytosis of USA300 in CD14 ⁺ monocytes.....	57
The peptides effect the IL-6 immune response of PBMCs to <i>S.aureus</i> but not TNF- α response	58
L15 and L13 in combination with different TLR stimulants couldn't rescue larvae from USA300 infection	59
Potassium derivative of Rom, FH-54, is active against Rom resistant <i>S.aureus</i>	61
Rom resistance is facilitated by contact of PG with Rom, which nullifies its antibacterial activity.....	61
Rom is active against pathogenic Gram-positive gut anaerobes	66
Synthesis of the sodium salt of PPAP 22, named PPAP 53, has improved solubility	68
PPAP 22 and PPAP 53 had no adverse effect on larvae but could not rescue larvae in an infection model	69
PPAP 23 showed a beneficial but not full protective effect on <i>S. aureus</i> septic arthritis mouse model.....	71
The coelomic fluid of the larvae antagonized the activity of PPAP 53.....	72
Bovine serum and albumin neutralized the activity of PPAP 53.....	73
<i>In silico</i> docking studies showed PPAP53 binds to the Heme binding pocket of BSA	75
Addition of known BSA ligands couldn't improve the <i>in vitro</i> bactericidal activity of PPAP53 in presence of BSA.....	77
PPAP23 is active against pathogenic Gram-positive gut anaerobes	77

Discussion	82
Conclusion.....	89
References	90
Appendix.....	104
Appendix A: Abbreviations	105
Appendix B: List of figures	107
Appendix C: List of tables	112
Appendix D: Publications and personal contributions to publications	113
Appendix E: RightsLink Permission	116

Preparatory statement

This thesis represents a monograph thesis of Aparna Viswanathan Ammanath. Sections from this thesis have been published, are submitted for peer review in journals or are intended to be submitted for publication. This thesis may contain similar passages and/or figures/tables adapted from these manuscripts without distinctly stating their origin, as the attached manuscripts are important part of this thesis. The above said manuscripts have been authored or co-authored by me and were the part of my doctoral thesis work. My contributions to each publication can be found in page 113.

The copyright of this thesis belongs to Aparna Viswanathan Ammanath and third parties that are indicated in the respective sections. Unauthorized publications are prohibited.

Abstract

Owing to the development of antibiotic resistance in microorganisms, new anti-microbial and anti-infective agents are of dire need to keep these pathogens at bay. These agents are mainly derived from the pathogen (bacteria or fungi) itself or from different plant extracts.

In our previous work, it was observed that Lipoprotein like lipoprotein (Lpl) is an essential virulence factor in *Staphylococcus aureus*. Lpl is membrane bound and encoded in a genomic island called vSaa. Lpl causes the invasion of *S. aureus* into the HaCaT keratinocyte cells through its interaction with Hsp90 α receptor. Lpl1 administration also surges the murine kidney abscess - bacterial burden. Our aim was to identify peptides that can block Hsp90 and reduce the *S.aureus* pathogenicity caused by Lpl.

Here, we show 2 small peptides, named L15 and its derivative, L13, both part of Lpl1 have anti-infective action towards *Staphylococcus aureus*. Pretreatment with L15 and L13 reduced the invasion of *S. aureus* USA300 into HaCaT keratinocytes, N/TERT-1 primary keratinocytes and *S. aureus* phagocytosis in human monocytes. The peptides were water soluble, non-cytotoxic and non-hemolytic at the tested concentrations. Dot blot studies showed that there is direct interaction of the peptides with Hsp90 α .

L15 and L13 significantly decreased lethality of *S. aureus* bacteremia in *Galleria mellonella* insect larvae model, but did not affect growth or hemolytic activity of *S. aureus in vitro*. In a mouse bacteremia model L15 was found to significantly decrease weight loss and lethality. In effect the small peptides showed the opposite effect from their mother protein, in terms of the invasion of *S. aureus* into host cell and mice bacteremia model.

Although the molecular bases behind the protective effect of L15 remain unclear, *in vitro* data indicate that treatment with L15 or L13 and simultaneous infection with *S. aureus* significantly increase IL-6 production in host immune cells. Our findings highlight Hsp90-interacting peptides as potential anti-infective agents

In a separate work, non-peptide, anti-microbial phytochemicals- Rhodomyrtone (Rom) and Polycyclic polyprenylated acylphloroglucinols (PPAP), capable of inhibiting *S.aureus in vitro* are described. A single point mutation at farR makes *S.aureus*

resistant to Rom. The antibacterial activity of Rom was targeted towards the cell membrane by interacting with its phosphatidylglycerol (PG). Rom^R mutants were seen to excrete far more PGs, thereby neutralizing the Rom before it reaches the cell membrane.

PPAP, though very much active *in vitro*, failed to rescue *G. mellonella* larvae from *S.aureus* infection. The reason was found to be the neutralization of PPAPs by the serum albumin proteins found in the larval coelomic fluid. *In silico* docking studies showed that PPAP is binding to the Heme binding pocket of bovine serum albumin. On the other hand, PPAP was observed to have a beneficial but not fully protective effect in *S. aureus* septic arthritis mouse model.

Zusammenfassung

Aufgrund der bei Mikroorganismen steigenden Entwicklung von Antibiotikaresistenzen, werden dringend neue antimikrobielle und antiinfektiöse Wirkstoffe benötigt, um diese Krankheitserreger in Schach zu halten. Diese Substanzen werden hauptsächlich aus Pathogenen (Bakterien oder Pilze) oder aus verschiedenen Pflanzenextrakten gewonnen.

Das *Lipoprotein like lipoprotein* (Lpl), welches in einer genomischen Insel namens *vSaa* kodiert wird, ist membrangebunden und ein wesentlicher Virulenzfaktor von *Staphylococcus aureus*. Durch die Interaktion von Lpl mit dem Hsp90 α -Rezeptor, wird die Invasion von *S. aureus* in HaCaT-Keratinocyten verursacht. Zudem erhöht die Verabreichung von Lpl1, die bakterielle Belastung bei Nierenabszesse in der Maus.

Hier zeigen wir, dass zwei kleine Peptide, L15 und sein Derivat L13, welche beide Bestandteile von Lpl1 sind, eine antiinfektiöse Wirkung auf *Staphylococcus aureus* haben. Die Vorbehandlung der Zellen mit L15 und L13 verringerte die Invasion von *S. aureus* USA300 in HaCaT-Keratinocyten und primären N/TERT-1-Keratinocyten, sowie die Phagozytose von *S. aureus* in menschliche Monozyten. Die Peptide waren in den getesteten Konzentrationen wasserlöslich, nicht zytotoxisch und nicht hämolytisch. Dot-Blot-Studien zeigten, dass es eine direkte Interaktion der Peptide mit Hsp90 α gibt.

L15 und L13 verringerten die Letalität von *S. aureus* Bakteriämie im *Galleria mellonella* Insektenlarvenmodell signifikant. Jedoch war weder das Wachstum, noch die hämolytische Aktivität von *S. aureus in vitro* beeinflusst. Anhand eines Bakteriämie Modells in Mäusen wurde festgestellt, dass L15 den Gewichtsverlust und die Sterblichkeit deutlich verringert. Die kleinen Peptide zeigten in Bezug auf die Invasion von *S. aureus* in die Wirtszelle und dem Bakteriämie Modell in Mäusen, die entgegengesetzte Wirkung, verglichen zum Mutterprotein.

Obwohl die molekularen Grundlagen für die schützende Wirkung von L15 noch unklar sind, deuten *in vitro* Daten, auf eine deutlich erhöhte IL-6 Produktion in den Immunzellen des Wirts, nach einer Behandlung mit L15 oder L13 und der gleichzeitigen Infektion mit *S. aureus*, hin. Unsere Ergebnisse weisen auf Hsp90-interagierende Peptide als potenzielle Antiinfektiva hin.

In einer separaten Arbeit werden nicht-peptidische, antimikrobielle Phytochemikalien - Rhodomyrton (Rom) und polyzyklische polyprenylierte Acylphloroglucinole (PPAP) - beschrieben, welche in der Lage sind, *S. aureus in vitro* zu hemmen. Eine einzige Punktmutation in *farR* verursacht in *S. aureus* eine Resistenz gegenüber Rom. Die antibakterielle Aktivität von Rom ist, aufgrund dessen Interaktion mit Phosphatidylglycerin (PG), auf die Zellmembran ausgerichtet. Es wurde festgestellt, dass Rom^R Mutanten viel mehr PGs ausscheiden, wodurch Rom neutralisiert wird, bevor es die Zellmembran erreicht.

Obwohl PPAP *in vitro* sehr aktiv war, gelang es nicht, *G. mellonella* Larven vor einer *S. aureus* Infektion zu schützen. Dies resultiert aus der Neutralisierung von PPAPs durch Serumalbuminproteine in der Coelomflüssigkeit der Larven. *In silico docking* Studien zeigten, dass PPAP an die Häm-Bindungstasche von Rinderserumalbumin bindet. Außerdem wurde beobachtet, dass PPAP im Mausmodell, mit einer *S. aureus* verursachten septischen Arthritis, eine positive, aber nicht vollständig schützende Wirkung hat.

Chapter 1

General Introduction

***Staphylococcus aureus* and its intracellular survival**

Staphylococcus aureus is a gram-positive bacterium commonly found on human epithelial surfaces. Nearly 30% of the human population harbors the bacteria on their skin without any signs of infections (Kluytmans *et al.*, 1997, Gorwitz *et al.*, 2008, Tong *et al.*, 2015). Sometimes this opportunistic human pathogenic bacterial species can cause grave community acquired and nosocomial infections, comprising wound infection, pneumonia, osteomyelitis, endocarditis, abscess formation, and sepsis/septic shock (Wertheim *et al.*, 2005, Deurenberg & Stobberingh, 2008, Krismer *et al.*, 2017). Management of these infections has become challenging due to the emergence of antibiotic-resistant strains and the capability of *S. aureus* to invade and persist within host cells (Moran *et al.*, 2006, Alva-Murillo *et al.*, 2014).

Lots of studies have shown the capability of *S. aureus* in its invasiveness and persistence within professional phagocytic cells and non-professional phagocytic cells (NPPCs), such as osteoblast, endothelial, fibroblast, epithelial, or kidney cells (Hudson *et al.*, 1995, Vesga *et al.*, 1996, Bayles *et al.*, 1998). For example, Tranchemontagne *et al.* showed that *S. aureus* persisted in the macrophages by blocking the development of phagolysosome (Tranchemontagne *et al.*, 2016).

S. aureus owns a collection of virulence factors (i.e. enzymes, invasins, adhesins, toxins) that adds to the pathogenesis of infection, supporting its colonization, dissemination, and transmission. *S. aureus* start the invasion process by attaching to cell membrane of the host cell via the adhesins, like fibronectin-binding proteins A (FnBPA), autolysin (Atl), Extracellular adherence protein (Eap), fibronectin-binding proteins B (FnBPB) and iron-regulated surface determinant B (IsdB) (Sinha *et al.*, 1999, Haggar *et al.*, 2003, Hirschhausen *et al.*, 2010, Zapotoczna *et al.*, 2013). The main method for *S. aureus* internalization into non-professional phagocytes is supposed to be facilitated by FnBPs that network with human $\alpha 5\beta 1$ integrins via Fn as a bridging molecule. FnBPs also interact with human Hsp60 thereby ensuring an efficient *S. aureus* internalization into epithelial cells (Dziewanowska *et al.*, 1999, Dziewanowska *et al.*, 2000). This interaction can be direct or indirect, or Hsp60 may work as a co-receptor for $\alpha 5\beta 1$ integrins (Fowler *et al.*, 2000). The *S. aureus* extracellular adherence protein Eap has been observed to help *S. aureus* Newman

internalization into fibroblasts and epithelial cells. Eap is shown to interact with different plasma proteins, like prothrombin, fibrinogen and fibronectin (Haggar *et al.*, 2003). The autolysins- Atl from *S. aureus* and AtlE from *S. epidermidis* to promote staphylococcal internalization by interacting with the host cell receptor, the heat shock cognate protein Hsc70. The Atl-mediated internalization seems to be the effect of a direct contact between Atl and Hsc70. However, there is an extra interaction of Atl with the host cell integrin $\alpha 5\beta 1$ with Fn as a bridging molecule. The bacterium adheres to kidney cells, epithelial cells and platelets by employing an iron-regulated surface determinant B protein IsdB, mediated by integrins (Zapotoczna *et al.*, 2013). Lipoproteins (Lpp) are also known to trigger the host cell invasion in epithelial cells (Nguyen *et al.*, 2015). This bridging of bacteria and host cell proteins triggers bacterial uptake by mechanism driven by the host cells that involves actin remodeling, Src family kinases and focal adhesion kinase (Agerer *et al.*, 2005, Sinha & Herrmann, 2005).

Lipoproteins

The first Lipoprotein (Lpp) elucidated was from *E. coli* and is called Braun's Lipoprotein (Hantke & Braun, 1973). Lpp is attached with its N-terminal lipid structure in the outer membrane of nearly all Gram-negative bacteria. In Gram+ bacteria, the Lpp's lipid moieties are attached in the outer layer of the cytoplasmic membrane and their protein portions extend to the cell wall.

Biosynthesis of Lipoproteins

Lipid modification enables the binding of hydrophilic proteins in bacteria to the hydrophobic cell wall phospholipids. Here in lipoproteins, an acyl moiety is attached to the protein, which provides a membrane anchor for its easy function. Lipoproteins are synthesized in the cytoplasm as precursors and are then translocated across the cytoplasmic membrane. These precursors possess an N-terminal signal peptide with a characteristic "lipobox" consensus region at its C-terminal. In the lipobox sequence: Leu-(Ala/Ser)-(Gly/Ala)-Cys, the last cysteine is modified by covalent attachment of a diacylglycerol moiety to its thiol group by the enzyme lipoprotein diacylglyceryl transferase (Lgt). Following lipid modification, the signal sequence of the lipidated prolipoprotein is cleaved just before the cysteine residue by lipoprotein signal

peptidase (Lsp). This leaves the cysteine of the Lipobox as the new N-terminal residue of the lipoprotein or the mature lipoprotein in Gram-positive bacteria.

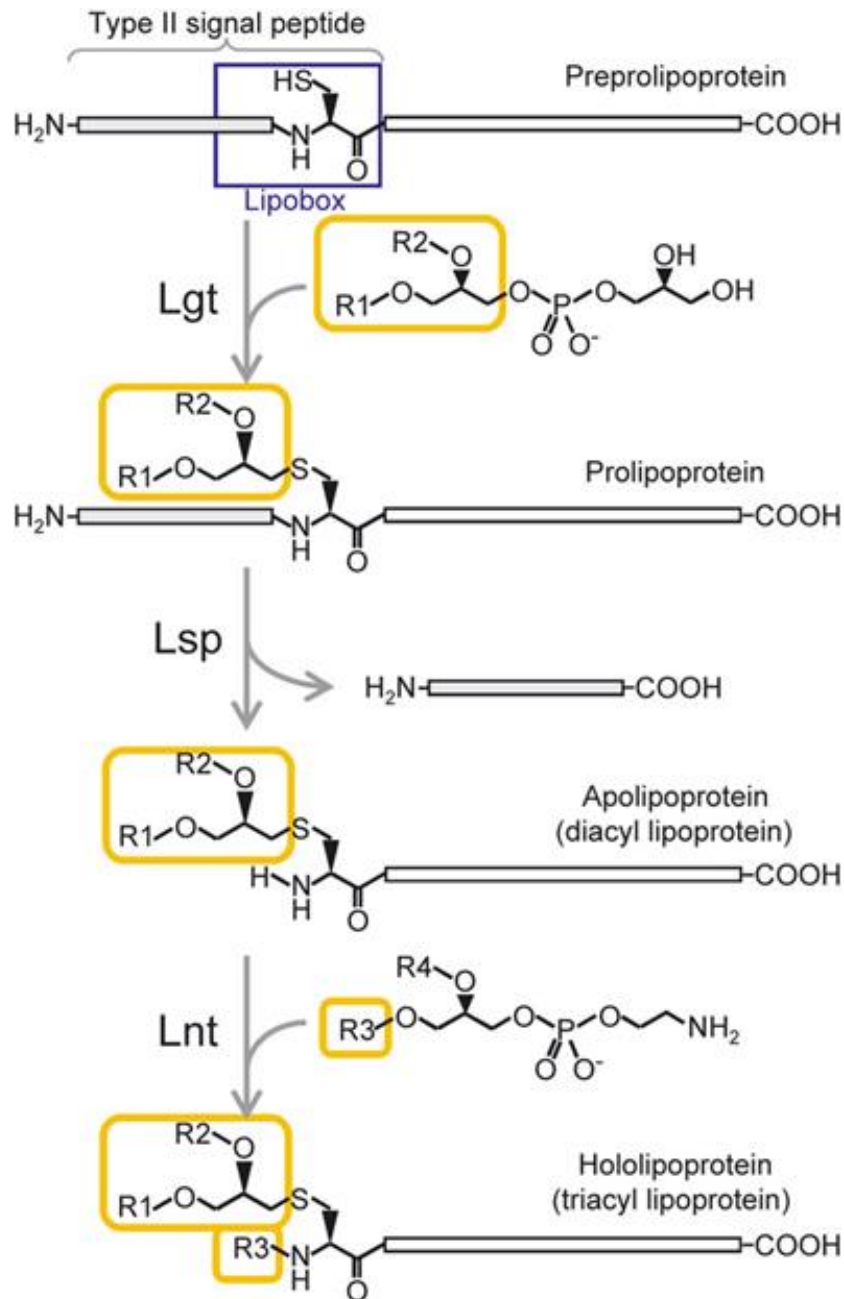


Figure 1.1. Biosynthesis of lipoprotein in bacteria. Adapted with Rightslink permission from (Nakayama *et al.*, 2012)

In gram negative bacteria, the Lsp catalyzed lipoprotein is further modified at the N-terminal cysteine group by acylation reaction (Addition of an amide – linked acyl group). This step is catalyzed by lipoprotein N-acyl transferase (Lnt) (Kovacs-Simon *et al.*, 2011) (Figure. 1.1). Both the membrane phospholipids-derived amino-terminal acyl groups (in gram –ve bacteria) and the diacylglycerol group contributes to tight

anchorage of the lipoprotein to the membrane (Hantke & Braun, 1973) . The enzymes involved in the biosynthesis of lipoproteins have been employed as a target for the synthesis of new antibacterial agents. This is because of the nonexistence of any homologues in eukaryotes.

Functions of bacterial lipoproteins

Bacterial lipoproteins have different functions varying from virulence in pathogenic bacteria to nutrient uptake signal transduction etc. The functions of bacterial lipoproteins are given in detail below. Nguyen et al., compared the Lpp of 14 bacterial species from the genera of *Bacillus*, *Clostridium*, *Enterococcus*, *Listeria*, *Mycobacterium*, *Staphylococcus* and *Streptococcus*. The number of Lpp genes in each of the 14 mentioned species are different but accounts for a substantial part of the genome (1-3 %) (Nguyen et al., 2020).

Functions of Lpps are

1. Transportation: *S. aureus* USA300 (MRSA) has 67 Lpps, in which nearly 1/3rd are involved in transportation of zinc (Zn), iron (Fe), manganese (Mn), Nickel (Ni), molybdenum (Mo), Cobalt (Co), aminoacids, sugars etc. Different Lpps involved in the transport are mentioned below.
 - Iron acquisition: *S.aureus* has 8 widely iron transporting Lpps which include FhuD1, FhuD2 (both bind to iron(III)-hydroxamate siderophores and present it to the ABC transporter – FhuCBG), SirABC (transport of staphylobactin, ferric enterobactin or ferric citrate and ferric hydroxamates) and FepA (part of FepABC - containing FepA (Fe binding Lpp), FepB (with TAT signal peptide) and FepC (transport of Fe across the membrane)) (Sebulsky et al., 2000, Dale et al., 2004, Biswas et al., 2009). The pathogenicity of staphylococci was found to be linked directly to lipoprotein dependent Fe-uptake systems (Shahmirzadi et al., 2016). In *S.pyogenes*, both MtsA (part of MtsABS transporter) and SiaA (part of SiaABC transporter) are Lpp involved in Fe acquisition (Sun et al., 2008, Sun et al., 2010).
 - Other cation and anion transporters: the Lpp MntC in *S.aureus* is involved in the transport of Mn. Homologues of MntC were found in bacilli as MntA and streptococci as PsaA (in *Streptococcus agalactiae* and *Streptococcus*

pneumoniae). 3 Lpp in *S.aureus* were glossed as Nickel transporters. Other Lpps functioning as cationic transporters include Cnt (Opp1) (Ni and Co transport at zinc reduced conditions in *S.aureus*), ModA (involved in Mo transport), AdcA and AdcAll (zinc transport in *Streptococcus*) (Neubauer *et al.*, 1999, Remy *et al.*, 2013, Tedde *et al.*, 2016). In USA300, the annotated Lpps - USA300_1283, USA300_0145 and USA300_0175 are involved in the transport of phosphate, phosphonate and nitrate respectively (Shahmirzadi *et al.*, 2016).

- Amino acid transport: *S.aureus* has 7 identified Lpps involved in the transport of aminoacids and short peptides. These includes Opp3 (involved intransport of oligopeptides) and GmpC (for transport of glycyl - methionine) (Williams *et al.*, 2004, Hiron *et al.*, 2007). Other Lpps functioning as amino acid/peptide transporters are OppA (from OppABCD(F) system), AppA (from AppDFABC transport system) and MetQ (from MetQNP transporter) (Koide & Hoch, 1994). MetQ trasports methionine in streptococci and is found to be significant in its virulence and growth function (Basavanna *et al.*, 2013).
 - Sugar and lipid transport: The only Lpp involved in the sugar transport is the maltose ABC transporter (Sauvageot *et al.*, 2017). The Mce Lpps in *Mycobacterium tuberculosis* transports cholesterol through the cell envelope. The Mce is crucial in the host signalling and the bacterial growth with cholesterol as the only carbon source (Wilburn *et al.*, 2018).
2. Cell wall biosynthesis and degradation: Studies about the role of Lpps in cell wall biosynthesis and degradation are very few. A papain-like cysteine peptidase called New Lipoprotein C/Protein of 60-kDa (NlpC/P60) is said to catalyse D-γ-glutamyl-meso-diaminopimelate or N-acetylmuramate-L-alanine linkages (Anantharaman & Aravind, 2003, Vermassen *et al.*, 2019). Lpps functioning as penicillin binding proteins, cell elongation specific DD-transpeptidase, and polysaccharide deacetylase were seen in some Bacilli. The lytA Lpp in Bacillus group, is a part of the operon lytRABC, which regulates the N-acetylmuramoyl-L-alanine amidase gene (Lazarevic *et al.*, 1992).
 3. As foldases and Enzymes:
 - YidC first found in *E.coli* is a membrane insertase Lpp that helps in the assembly and insertion of various proteins in the bacterial membrane (Samuelson *et al.*, 2000).

- PrsA or Peptidylprolyl Isomerase, a membrane bound Lpp is crucial in protein synthesis in *Bacillus subtilis* (Kontinen & Sarvas, 1993). PrsA is also known to fast-track the folding of proteins encompassing cis- proline (Gothel & Marahiel, 1999).
- SCO or Synthesis of Cytochrome c Oxidase (in Bacillu species) and its homologues (QoxA in *S. aureus*, Etrx1 and Etrx2 in *S. pneumonia*) are essential in the respiratory chain and sometimes during oxidative stress (Gotz & Mayer, 2013, Saleh *et al.*, 2013, Xu *et al.*, 2015).
- Lpp-penicillinases are found in both membrane bound and secreted free form with their function as β -lactamases in many bacterial species (Nielsen & Lampen, 1982). Lpps are also known to have protease, phosphatase, peptidase, esterase or lipase functions. The Lpp in *Streptococcus equisimilis*, called LppC does the role of as an acid phosphatase (Wolschendorf *et al.*, 2007).
- LanI or Lantibiotic Immunity Lpp in gram positive species makes the pathogen resistant to nisin specifically (Hacker *et al.*, 2015, Geiger *et al.*, 2019).
- Sex pheromones: Derivatives of signal sequences from the C-terminals of Lpp are employed as sex hormones in some bacterial species including *S. aureus* (cAM373), *S. epidermidis*, *E. faecalis* (cAM373), *L. monocytogens* and *B. subtilis*. These hormones expedite the conjugative transfer of certain plasmids in these bacteria (Dunny & Leonard, 1997, Flannagan & Clewell, 2002).

The information about many Lpps in terms of their role and importance is still incomplete. Although Lpps are seen in nearly every bacterial species, and is conserved in many, each Lpp is unique subject to the habitat and genetic makeup of the bacteria.

Lpl, A Special Class of Lpp in *S.aureus*, contributes to Invasion and virulence

Most *S. aureus* strains contain a pathogenicity island, *vSaa*, which encodes a set of lipoprotein-like gene cluster called *lpl* (lipoprotein like lipoprotein). Particularly, in highly epidemic strains the *lpl* cluster comprises up to 10 homologous tandemly arranged *lpl* genes (Nguyen *et al.*, 2015). It has been found that the *lpl* gene cluster contributes to internalization into NPPCs such as keratinocytes and epithelial cells. Here, USA300 wt, USA300 Δ lpl mutant and the respective complemented mutant were checked for its invasion capacity differentiated primary keratinocyte cells. In cells infected with Δ lpl

mutant, the number of invaded bacteria were 2.5 fold lower compared to the wild type USA300 strain.

On complementation of the same gene, the intracellular bacterial count went up to 1.5 in comparison to the wild type, suggesting the significance of *lpl* gene cluster in invasion in keratinocytes. *S. carnosus*, a relatively non-pathogenic bacteria doesn't have a lipoprotein cluster. A mutant of *S. carnosus* which expresses the Lpl - (*S. carnosus* (pTX30::lpl)) showed higher invasion potential as compared to *S. carnosus* wt and *S. carnosus* (pTX30). This result reinforced the significance of *lpl* gene cluster in invasion in keratinocytes. Similar trend was also seen on HeLa cells. They could also observe a cell cycle delay (G2-M transition) in HeLa cells on exposure to Lpl proteins.

The importance of *lpl* gene cluster in virulence were also seen *in vivo*. On challenging of Balb/C mice with USA300 wt and USA300 Δ lpl mutant, Nguyen *et al.*, found that, the bacterial burden in the kidney of Δ lpl mutant group were significantly lower than the USA300 wt infected group (Nguyen *et al.*, 2015). Lpl1 has been used as a model protein in the mice experiments.

Mohammad M *et al.*, injected Lpl1 into mice knee joint intra-articularly and saw macroscopic inflammation at the joints after 24hrs (Mohammad *et al.*, 2019). They could also observe synovitis and severe bone erosions indicating an *S. aureus* septic arthritis. The Lpl1 without the signal peptide called Lpl1 (-sp), failed to induce arthritis suggesting that the lipid moiety of Lpp is responsible for the arthritic induction. It was also observed that the TLR2 is required for the monocyte and neutrophil migration to synovial site after the Lpl1 administration.

Lpl protein triggers host cell invasion via activation of Hsp90 receptor

Recently it has been found that Lpl1 triggers the invasion into HaCaT cells by activating the Hsp90 α of the latter (Tribelli *et al.*, 2020). Hsp90 is a chaperone proteins and are highly expressed in most of the eukaryotic cells. Because of its involvement in the stabilization of lots of oncogenic proteins, Hsp90 inhibitors are widely studied as cancer treatment drugs. Hsp90 α is said to be membrane bound, but is also found as secreted

form in response to tissue injury (Guo *et al.*, 2017). Blocking of the keratinocyte Hsp90 using antibodies resulted in reduced USA300 invasion and adherence into the host cells. The reduction in USA300 invasion to Hsp90 α silenced HaCaT cells added to strengthening the above said theory. Lpl1-Hsp90 interaction induces F-actin formation, thus, triggering an endocytosis-like internalization (Figure 1.2). Even though there is direct interaction with Lpl1 and Hsp90, Tribelli *et al.*, couldn't see any resultant effect on the ATPase activity of Hsp90.

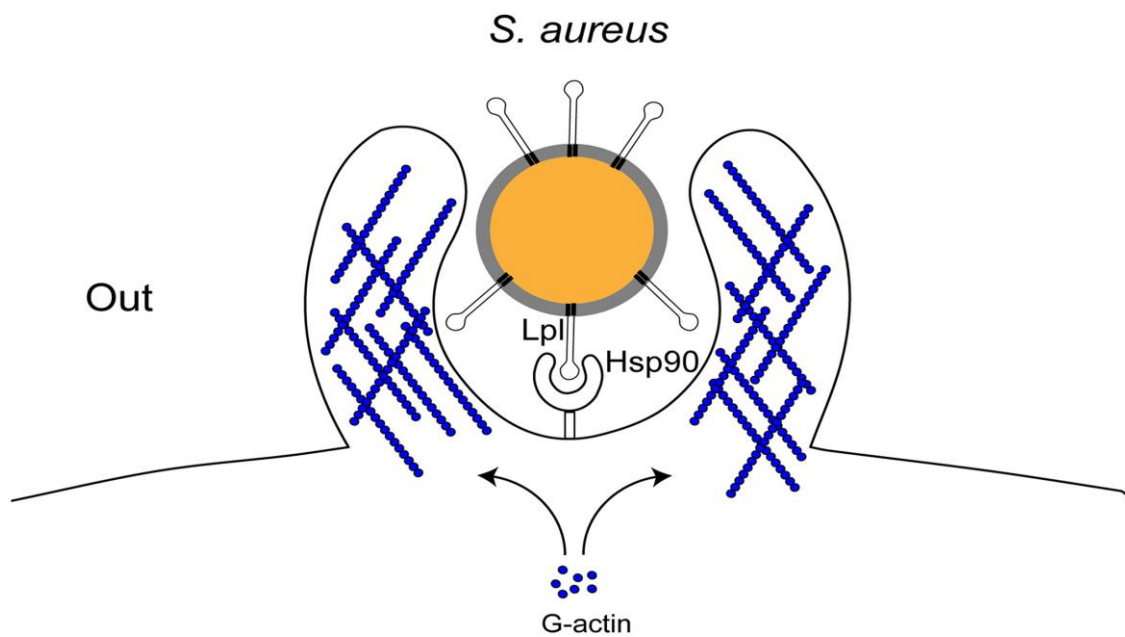


Figure 1.2. Proposed model of Lpl-Hsp90 interaction during USA300 invasion in keratinocyte cell. The C-terminal region of Lpl1 interacts with Hsp90. This interaction triggers F-actin formation and the bacteria is taken in by an endocytosis like process. G-actin: monomer of actin protein, F-actin: filamentous actin. Adapted from (Tribelli *et al.*, 2020).

***Galleria mellonella* larvae as an infection model**

Galleria mellonella (order *Lepidoptera*, family *Pyralidae*) also known as the greater wax moth or honeycomb moth has been widely studied as an infection model to study microbial pathogenesis and efficacy of different drugs. *G. mellonella* larvae are cheaper to acquire and can be easily maintained in large numbers. The development of *G. mellonella* infection model is simple and doesn't require much high end lab equipment. The lack of ethical constraints in *G. mellonella* study and their short life cycle makes them ideal candidate for these studies. The survival of *G.*

G. mellonella larvae at 37°C makes them more preferable in comparison to other commonly employed invertebrate models such as *Drosophila melanogaster* and *Caenorhabditis elegans* (Tsai *et al.*, 2016). Although the greater wax moth lack an adaptive immune response, their innate immune response shows remarkable similarities with the immune response in vertebrates. The innate immune system includes both humoral and cellular immune response. The humoral immune reaction is mediated by effector molecules that are able to kill or trap the pathogen. These effectors can be opsonins or antimicrobial peptides (AMPs).

Opsonins in *G. mellonella* include peptidoglycan recognition proteins (PGRPs), apolipoprotein III (apoL-III), cationic protein 8 (GmCP8) and hemolins (Seitz *et al.*, 2003). PGRPs binds to the peptidoglycan of bacteria and were identified among one of the genes induced by LPS in the hemocyte (Seitz *et al.*, 2003, Dziarski & Gupta, 2006). Apolipoprotein III, a pattern recognition molecule binds to hydrophobic ligands - lipopolysaccharides and lipoteichoic acids, activating the innate immune response (Halwani *et al.*, 2000, Pratt & Weers, 2004). GmCP8 work as a multi ligand protein in the phagocytosis of pathogens (Kim *et al.*, 2010). Hemolins are expressed in the silk glands and nervous system of larvae. Hemolins, generally upregulated when triggered by β -glucans, marks the apoptic/infected cells for elimination by hemocytes (Shaik & Sehgal, 2009, Mowlds *et al.*, 2010).

The greater wax moth have a wide array of anti-microbial peptides which includes cecropin, lysozyme, moricin like peptides, galliomyacin, gloverin, defensin, gallerimycin, apolipoprotein III and x-tox. In addition *G. mellonella*'s AMPs also include Gm proline-rich peptides 1 and 2, inducible serine protease inhibitor 2, heliocin-like peptide and Gm anionic peptide 1 and 2 (Cytrynska *et al.*, 2007, Brown *et al.*, 2009). Lysozymes catalyzes the hydrolysis of the β -1, 4 linkage between N-acetylglucosamine and N-acetylmuramic acid in the cell wall peptidoglycan (Sowa-Jasilek *et al.*, 2014). It was observed that the synergistic action of apoL-III and lysozyme increases the permeability of Gram-negative bacteria (Zdybicka-Barabas *et al.*, 2013). Cecropins and moricins (α -helical peptides) and defensins (cationic peptides) causes ion leakage and subsequent cell lysis in both Gram + and -ve bacteria by forming pores in the cell walls and membranes (Kim *et al.*, 2004, Brown *et al.*, 2008). Studies have shown that the activity of cecropin is sometimes enhanced by apoL-III. *G. mellonella* also have small peptides of size ranging from 2-4 kDa, called the proline-rich peptides that can

enhance the permeability of bacterial membrane and are known to inhibit the growth of yeast (Cytrynska *et al.*, 2007). Another AMP, gloverin binds to LPS of the Gram-ve bacteria and causes membrane permeability by inhibiting the synthesis of some vital outer membrane proteins (Kawaoka *et al.*, 2008). Other AMPs include gallerimycin, that can inhibit fungi and X-tox, whose function is still unknown (Langen *et al.*, 2006).

Plant derived antimicrobials

The abuse or overuse of antibiotics for every human ailment has resulted in antibiotic resistance in pathogens (Yu *et al.*, 2020). Antibiotic resistance is one of the prominent reason for increased mortality and morbidity in patients with infections, and this has caused a giant economic burden on our healthcare system (The Lancet Infectious, 2017). In 2017, World Health Organization (WHO) published its first list of pathogens that are antibiotic resistant, and are a threat to the population's health. This list covers 12 bacterial families, for which new antibiotics against them are of dire need. *Staphylococcus aureus* is included in this 12 family list, as a high propriety organism (Khare *et al.*, 2021). The Centers for Disease Control and Prevention (CDC) and the European Centre for Disease Prevention and Control (ECDC), classify pathogens into multidrug resistant (MDR), extensively drug resistant (XDR) or pandrug resistant (PDR) based on their resistance to antibiotics. Pathogens resistant towards more than one class of antibiotics are called Multi drug resistant pathogens.

Secondary metabolites from different plants exhibit promises in its ability to kill these resistant pathogens. Many plant extracts (in crude or modified form) have been employed in cosmetics and food industry to prevent product spoilage. Phytochemicals such as capsaicin, colchicine, paclitaxel, and reserpine has been approved by the Food and Drug Administration (FDA), and are effective against many MDR pathogens. The mode of action of these phytochemicals were mainly found to be- by inhibiting bacterial replications of the efflux pumps or by increasing the bacterial cell permeability to anti-microbial.

Phytochemicals can be essential oils, alkaloids, flavonoids or phenolic compounds. For example, essential oils extracted from the barks of cinnamon has been proved to be strongly bactericidal against MDR *S.aureus* (Naveed *et al.*, 2013). Piperine, an alkaloid from *Piper nigrum* is known for its activity against MRSA by the inhibition of the bacterial efflux pump (Khan *et al.*, 2006, Khameneh *et al.*, 2015). Catechin, an

antibacterial flavonoid mainly seen in tea and legumes are known to attack the methicillin-resistant *Staphylococcus aureus* (MRSA) membrane, resulting in potassium leakage (Cushnie *et al.*, 2008). Another phenolic-acid phytochemical, gallic acid is observed to have solid antibacterial activity against *S. aureus*, *S. agalatae*, *P. aeruginosa*, *E. fecalis*, *E. coli* etc. (Cueva *et al.*, 2012). Although there are several prosperous examples of phytochemicals against antibiotic resistant infections, most of them fail to reach the commercial pharmaceutical market and this needs to be remedied.

Rhodomyrtone

Rom or rhodomrytone, an acylphloroglucinol isolated from *Rhodomyrtus tomentosa* is found to be active against different gram +ve bacteria like *Staphylococcus aureus*, *Streptococcus pyogenes*, *Streptococcus pneumoniae*, *Propionibacterium acnes* and multidrug-resistant *Enterococcus faecalis* (Voravuthikunchai *et al.*, 2010, Limsuwan *et al.*, 2011, Saising & Voravuthikunchai, 2012, Wunnoo *et al.*, 2021). Rom's anti-microbial action is directed towards the bacterial cell membrane. The binding of Rom to the phosphatidylglycerol head of the phospholipid membrane causes the membrane to fold on to itself and subsequently its disruption. This disruption of cell membrane results in the leakage of ATP and different cytoplasmic proteins thereby bringing down the membrane potential (Saising *et al.*, 2018). Rom was observed to reduce the FtsZ polymerization and inhibit GTPase activity in *Bacillus subtilis*. FtsZ is a protein that drives the cell division in bacteria and is a homolog of tubulin in eukaryotes. FtsZ polymerized to form a Z-ring, causing the cell wall and membrane to constrict and form septum, resulting in the creation of 2 daughter cells. FtsZ is crucial in every bacteria and the polymerization requires GTP (Saeloh *et al.*, 2017).

Nyugen *et al.*, were able to develop Rom resistant *S.aureus* HG001 mutant strains by continuous subculture of the wild type strain in Rom supplemented media. The whole genome sequencing of the resistant mutant enabled them to identify a specific single point mutation instigating the Rom resistance in HG001. This point mutation was a change in the codon TGC to CGC resulting in change in the amino acid from cysteine (Cys) to arginine (Arg) in the coding region of *farR* (regulator of fatty acid (FA) resistance) at position 116 (Nguyen *et al.*, 2019). *FarR* expresses a regulator which controls *farE*. *FarE* is a transmembrane protein which functions as an efflux pump for multiple drugs (Alnaseri *et al.*, 2015). The point mutation in *farR* (*farR*^{*}) inactivates the

repressor function. This leads to an up-regulation of *farE*, thereby increasing the resistance of the strains against FA antimicrobials. More FarE means more efflux of FAs from bacterial cells. Nyugen et al., could also observe that the genes *psmβ1* and *hla*, encoding toxins and *sspB* and *gehA*, encoding secreted enzymes were also upregulated in Rom^R strain, resulting in enhanced virulence of the mutant in mouse pneumonia model. (Nguyen *et al.*, 2019) (Figure 1.3B).

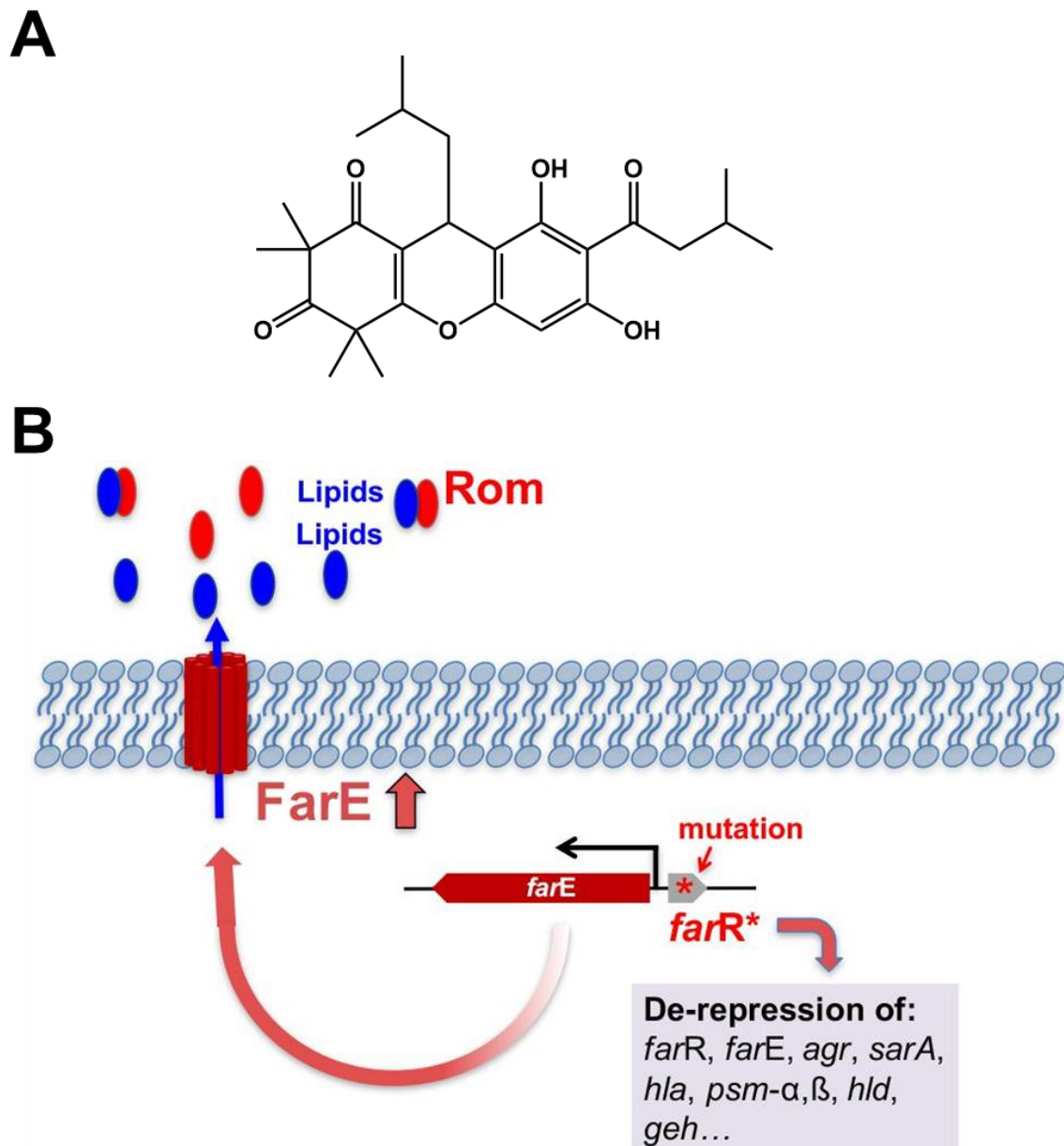


Figure 1.3. (A) Structure of Rom drawn using ChemDraw Professional 16.0. (B) Mechanism of Rom resistance in Rom^R mutant facilitated by the FarE. Reprinted under the Creative Commons Attribution License (CC BY) from (Nguyen *et al.*, 2019).

Polycyclic polyprenylated acylphloroglucinols (PPAPs)

Polycyclic polyprenylated acylphloroglucinols (PPAPs) from *Hypericum perforatum* or St. John's wort, is a well-known antidepressant and its derivatives are active against different microbes (Barnes *et al.*, 2001). PPAP features a bicycle [3.3.1]nonane-2,4,9-trione and can be classified into 3 types depending on the position of the exocyclic acyl group. They are- type A with acyl group at C1, type B with acyl group at C3, and type C with acyl group at C5 position (Figure 1.4). Hyperforin, the first PPAP isolated, is type A PPAP used for the treatment of depression, schizophrenia and anxiety (Ciochina & Grossman, 2006).

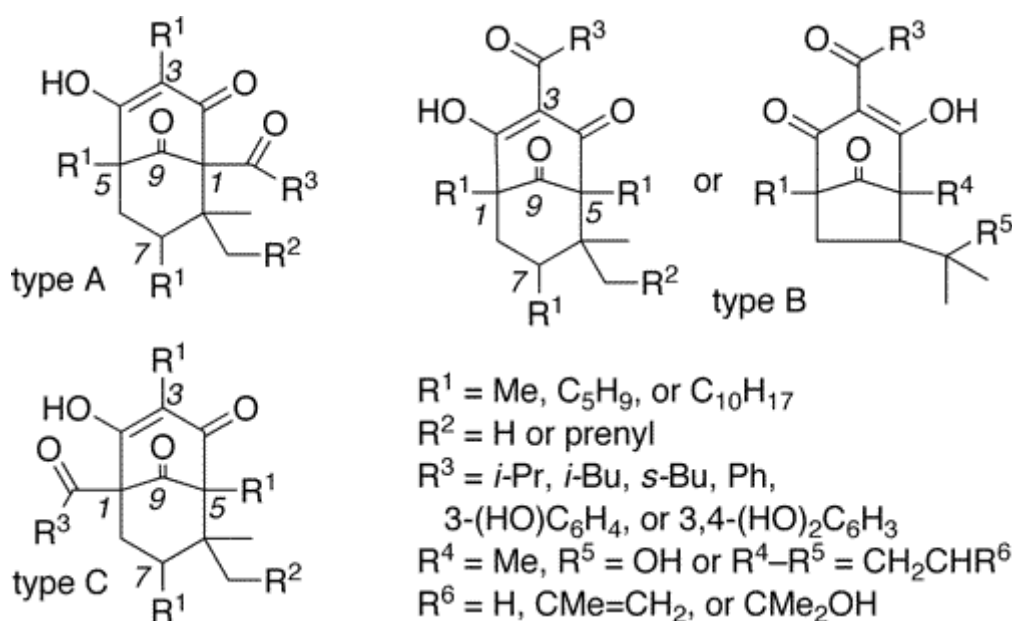


Figure 1.4. Type A, B and C PPAPs. Adapted with permission from (Ciochina & Grossman, 2006). Copyright 2022 American Chemical Society.

Wang *et al.*, synthesized a type B PPAP called PPAP23, which was found to be active against different gram positive bacterial strains. PPAP23 showed an MIC of 1 $\mu\text{g/ml}$ same as that of vancomycin against *S. aureus* USA300. The compound was also found to be active against *Staphylococcus aureus* Mu50, a VISA strain, *Enterococcus faecium* 4147, vancomycin-resistant *Enterococcus faecalis* VRE366, *Enterococcus faecium* VRE392, as well as *Streptococcus pneumoniae* ATCC49619 and *Listeria monocytogenes* ATCC19118 with MIC values < 5 $\mu\text{g/mL}$ (Guttruff *et al.*, 2017). Wang *et al.*, didn't observe any membrane depolarization or pore formation in *S. aureus* USA300 upon PPAP23 treatment, but noticed extensive ATP leakage and reduced consumption of oxygen in the bacteria. This suggested that PPAP targets the bacterial

membrane and its respiration (Figure 1.5). The exposure to PPAP also caused in the loss of bacterial resistance to osmotic pressure. PPAP was also seen to hinder with the bacterial iron metabolism. Genes involved in iron acquisition were downregulated and the one involved in iron storage was upregulated. PPAP23 also caused ROS production in the bacterial cell (Wang *et al.*, 2019).

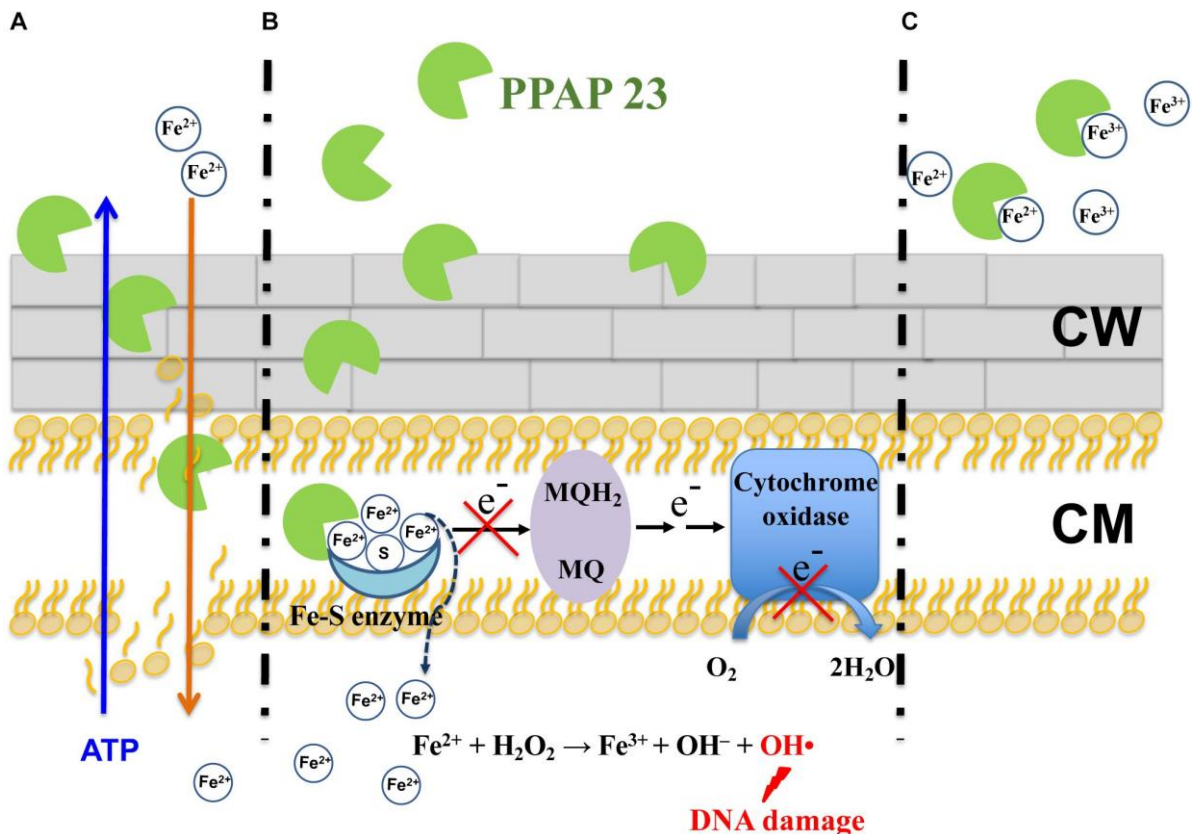


Figure 1.5. Proposed antibacterial action of PPAP23. (A) PPAP 23 affects the membrane integrity by interacting with the lipophilic pocket of the membrane. Disintegrated membrane results in the diffusing out of ATP and diffusing in of iron to the bacterial cells. (B) PPAP 23 chelates iron from Fe-S cluster enzymes causing the inactivation of Fe-S cluster enzyme. This can disturb the cell respiration (through the enzymes involved) or DNA damage and cell death (due to iron overload). (C) PPAP 23's antimicrobial activity is lessened when it is iron bound. MQH₂, menaquinol; MQ, menaquinone; CW, cell wall; CM, cytoplasmic membrane. Adapted with permission from (Wang *et al.*, 2019) with Creative Commons public licenses.

Objectives

This work is a continuation of the previous work where Hsp90 α was recognized as the host cell receptor for Lpl in USA300. The potential of Lpl1 fragments of different sizes were analyzed for their influence in USA300 invasion into HaCaT cells. A 15 amino acid fragment of Lpl1 called L15 (NH₂-TAKGHYFVTTTFYRNG-COOH) and its derivative L13 (NH₂-GHYFVTTTFY-COOH) were seen to bind directly to the Hsp90 α , but unlike Lpl1, reduces the invasion of bacteria into the keratinocytes. This intrigued us to check its potential on the invasion of USA300 on primary keratinocytes (N/TERT-1) and monocytes. The cytotoxic effect of these peptides on different eukaryotic cells and their hemolytic activities were also tested.

Next, we checked if the peptides can rescue *Galleria mellonella* larvae from different strains of *S.aureus* infection. The efficacy of the peptides in rescuing the same larvae from infection caused by bacteria including *E. coli*, *P. aeruginosa* were also studied. Growth curve kinetics study and hemolytic activity of *S.aureus* on treatment with L15 and L13 were conducted to identify if the larval rescue is the result of the peptides compromising the growth or virulence of the bacteria. Once it was seen that the peptides indeed could protect the larvae from *S.aureus* bacteremia, the same study was replicated in mice model with L15 as the model peptide.

Next, immune stimulation experiments were carried out to see the effect of L15 on PBMC cells alone and also in combination with USA300 infection. Multiple sequence alignment of lipoprotein analogs in different bacteria as well as similarity between different Lpls (Lpl1 - 9) were examined. Additionally, the potential of the peptides in rescue of larvae from *S. aureus* bacteremia in combination with different TLR ligands were also analyzed.

The group of Martin Maier, Institut für Organische Chemie, Universität Tübingen, was not only able to chemically synthesize Rom but also its isomer, rhodomycosone B; both isomers showed similar high antimicrobial activity. Despite its antibacterial activity on a broad spectrum of bacteria, the complete mode of action of Rom is still unknown other than the observation that Rom targets the cell membrane (Saising *et al.*, 2018).

The objective of this paper is to cement our previous *in silico* data and hypothesis that Rom binds to the phosphatidylglycerol (PG) group of the cell membrane by employing lipidomic analysis *in vitro* and to understand further about the molecular mechanism of Rom resistance. More Rom derivatives were also synthesized to develop a Rom derivative molecule that is also active against the Rom^R strain. The solubility of Rom derivatives was another criterion during the derivative synthesis. Most Rom derivatives are insoluble in water and are soluble only in DMSO. The activity of Rom against different anaerobic strains were also tested.

To assess the role of *farE* in Rom resistance, the said gene was deleted in *S.aureus* HG001 and the corresponding Rom^R strain and was checked for its sensitivity to rhodomycinone. Next, a lipidomic analysis of the culture supernatants was carried out to check whether the cause of Rom resistance was due to (1) Expulsion of Rom by the FarE pump or (2) Neutralization of Rom by the excreted PGs. Static and dynamic light scattering and Isothermal titration calorimetry experiments were carried out to check the interaction of Rom with PG. In static & dynamic light scattering studies, one can measure the diameter of Rom and PG vesicles separately and this diameter will increase if there is an interaction. The effect of another membrane protein MprF on Rom resistance was also investigated. MprF synthesizes Lys-PG and rescues the bacteria from lipopeptide antibiotics and cationic antimicrobial peptides. Additionally, we tested whether resistance to Rom can lead to cross-resistance in other antibiotics.

PPAP23 was found to be active against *S.aureus* and other anaerobes including *Clostridium difficile*, *Clostridium perfringens*, *Streptococcus salivarius*, *Ruminococcus gnavus*, *Clostridium ramosum*, *Blautia obeum* and *Parabacteroides distasonis*. A new water-soluble derivative of PPAP23, called PPAP53 was synthesized. Both PPAP23 and PPAP53 have similar MICs (0.5 -1 µg/ml) against *S.aureus*. Despite its promising antibacterial activity *in vitro*, both PPAP23 and PPAP53 were unsuccessful in providing a protecting effect on *S.aureus* infected *Galleria mellonella* larvae upon treatment. The control vancomycin protected 100% larvae from infective death. The objective of this paper is to understand the reason why PPAP fails to rescue the larvae from infection and identify the compound (serum albumin) in larval coelomic fluid responsible for its neutralization.

Once identified, further *in vitro* bacterial growth curve kinetics will be carried out to understand the bactericidal effect PPAP in combination with neutralization molecule - serum albumin. *In silico* docking studies will also be carried to identify the site of interaction of PPAP and the neutralization molecule (serum albumin). Further growth kinetics experiments involve blocking different sites of serum albumin with its ligands and then testing the efficacy of PPAP in killing *S. aureus* USA300 in the presence of the ligand saturated albumin. The cytotoxicity of PPAP23 (and some derivatives) in presence and absence of albumin proteins were also tested using MTT assay. The effect of PPAP23 on mice septic arthritis were also investigated. This is done by comparing the severity of clinical arthritis, the body weight development, Kidney abscess scores and quantity of *S. aureus* in kidneys of infected mice and that of infected mice treated with PPAP.

Chapter 2

Materials and Methods

Materials**Chemicals and media**

Chemicals and media	Manufacturer
Acetic acid	Sigma-Aldrich
ActinGreen™ 488 ReadyProbes®	Thermo Fischer, Germany
alkaline phosphatase conjugated goat- α -mouse IgG	Sigma-Aldrich, Germany
Ampicillin	AppliChem GmbH, Darmstadt, Germany
Anti-Hsp90 antibody	Abcam, Germany
anti-human CD14 microbeads	Miltenyi Biotech, Bergisch-Gladbach, Germany
Bovine serum albumin	Sigma-Aldrich Chemie GmbH, Munich, Germany
CD14-FITC	BD Biosciences, Heidelberg, Germany
CD45-PE	BD Biosciences, Heidelberg, Germany
DMEM, high glucose, with phenol red	Thermo Fisher Scientific, Schwerte, Germany
DMSO ≥ 99 %	Carl Roth GmbH & Co. KG, Karlsruhe, Germany
DNase I	Appllichem GmbH, Darmstadt, Germany
Ethanol	Sigma-Aldrich
Ethylene diamine tetraacetic acid (EDTA)	Appllichem GmbH, Darmstadt, Germany
Ethylene diamine tetraacetic acid (EDTA)	Appllichem GmbH, Darmstadt, Germany
Geldanamcin	Sigma-Aldrich Chemie GmbH, Munich, Germany
Gibco Roswell Park Memorial Institute 1640 Medium (RPMI 1640)	Thermo Fisher, Waltham, MA, USA

Glucose D(+)	Carl Roth GmbH & Co. KG, Karlsruhe, Germany
Hydrochloric Acid	Sigma-Aldrich Chemie GmbH, Munich, Germany
Isopropanol	Sigma-Aldrich Chemie GmbH, Munich, Germany
Kanamycin	Carl Roth GmbH & Co. KG, Karlsruhe, Germany
Keratinocyte serum-free medium (K-SFM)	Gibco, Invitrogen Corp.
LB media	Carl Roth GmbH & Co. KG, Karlsruhe, Germany
L-Glutamine	Thermo Fisher Scientific, Schwerte, Germany
Magnesium chloride	Sigma-Aldrich Chemie GmbH, Munich, Germany
Milk powder, blotting grade	Carl Roth GmbH & Co. KG, Karlsruhe, Germany
Penicillin Streptomycin	Thermo Fisher Scientific, Schwerte, Germany
Phosphate Buffered Saline (PBS), 1x	Thermo Fisher Scientific, Schwerte, Germany
Pierce™ BCA Protein Assay Kit	Thermo Fisher Scientific, Schwerte, Germany
Propidium iodide	BD Biosciences, Heidelberg, 436 Germany
Recombinant Hsp90α	Thermo Fisher Scientific, Schwerte, Germany
Roti®-Quant, 5X concentrate	Carl Roth GmbH & Co. KG, Karlsruhe, Germany
Sodium chloride	Carl Roth GmbH & Co. KG, Karlsruhe, Germany
Sodium dodecyl sulfate (SDS)	Carl Roth GmbH & Co. KG, Karlsruhe, Germany

Triethylamine (TEA)	Carl Roth GmbH & Co. KG, Karlsruhe, Germany
Triton X-100	Carl Roth GmbH & Co. KG, Karlsruhe, Germany
Gibco Trypsin-EDTA (0.25%), with phenol red	Thermo Fisher, Waltham, MA, USA

Consumables/ Standard labware

Consumables	Manufacturer
0.2 μ filter tips	Sarstedt
0.45 μ filter tips	Sarstedt
10 mL pipette	Greiner
12 well plate Cell culture	Greiner
24 well plates Cell culture	Greiner
25 mL pipette	Greiner
48 well plate (Growth curve)	Greiner
48 well plates Cell culture	Greiner
6 well plates Cell culture	Greiner
96 well F bottom	Greiner
96 well lid with CR	Greiner
96 well plates Cell culture	Greiner
96 well U bottom	Greiner
96 well U bottom black plates	Greiner
Cell Scraper	Cornig
Cryopreservation tubes	Greiner
Cuvette	Sarstedt
ELISA plates	Cornig Sigma
Eppendorfs 1.5 mL	Fischer scientific
Eppendorfs 2 mL	Fischer scientific
Eppendorfs 5 mL	Fischer scientific
Falcon tube 15 mL	Greiner
Flacon tube 50 mL	Greiner

Gloves	Haeberle
Inoculation loop 10 uL	Sarstedt
Inoculation loop 1uL	Sarstedt
Pipette tips 10 µL	Axygene from sigma
Pipette tips 100 µL	Greiner
Pipette tips 1000 µL	Greiner
PP tube 14ml	Greiner
RAININ pipette tips 1200 µL	Mettler Toledo
RAININ pipette tips 200 µL	Mettler Toledo
Reservoir	Fischer Scientific
Square Petri plates	Fischer scientific
Syringe 10 mL	Haeberle
Syringe 20 mL	Haeberle
Syringe 5 mL	Haeberle
T spreader	TH Geyer
T-25 Cell culture flask	Greiner
T-75 Cell culture flask	Greiner

Technical equipment

Equipment	Manufacturer
Centrifuge 5424R	Eppendorf AG, Hamburg, Germany
Centrifuge 5810R	Eppendorf AG, Hamburg, Germany
CO2 Incubator, BBD 6220	Heraeus Instruments
Flow cytometer BD Accuri C6	BD Biosciences, Heidelberg, Germany
Laminar flow hood	Tecnoflow, Cesate MI, Italy
Magnet stirrer RCT basic	IKA Werke GmbH, Staufen, Germany
Microscope, Zeiss Axioplan 2	Zeiss, Oberkochen, Germany
Multichannel pipette	Eppendorf AG, Hamburg, Germany
pH meter	Mettler Toledo GmbH, Giessen, Germany
Pipetts	Brand GmbH & Co KG, Wertheim, Germany
Pipettboy	Integra BioSciences, Fernwald, Germany
Refrigerator	Liebherr, Germany

Spectrometer NanoDrop 2000	Thermo Scientific, Schwerte, Germany
Sterile hood	BDK GmbH, Sonnenbühl-Genkingen, Germany
Varioskan LUX multimode microplate reader	Thermo Scientific, Schwerte, Germany
Vortex Genie 2	Scientific Industries, Karlsruhe, Germany
Water bath	GFL Technology, Lauda-Koenigshofen, Germany

Mammalian cell lines

Name	Type Of Cell Line	Source
CD14 ⁺ Monocytes	CD14 ⁺ Monocytes	German Red Cross Blood transfusion west (Hagen, Germany)
HaCaT	Immortalized Keratinocyte Cells	German Cancer Research Center (DKFZ)
HEK	Human Embryonic Kidney Cells	ATCC
HL-60	Acute Monocytic Leukemia	German Collection of Microorganisms and Cell Cultures (DSMZ)
HT-29	Human Colon Cancer Cells	ATCC
MM6	MONO MAC 6, Acute Monocytic Leukemia	German Collection of Microorganisms and Cell Cultures (DSMZ)
N/TERT-1	Immortal Keratinocyte Cell Line	Dr. J. Rheinwald, Harvard Medical School, Boston, USA
PBMC	Peripheral Mononuclear Blood Cells	German Red Cross Blood transfusion west (Hagen, Germany) and the Transfusion Blood Bank of the Medical Clinic Tübingen

Bacterial strains

Strain	Source
<i>Escheria coli</i> K12	ATCC
<i>Pseudomonas aeruginosa</i> PA01	ATCC
<i>Staphylococcus aureus</i> HG001	Microbial Genetics, Uni. Tübingen
<i>Staphylococcus aureus</i> Newman	ATCC
<i>Staphylococcus aureus</i> USA300	ATCC

Methods

Bacterial strains, growth conditions and antibiotics

S. aureus strains was grown in Tryptic Soy Broth (TSB, Difco) to the desired phase as specified in each experiment. Mueller Hinton Broth (MHB) was used for the MIC determination. Fetal bovine serum, bovine serum albumin, IgG from bovine serum, and fibronectin from bovine plasma were purchased from Sigma. Fetal bovine serum (FBS) and bovine serum albumin (BSA) were dissolved in the Mueller-Hinton Broth (MHB) to achieve the desired concentrations before being sterile filtered. Bovine IgG and fibronectin were dissolved in 0.9% NaCl and sterile filtered before further dilution in MHB. As antibiotics we used PPP 23, PPAP 22, and PPAP 53 which were all chemically synthesized in the AG Bernd Plietker. Rom and its derivatives were synthesized by AG Martin Maier.

Peptide synthesis

The amino acid sequences of peptides used in this study are given in Table 1. The peptides were synthesized by Apeptide (Shanghai, China) with a purity of >95%, dissolved in water at 1 mg/ml and stored at -20°C . 20 μM of L15, 30 μM of L13 and 5 μM of geldanamycin were used in in vitro studies unless mentioned otherwise.

Antibiotic susceptibility testing

The minimal inhibitory concentration is adopted as the parameter to measure the bacterial susceptibility to the antimicrobial drug (Gemmell *et al.*, 2006). The minimal inhibitory concentration determined by the microdilution method according to the guidelines of the Clinical and Laboratory Standards Institute document M07-A9 (Rennie *et al.*, 2012). Each antibiotic was serially diluted resulting in 50 µl antibiotic dilution in the respective well of a 96-well microtiter plate, 50 µl bacterial suspension of 10⁶ CFU/ml were added to the antibiotic dilution, and growth control. The microtiter plate was incubated at 37°C under continuous shaking for 18 hours or 24 hours before the measurement of OD with a microplate reader (TECAN Infinite M200). The MIC is the lowest concentration of an antibiotic that prevents the visible growth of a microorganism (Wiegand *et al.*, 2008).

Invasion studies in HaCaT and N/TERT-1 cells

The invasion protocol was adapted from our previous papers (Nguyen *et al.*, 2015, Tribelli *et al.*, 2020). Keratinocytes were seeded in a 24 well plate (Greiner, Frickenhausen, Germany) to attain a monolayer of ~10⁶ cells/well. *S. aureus* was grown overnight at 37°C, centrifuged and suspended in invasion medium (DMEM with 10% FBS for HaCaT and K-SFM for N/TERT-1 cells). The adherent keratinocytes were washed with PBS and supplemented with invasion medium followed by treatment with 20 µM of L15, 30 µM of L13 or 5 µM geldanamycin (Sigma-Aldrich, Germany) or monoclonal antibodies specific against Hsp90α (α-Hsp90α, Abcam) for 1 h. After 1h, 100 µl of bacterial suspension was added to each well to attain a MOI (multiplicity of infection) of 30 and incubated with cells for 1.5 h. After this, the extracellular bacteria were killed with treatment of 2.5 µg/ml lysostaphin (Sigma-Aldrich, Germany) for 1.5 h. The cells were then washed, lysed, mechanically detached by scraping, diluted and seeded on TSB plates to quantify the intracellular bacteria.

CD14⁺ monocyte isolation

Peripheral Blood Mononuclear cells (PBMCs) were isolated by density gradient centrifugation following the previous study (Nguyen *et al.*, 2022). From the pool of PBMCs, monocytes were isolated by positive selection with anti-human CD14 microbeads (Miltenyi Biotech, Bergisch-Gladbach, Germany) following a previously

reported protocol (Nguyen et al., 2022). The purity was analysed by flow cytometry on a BD Accuri C6 (BD Biosciences, Heidelberg, Germany) with anti-human CD14-FITC, CD45-PE and propidium iodide (BD Biosciences, Heidelberg, Germany) and ranged from 85% to 98%.

Phagocytosis assay

For phagocytosis 10^6 CD14⁺ monocytes were seeded in 1 ml medium (RPMI supplemented with L-Glutamine and 10% FCS) in a 12 well plate (Greiner, Germany). The cells were incubated with 20 μ M of L15, 30 μ M of L13 or with 5 μ M of Geldanamycin for 60 min at 37 °C and 5% CO₂ before addition of bacteria. For phagocytosis assay, bacterial cells were resuspended in 100 μ l RPMI medium at MOI of 30 and incubated with monocytes for 90 min. The cells were washed once with PBS and 0.5 ml of medium supplemented with 20 μ g/ml of Lysostaphin was added for 90 min to remove the extracellular bacteria. Then, monocytes were washed for 2 times with PBS and resuspended in 0.5 ml of milliQ dH₂O. The cells were scraped, and the lysed solution was transferred into a new 1.5 ml Eppendorf tube for a 5 min sonication. 10 μ l fractions of undiluted, 10^{-1} , 10^{-2} and 10^{-3} dilutions were inoculated on tryptic soy agar (TSA) plates and incubated overnight at 37 °C. The numbers of internalized bacteria were determined based on the manual counting of bacterial colony forming units (cfu) recovered on the agar plates.

Bacterial Growth kinetics

S. aureus precultured in TSB overnight were inoculated to OD~0.01 into a 48 well plate and L15 and L13 or 1X MIC PPAP53 and/or 1% BSA were added to study the effect of peptides on bacterial growth using Varioskan LUX Multimode Microplate Reader. With this instrument, a kinetic measurement of OD₅₇₈ nm was obtained every 1 h for a total of 24 h, at 37°C with continuous shaking.

Peptide - Hsp90 α interaction studies with immunoblotting

2 μ g of each peptide was blotted (dot blot) directly on PDV nitrocellulose membrane and blocked with 3% BSA. After washing, the membrane was then incubated with 20 μ g of recombinant Hsp90 α protein at 4 °C overnight. α -Hsp90 α was used as the

primary antibody and alkaline phosphatase conjugated goat- α -mouse IgG (Sigma-Aldrich, Germany) as the secondary antibody. Detection was done using BCIP®/NBT solution (Sigma, Germany).

F-actin formation

5×10^4 cells were seeded in black flat bottom 96 well cell culture microplate (Greiner, Germany) and incubated overnight. The cells were then incubated with peptides or geldanamycin for 1.5 h. After incubation, the cells were washed, permeabilised with 0.1% (v/v) Triton X-100 and stained with ActinGreen™ 488 ReadyProbes® (Thermo Fischer) for 30 min. After the staining, the cells were washed and measure for its fluorescence at Excitation/Emission: 495/518 nm (Luqman *et al.*, 2020)

Cytotoxicity studies

MTT (3-(4,5-dimethylthiazol-2-yl)-2,5-diphenyl tetrazolium bromide) assay was employed to analyze the cytotoxicity of peptides and geldanamycin to the cells. 5×10^5 cells were seeded in a 96 flat bottom well plate and incubated for 2.5h/ 24 h at 37 °C with 5% CO₂. The cells were then treated with increasing concentration (0 to 200 μ M) of peptides or geldanamycin for 24 h. After the incubation, 10 μ l of the MTT labelling reagent is added to each well to attain a final concentration 0.5 mg/ml, followed by 4 h incubation. Metabolically active cells convert the yellow tetrazolium salt to purple formazan crystals, which were solubilized using the solubilization solution (DMSO) and measured for absorbance at $\lambda_{\max}/\lambda_{\text{ref}}$ - 570/690 nm (Saising *et al.*, 2018).

Larval studies

The infection experiment was conducted as previously described (Popella *et al.*, 2016). *Galleria mellonella* larvae, purchased from Feeders & more GmbH, Germany, were sorted based on weight and used within one week. Ten larvae per group with weight average of 500mg/larvae were injected with bacteria and/or peptides on its last proleg using a BD insulin syringe. The dosage used for the experiment were 60 mg/kg for peptides, 5mg/kg of geldanamycin and 20 mg/kg for vancomycin. Each larva was injected with 10 μ l of L15 (last left proleg) 1h before administration of 10^6 cfu *S. aureus* (last right proleg). In case of PPAP studies, the overnight culture of *S. aureus* USA300

was washed with PBS twice to adjust to an OD₅₇₈ of 0.1, and 10 µl of bacterial suspension, corresponding to a dose of 10⁵ CFU was injected to the last left proleg of each larva; and 10 µl of PPAP 23/53, corresponding to a dose of 20 mg/kg was injected to the right proleg of each larva in the treatment group. Untreated larvae and larvae injected with PBS were in the control groups. The larvae were maintained at 37 °C and observed for mortality every day over the course of 5 days.

***Ex vivo* killing assay of *Galleria mellonella* larvae**

The body liquid from the larvae of *Galleria mellonella* was extracted and filtered sterile, and one larva could produce about 100 µl of larval liquid. To mimic the in-vivo larva infection assay, the *ex vivo* killing assay adopted the same amount of bacterial suspension and PPAP used in the infection model. Bacterial inoculum of 10⁵ CFU and 10 µg of PPAP was added to 100 µl of larva body liquid as the treatment group. Untreated larval liquid and larval liquid treated with PBS were the controls. The plate was incubated at 37 °C, overnight with a shaking speed of 20 rpm that resembles the movement of larvae. The viability of bacteria in each group was determined by the drop plate method (Herigstad *et al.*, 2001).

Hemolysin activity

6 mm Whatman empty Antibiotic Assay Discs were impregnated with L15 or L13 and allowed to dry. Once dried, the discs were placed on sheep blood agar plates, inoculated with *S. aureus* and incubated at 37 °C overnight. The halo obtained was measured and compared.

Mouse studies

Eight- to 10-week-old female NMRI mice were purchased from Envigo (Venray, Netherlands) and stored under standard temperature, light, and nutrition conditions in the animal facility of the Department of Rheumatology and Inflammation Research, University of Gothenburg. Due to its poor solubility in PBS, L13 was not used in mouse experiments. To study the effect of L15 on *S. aureus* bacteremia two separate experiments were performed. The mice were treated intraperitoneally with L15 (10 mg/kg) in 200 µl of PBS every 12 hours, starting 2-3 hours before inoculation with

bacteria and continuing until the animals were sacrificed. Mice were challenged with septic dose of 2×10^6 CFU/mouse of *S. aureus* Newman. To induce the *S. aureus* systemic infection in NMRI mice, 0.2 ml of *S. aureus* Newman suspension was inoculated intravenously into the tail vein of the mice. During the course of the experiments, the mice were regularly weighed until the mice were sacrificed. After sacrificing the mice at day 7, kidneys from mice were aseptically removed, homogenized, serially diluted with PBS and spread on agar plates containing 5 % horse blood. Plates were incubated at 37°C for 24 h and bacteria were quantified as CFUs. Kidneys from mice in bacteremia experiment were aseptically removed after the mice had been sacrificed. Kidneys were then homogenized, serially diluted with PBS and spread on agar plates containing 5 % horse blood. Plates were incubated at 37°C for 24 h and bacteria were quantified as CFUs. Before homogenisation, the kidneys were blindly assessed by one investigator (T.J.) for abscesses. A scoring system ranging from 0-3 was used (0- healthy kidneys; 1- 1 to 2 small abscesses on kidneys without structure changes; 2- more than 2 abscesses, but < 75% kidney tissue involved; and 3- large amounts of abscesses with >75% kidney tissue involved) (Ali *et al.*, 2015).

Immune stimulation

Human peripheral blood mononuclear cells (PBMCs) from buffy coat blood samples of healthy donors were stimulated with the indicated doses of L15 and L13 for 20 hours. For the subsequent bead-based immunoassay, the cell culture supernatants of a total of four buffy coats per immunoassay were used. Each of the stimulations was performed in biological duplicates. The secreted cytokines were then identified and quantified using the immunofluorescent bead-based immunoassay LEGENDplex® Human Macrophage/Microglia Panel (13-plex) and the corresponding Data Analysis Software from BioLegend. Muramyl Dipeptide (MDP) which activates the NOD-2 receptors was used as the positive control.

Bioinformatics analysis

The 3D structure of Lpl1 was predicted using the protein structure prediction server Robetta using RoseTTAFold modelling method (Baek *et al.*, 2021). The obtained .pdb

structure was then visualized in PyMOL by Schrödinger. The homologs of *S. aureus* USA300 Lpl1 in different bacteria were identified using the Protein BLAST tool on the NCBI server. The comparison of different lipoprotein homologs from different bacteria was done in Snap gene using Clustal Omega algorithm.

A well-defined crystal structure of BSA was downloaded from protein data bank (PDB ID: 3V03) (Majorek et al., 2012). The calcium and acetate ions attached to the crystal structure, as well as the water molecules used for crystallization were removed to get a clean structure of the BSA protein. 2D structure of PPAP was prepared and its geometry was optimised by energy minimisation in Chem3D 16.0. The structures are visualized and verified using PyMoL software. The PDBQT files of Protein and ligands were prepared using AutoDock Tools and blind docking was performed in AutoDock vina (Trott & Olson, 2010). During the preparation of PDBQT files polar hydrogens and Kollman charges are added for both the protein and ligand. The serum albumin was considered as a rigid structure and PPAP as the flexible one during docking.

Statistical analysis

GraphPad Prism was employed for statistical analysis. Student's t tests or one-way analysis of variance (ANOVA) were used to check the statistical significance of different results. P value > 0.05 was considered as not significant (ns). In figures, significant differences are represented as follows: * $p < 0.05$; ** $p < 0.01$; *** $p < 0.001$; and **** $p < 0.0001$.

Ethical Statement

The use of human peripheral blood mononuclear cells (PBMCs) from buffy coats was approved by the Ethics Committee of the Medical Association of Westphalia-Lippe and the University of Münster (Approval number 2021-063-f-S) and the Ethics Committee of the Medical Faculty of the University of Tübingen and the Medical Clinic Tübingen (approval number 084/2021BO2). Buffy coats were obtained from the German Red Cross Blood transfusion west (Hagen, Germany) and the Transfusion Blood Bank of the Medical Clinic Tübingen. The Ethics Committee of Animal Research of Gothenburg approved all experiments conducted on mice. The mouse experiments were performed

in accordance with the Swedish Board of Agriculture's regulations and recommendations on animal experiments.

Chapter 3

Results

Results

Studies on L15 and L13

L15 reduces USA300 invasion into keratinocytes

It has been shown in our previous papers that Ipl cluster be conducive to the invasion of USA300 into HaCaT cells. In the Δ Ipl mutant the, amount of invasion was 2.5 fold less as compared to the wild type. The peptides were synthesised from Apeptide (Shanghai, China) with a purity of >95%, solubilized in water at 1 mg/ml and stored at -20°C . 20 μM of L15, 30 μM of L13 and 5 μM of geldanamycin were used in *in vitro* studies if not stated otherwise. The invasion protocol was adapted from our previous paper (Tribelli *et al.*, 2020).

Preincubation of L15 and L13 with HaCaT cells reduced the invasion of USA300 into the former by nearly 59.9 and 54.7% respectively. Relative invasion of *S. aureus* into the HaCaT cells reduced from 1 ± 0 (untreated control) to 0.40 ± 0.09 on pre-treatment with L15 and 0.45 ± 0.06 on pre-treatment with L13. Enhanced invasion of USA300 into HaCaT cells were seen on pre-treatment with peptides L11 (1.57 ± 0.20), L26 (1.50 ± 0.17) and L27 (1.55 ± 0.17). Other test peptides didn't affect the invasion activity of bacteria into the cell (Table 1).

Geldanamycin, a benzoquinoid from *Streptomyces hygroscopicus*, was used as a positive control. It has been demonstrated in our previous paper that 5 μM geldanamycin showed significant reduction in USA300 internalisation (Tribelli *et al.*, 2020). Herealso, we could see that geldanamycin showed 75 % reduction of USA300 invasion into the HaCaT cells (relative invasion for geldanamycin group was 0.25 ± 0.13). Pre-treatment of HaCaT cells with α -Hsp90 α , also reduced the invasion of *S. aureus* by 89.3% (0.11 ± 0.09) (Fig. 3.1A).

We did the same studies on N/TERT-1 keratinocyte cell line using L15 and L13. N/TERT-1 were a kind gift from Dr. J. Rheinwald, Harvard Medical School, Boston, USA (Dickson *et al.*, 2000). N/TERT-1 cells are frequently employed as an auxiliary for primary keratinocyte cells due to the limited obtainability and high inter-donor inconsistency of the latter. N/TERT-1 cells are immortalised and are shown to work

essentially like primary human keratinocytes in expression of host defence genes and proteins, and epidermal differentiation (Smits *et al.*, 2017). Similar pattern was exhibited in N/TERT-1 cells. Intracellular *S.aureus* USA300 relative bacterial load was significantly reduced on pre-treatment with L15 (0.6 ± 0.05), L13 (0.37 ± 0.10), geldanamycin (0.24 ± 0.04) and α -Hsp90 α (0.25 ± 0.04) in N/TERT-1 cells as compared to the untreated control (Fig. 3.1B).

It should be noted that neither peptides (L15/L13) nor geldanamycin showed any inhibitory action towards the cell lines (Fig. 3.2A, B) or *S.aureus* for the duration of the experiment. Also, the addition L15 and L13 didn't influence the growth of *S.aureus* USA300 at 37°C (Fig. 3.2C).

Table 1. Effect of tested Lpl1-derived peptides on their invasion potential, F-actin formation and binding to Hsp90 α .

Name	Sequence	No of AA	Relative Invasion	Interaction with Hsp90 α	Relative F-actin level
L1	³⁴ GKGNETKED	9	1.02 ± 0.34	No	0.95 ± 0.49
L2	⁵⁵ TLDMPYIKNLED	12	1.12 ± 0.40	No	0.99 ± 0.13
L3	⁶⁷ LYDKEGYRDS	10	1.00 ± 0.11	No	1.03 ± 0.1
L4	⁷⁷ EFKKGDKGMWT	11	0.93 ± 0.12	No	0.94 ± 0.08
L5	⁸¹ GDKGMWTIYTDFAKSNKPGELDDEGMVLNLDNRNTR	34	1.59 ± 0.76	No	0.97 ± 0.08
L6	⁸⁵ MWTIYTDFAKS	11	0.98 ± 0.68	No	0.91 ± 0.1
L7	⁸⁸ IYTDFAKSNKPGEL	14	1.10 ± 0.18	No	1.03 ± 0.08
L8	⁹⁶ NKPGEL	6	1.28 ± 0.34	No	0.96 ± 0.05
L9	¹⁰² DDEGMVLNLD	10	1.0 ± 0.44	No	1.06 ± 0.07
L10	¹¹³ NTRTAKGHYFVTTFYRNG	18	1.10 ± 0.17	Yes	0.99 ± 0.08
L13	¹¹⁹ GHYFVTTY	9	0.45 ± 0.08	Yes	0.87 ± 0.03
L15	¹¹⁶ TAKGHYFVTTFYRNG	15	0.4 ± 0.09	Yes	0.83 ± 0.04
L11	¹¹⁶ TAKGHYFVTTFYRNGKLPDEKNYKIEMKNNKIILLDEVKDDKLLQKIENFKFFGQYANLKLKLRK	64	1.57 ± 0.20	No	1.49 ± 0.07
L12	¹²⁶ FYRNGKLPDEKNYKI	15	0.94 ± 0.11	No	0.98 ± 0.06
L14	¹³¹ KLPDEKNYKI	10	0.78 ± 0.26	No	0.98 ± 0.08
L16	¹³⁷ NYKIEMKNNKIILLD	15	0.92 ± 0.37	Yes	1.08 ± 0.23
L17	¹⁴¹ EMKNNKIIL	9	1.05 ± 0.26	No	1.09 ± 0.20
L18	¹⁴⁴ NNKIILLDEVKDDKL	15	1.05 ± 0.36	No	1.09 ± 0.22
L19	¹⁵¹ DEVKDDKLLKQKIENF	15	1.29 ± 0.37	No	0.97 ± 0.11

L20	¹⁶² ENFKFFGQYAN	12	1.15 ± 0.20	No	1.03 ± 0.11
L21	¹⁶³ ENFKFFGQYANLKELRK	17	1.20 ± 0.25	Yes	1.09 ± 0.13
L22	¹⁷⁷ LRKYNNGDVSINENVPSYDV	20	1.29 ± 0.13	No	0.97 ± 0.09
L23	¹⁸⁰ YNNGDVSINENVPSYDVEYKMSNK	24	1.09 ± 0.46	No	0.96 ± 0.05
L24	¹⁹⁴ YDVEYKMSNK	10	0.95 ± 0.12	No	0.94 ± 0.08
L25	²⁰⁴ DEIVKELRSRYNIST	15	1.0 ± 0.06	No	1.03 ± 0.16
L26	²⁰⁴ DEIVKELRSRYNISTEKSPILKMHD GDLKGSSVGYRKLEI DFSKRENSKLSVIEFLSYKPAKK	64	1.50 ± 0.17	Yes	1.25 ± 0.13
L27	²¹¹ RSRYNISTEKSPILKMHDGDLKGSS VGYRKLEIDFSKRENSK	38	1.55 ± 0.17	Yes	1.36 ± 0.12
L28	²¹⁷ STEKSPILKMHDGD	15	1.0 ± 0.27	No	0.90 ± 0.04
L29	²²⁷ HIDGDLKGSSVGYRK	15	1.21 ± 0.33	No	0.90 ± 0.05
L30	²⁴⁶ FSKRENSKLSVIEFL	15	1.24 ± 0.32	No	0.96 ± 0.1
	Control: Geldanamycin		0.25 ± 0.13	NA	0.88 ± 0.03

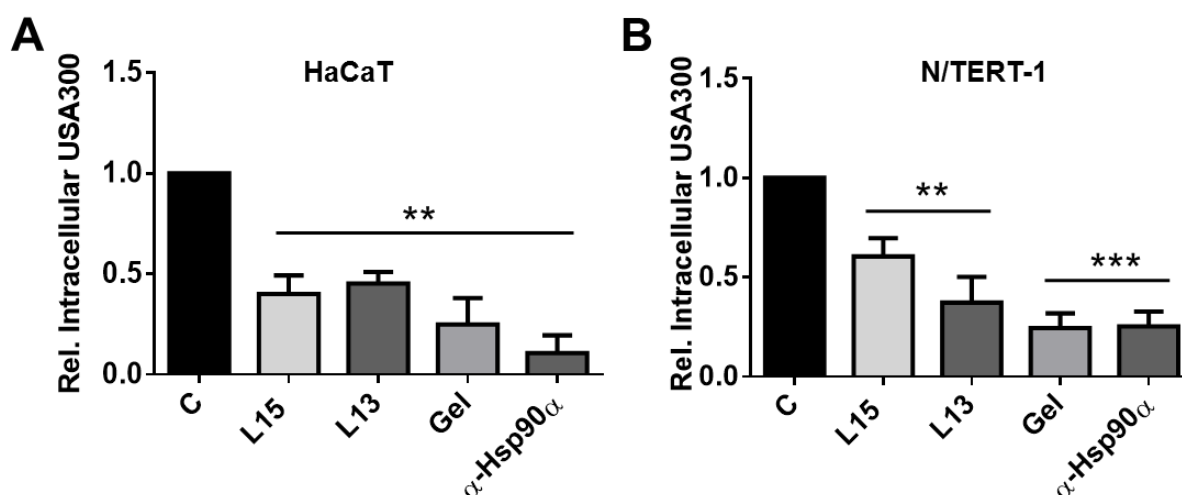


Figure 3.1. L15 and L13 hinders the invasion of *S.aureus* USA300 into (A) HaCaT and (B) N/TERT-1 cell lines upon pretreatment for 1.5h. Pretreatment of cells with geldanamycin, a well-known Hsp90 inhibitor or with α -Hsp90 α (Hsp90 α) antibody also inhibited USA300 invasion into the keratinocytes. Error bars show standard deviation of the mean of 3 biological replicates. P values were obtained by student's T-test. : * p < 0.05; ** p < 0.01; *** p < 0.001; and **** p < 0.0001.

L15 and L13 directly interacts with Hsp90 α

LpI1 was shown to directly interact with Hsp90 α in our previous studies (Tribelli *et al.*, 2020). Here also, we did the same experiment with the peptides. The synthetic peptides were directly blotted on the nitrocellulose membrane and checked for its binding to Hsp90 α using alkaline phosphatase assay. We could see direct interaction

of L15/L13 and purified Hsp90 α using dot blot studies (Table 1). Other peptides which showed direct interaction with Hsp90 α were L10, L16, L21, L26 and L27. No interaction was observed with Bovine serum albumin (BSA) which was used as a control.

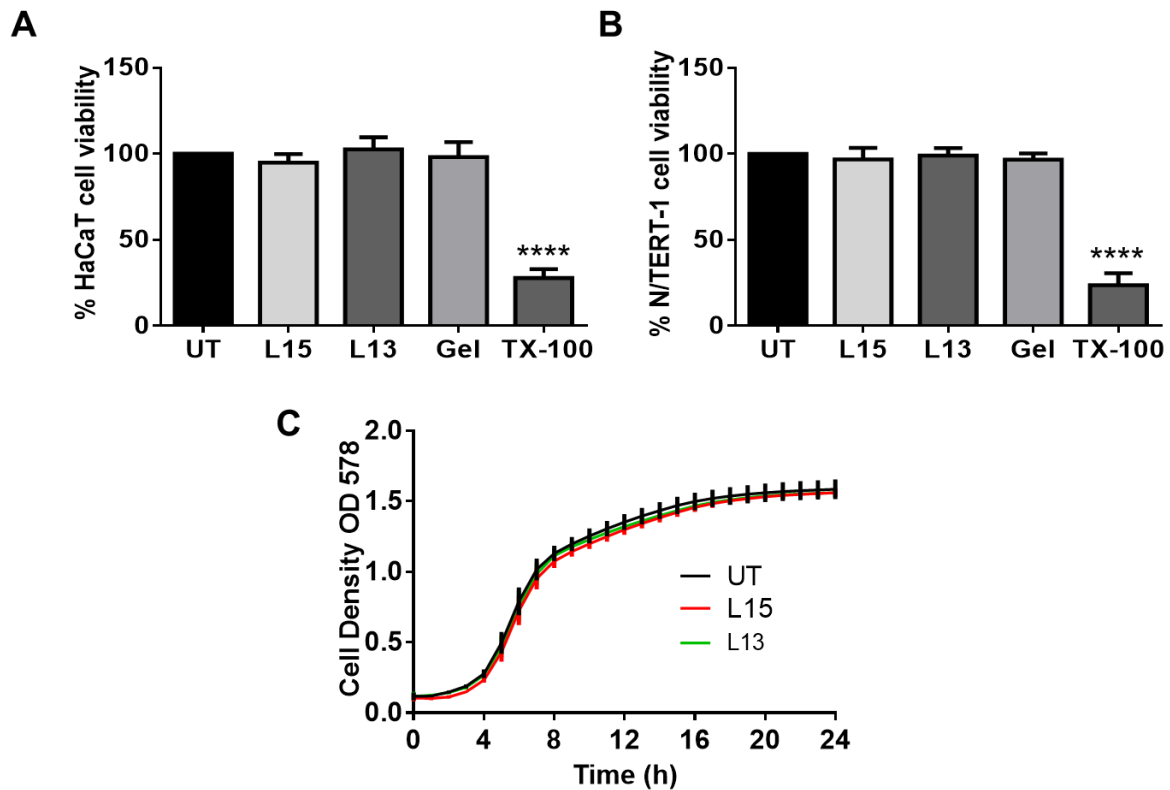


Figure 3.2. L15, L13 and geldanamycin doesn't have any effect on cell lines (A) HaCaT and (B) N/TERT-1 during treatment time. (C) L13, L15 doesn't affect the USA300 growth in TSB at 37 °C.

L15- Hsp90 α interaction reduces F-actin levels in keratinocytes

The mother protein Ipl1 was shown to boost the F-actin levels in HaCaT cells in our previous paper (Tribelli *et al.*, 2020). It is also reported that 17-allylamino-demethoxy-geldanamycin (17-AAG) decreased the F-actin levels upon Hsp90 inhibition in breast cancer cells (Taiyab & Rao Ch, 2011). We checked if L15 is affecting the actin polymerisation, since it is interacting with Hsp90 α . Indeed, a significant reduction in F-actin levels were seen in both keratinocytes on treatment with L15, L13 and geldanamycin (Fig. 3.3A, B). In HaCaT cells, relative F-actin levels went down to 0.83 ± 0.04 for L15, 0.87 ± 0.03 for L13 and 0.88 ± 0.03 for geldanamycin. Relative F-actin levels in N/TERT-1 cells for L15, L13 and geldanamycin were 0.9 ± 0.02 , 0.81 ± 0.03 and 0.82 ± 0.03 respectively. As expected enhanced F-actin levels were seen when L11, L26 and L27 were introduced to HaCaT cells (Table 1).

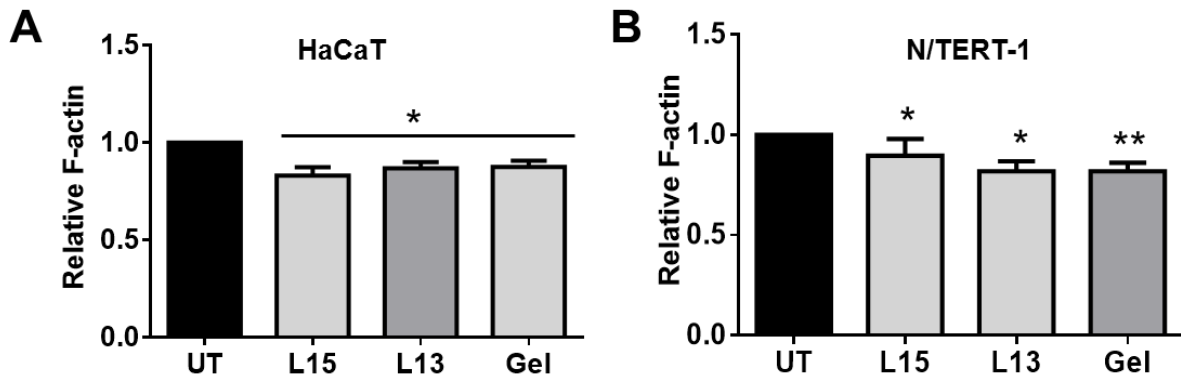


Figure 3.3. L15, L13 and geldanamycin interaction with Hsp90 α effects the F-actin formation in (A) HaCaT and (B) N/TERT-1 cells. A significant reduction of F-actin levels were observed on treatment of keratinocytes with peptides and geldanamycin. Error bars show standard deviation of the mean of 3 biological replicates. P values were obtained by student's T-test. : * p < 0.05; ** p < 0.01; *** p < 0.001; and **** p < 0.0001

L15 and L13 are non-toxic to cells *in vitro*

10-50 μ M of L15 and L13 were checked for its cytotoxicity on HaCaT- human Keratinocyte cell line, HEK-human embryonic kidney cells, HT-29 - human colorectal adenocarcinoma cell line and MM6 cell line - human monocytic cell line for a 24h time period using MTT assay (Fig. 3.4A-D).

The percentage of viable cells on treatment with L15 for 24h ranged from 90.36 ± 2.89 (10 μ M) to 93.56 ± 3.96 (50 μ M) for HaCaT cells and 86.53 ± 6.23 (10 μ M) and 93.12 ± 4.96 (50 μ M) for HEK cells. For HT-29 cells, L15 showed cell viability from 100.32 ± 4.07 % and 97.03 ± 4.44 % for 50 and 10 μ M respectively. MMT studies on MM6 cells indicated % viability of 111.45 ± 7.96 for 50 μ M and 101.31 ± 3.52 for 10 μ M L15.

Treatment with 50 μ M of L13 resulted in percentage cell viability of 92.62 ± 6.08 for HaCaT, 89.0 ± 5.52 for HEK, 97.07 ± 5.55 for HT-29 and 90.01 ± 8.58 for MM6 cells. 10 μ M of L13 showed a cell viability of 98.03 ± 8.62 % (HaCaT), 91.47 ± 8.21 % (HEK), and 93.36 ± 4.95 % (HT-29) and 104.65 ± 10.48 % (MM6).

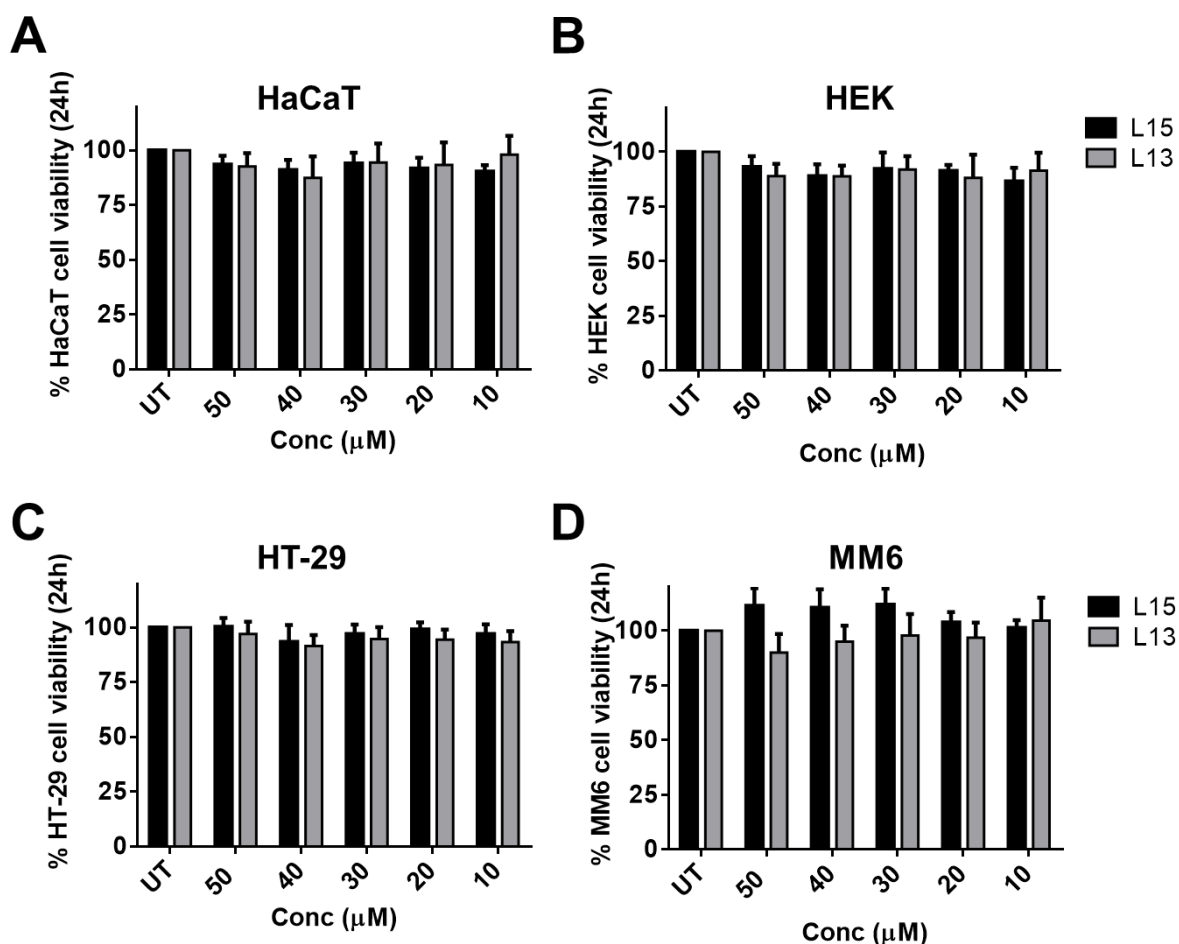


Figure 3.4. L13/L15 is non-toxic to (A) HaCaT, (B) HEK, (C) HT-29 and (D) MM6 cells *in vitro*. Error bars show standard deviation of the mean of 3 biological replicates. P values were obtained by student's T-test. : * $p < 0.05$; ** $p < 0.01$; *** $p < 0.001$; and **** $p < 0.0001$.

L15/L13 rescues larvae from *S. aureus* infection

The larvae of *Galleria mellonella* or greater wax moth has been well recognized as an experimental model to study the virulence of different pathogens as well as to evaluate the efficacy of various anti-microbial compounds. The large size of the larvae warrants easy handling and direct injection of inoculate into the larval hemocoel. *Galleria mellonella*, purchased from Feeders & more GmbH, Germany, were sorted based on weight and used within one week. Each group consists of 10 larvae with weight average of 500mg/larvae, and were injected with bacteria and/or peptides on its last proleg using a BD insulin syringe. The dosage used for the experiment were 60 mg/kg for peptides, 5mg/kg of geldanamycin and 20mg/kg for vancomycin. Each larvae were injected with 10μl of L15 (last left proleg) 1h before administration of $1-5 \times 10^6$ cfu *S. aureus* (last right proleg). The larvae were maintained at 37 °C and observed for its

mortality every day for the study period of 5 days. For *E.coli* K12 and *P. aeruginosa* PA01, the MOI used was 10^6 cfu/larvae and 10^2 cfu/larvae respectively (Zheng *et al.*, 2017, Brochado *et al.*, 2018). The larvae were injected with 10 μ l of L15/L13/geldanamycin 1 h before inoculating *S.aureus* USA300/ Newman/ HG001 into its hemocoel. The larvae were then checked for its mortality for 5 days.

Larvae were injected with different concentrations of (Fig. 3.5A) L15 and (Fig. 3.5B) L13 to find the optimum dosage against USA300 infection. From the results, the optimum dosage was decided as 60mg/kg. Fig. 3.5C shows the larvae infected by *S. aureus* USA300. All infected untreated larvae died by the end of 3rd day. On day 5, L15 could rescue 30% and L13 could rescue 23.33 % of the larvae. Geldanamycin was unsuccessful in saving larvae from infection (they all died by 3rd day). Vancomycin rescued 100% of the larvae and was used as a positive control.

Similar results were obtained for *S. aureus* HG001 infection (data not shown). The percentage larvae alive on 5th day for L15 and L13 were 33.33 and 26.67 % respectively. All infected untreated larvae died by the end of 3rd day. L15 and L13 showed higher rescuing activity for larvae when infected with *S. aureus* Newman (Fig. 3.5D). L15 was able to save 36.67 % of larvae whereas L13 saved 46.67%. The tested doses of peptides, geldanamycin and vancomycin were non-toxic to larvae.

We also tested whether L15 or L13 could affect the pathogenicity of *S. aureus*. A simple disc diffusion assay was done, where *S. aureus* added to pre-impregnated L15 or L13 discs were incubated on sheep blood agar plate overnight at 37°C. The pathogenicity was correlated with the haemolytic activity of the bacteria and the halo formed on the plate was measured and compared with the control. The result suggested that the expression of α -haemolysin or the pathogenicity remained unaffected in *S. aureus* on treatment with L15 and L13 (Fig. 3.6).

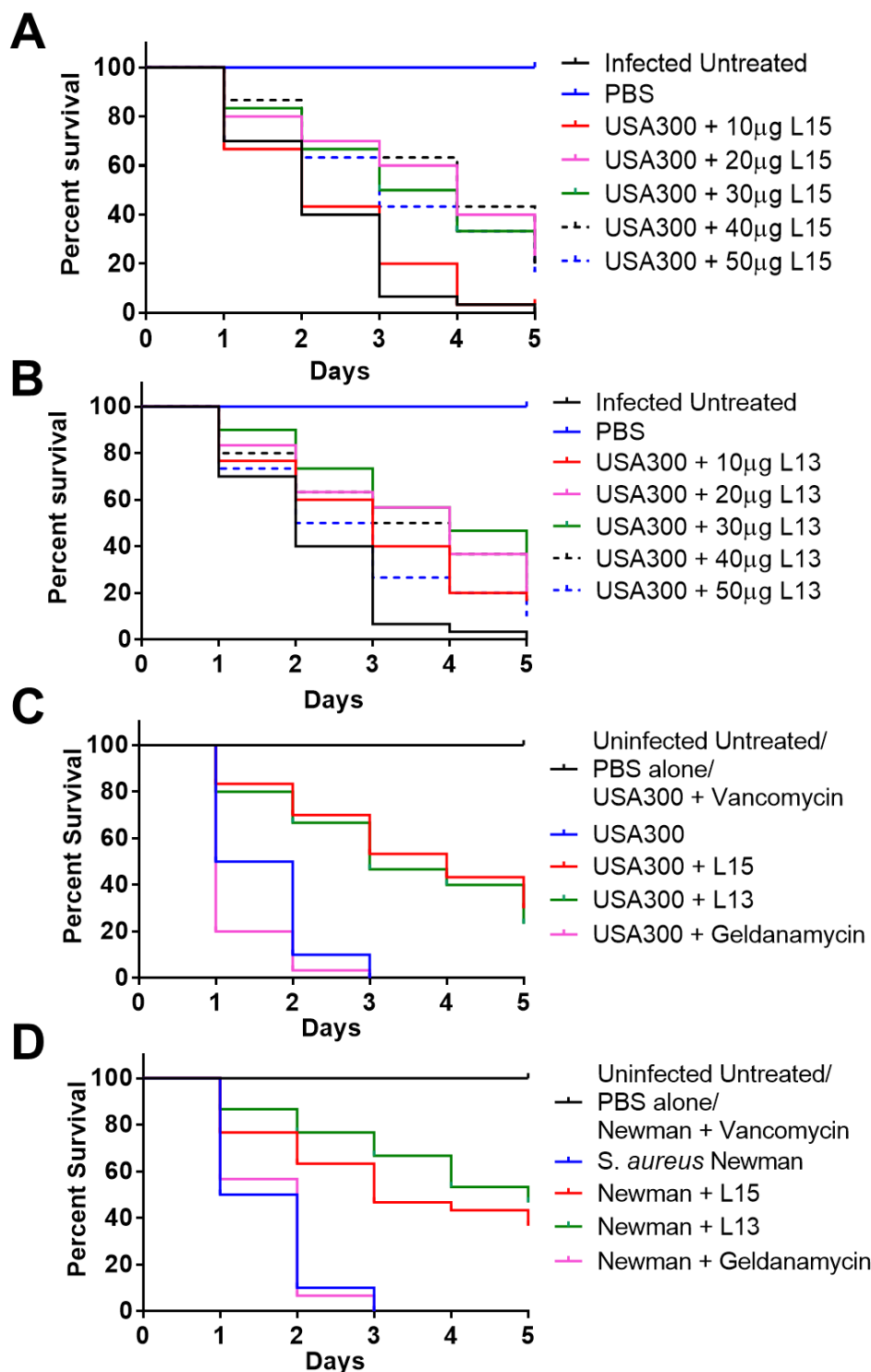


Figure 3.5. L15/L13 rescues larvae from *S.aureus* infection. Each group consists of 10 larvae with weight average of 500mg/larvae, and were administered with bacteria and/or peptides on its last proleg using a BD insulin syringe. Larvae were injected with different concentrations of (A) L15 and (B) L13 to find the optimum dosage against USA300 infection. Each larvae were injected with 10 μ l of L15 (last left proleg) 1h before injection of 10⁶ cfu *S. aureus* (last right proleg) (C) USA300 and (D) Newman. The larvae were maintained at 37 °C and checked for its mortality every day for the study period of 5 days. Total of 3 biological replicates are represented in the graph.

Mice studies

To study the effect of L15 treatment on *S. aureus* systemic infection, NMRI mice infected with *S. aureus* Newman were treated with L15 (10 mg/kg) and clinical outcomes were monitored during the course of disease. Mice infected with *S. aureus* started to lose weight after infection. The mice treated with L15 had significant better weight development during the whole course of infection compared with the control mice who received PBS or distilled water (Fig. 3.7A). No significant difference was found regarding the bacterial load in kidneys (Fig. 3.7B). Regarding the mortality rate, forty percent of animals in the control group died, whereas all mice treated with L15 survived during 7 days of observation time (Fig. 3.7C), suggesting that L15 treatment prevents the lethal *S. aureus* bacteremia.

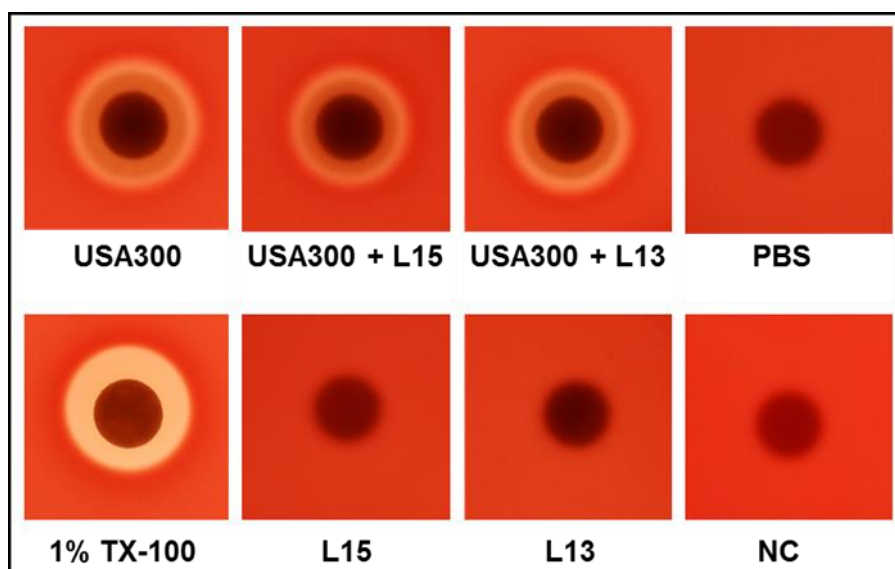


Figure 3.6. L13, L15 doesn't affect the hemolysin activity of USA300

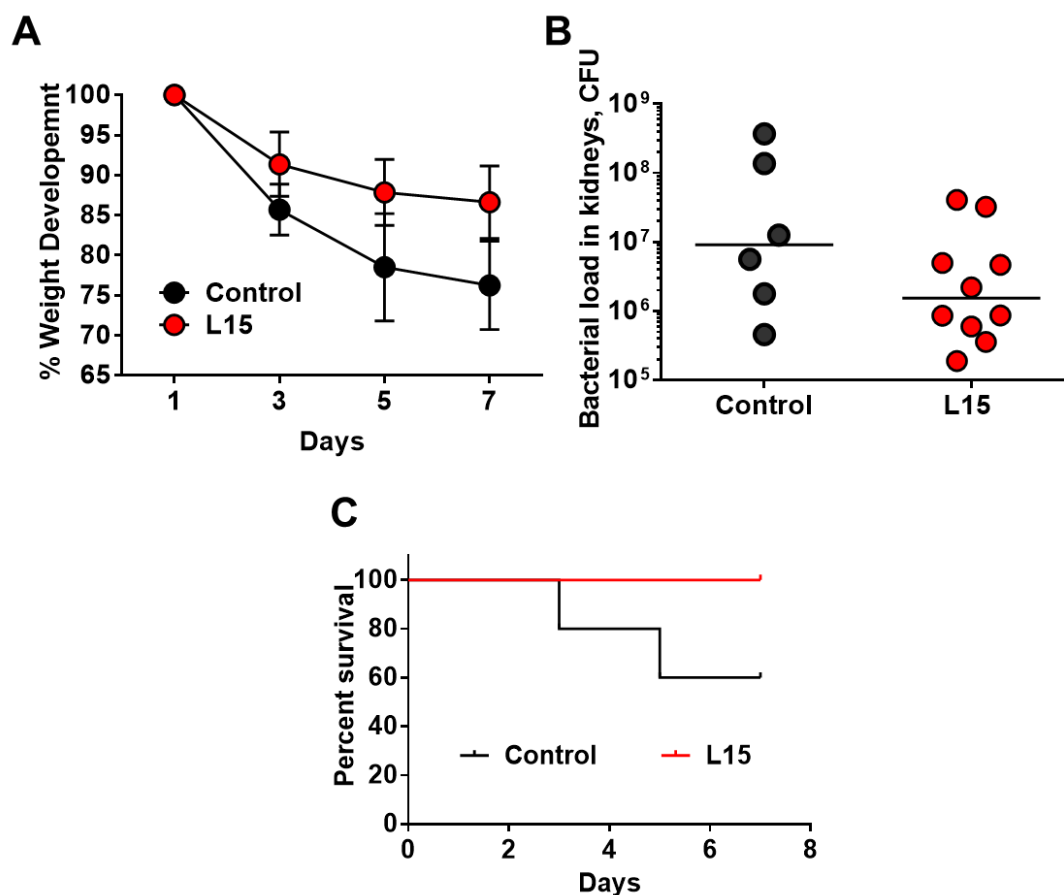


Figure 3.7. L15 treatment reduces systemic *S. aureus* infection. NMRI mice infected intravenously with *S. aureus* Newman strain (2×10^6 CFU/mouse) were treated with L15 intraperitoneally (10mg/kg) or PBS for control starting two hours before inoculation and continuing twice daily until animals were euthanized on day 7. (A) Weight development observed during 7 days. (B) Bacterial load in kidneys on day 7 post-infection. (C) Survival graph of mice infected with *S. aureus*.

Multiple sequence alignment

The homologs of *S. aureus* USA300 Lpl1 in different bacteria were identified using the Protein BLAST from NCBI database. The comparison of different Lpl (Lpl1-9) in *S. aureus* and the lipoprotein homologs from different bacteria were done in Snap gene using Clustal Omega algorithm.

The homolog identification of Lpl1 in USA300 using Protein BLAST revealed lipoproteins in different bacteria with high similarity (Fig. 3.8). Lipoproteins from *Staphylococcus hyicus*, *Staphylococcus schweitzeri* and *Staphylococcus argenteus* showed a percentage identity of 88.64, 97.75 and 88.72 respectively. The corresponding L15 and L13 homolog sequences in these lipoproteins were exactly

similar. *Listeria monocytogenes* had a lipoprotein with sequence similarity of 80.49% with that of Lp1, whereas the same was 74.62 % for *Lactobacillus ruminis*. *Escherichia coli*, *Klebsiella pneumoniae* and *Pseudomonas aeruginosa* also exhibited highly similar lipoprotein with percentage sequence similarity of 75.76, 90.51 and 85.05 respectively. The corresponding L15 homolog of *Pseudomonas aeruginosa* was exactly similar to L15 of *S. aureus*.

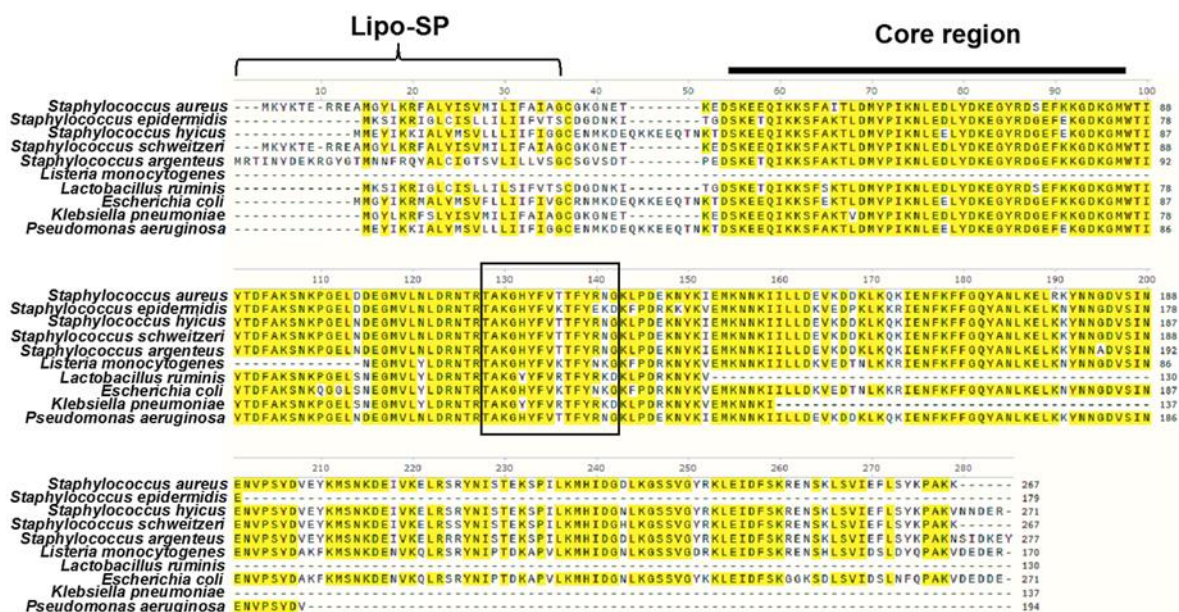


Figure 3.8. Multiple sequence alignments of Lp1 from *S. aureus* USA300 with other bacteria. These include *Staphylococcus epidermidis* SE62, *Staphylococcus hyicus* NCTC 8294, *Staphylococcus schweitzeri* NCTC 13712, *Staphylococcus argenteus* B3-25B, *Listeria monocytogenes* ATCC 15313, *Ligilactobacillus ruminis* ATCC 27780, *Escherichia coli* NCTC 9001, *Klebsiella pneumoniae* NCTC 9633 and *Pseudomonas aeruginosa* PA216. The lipoprotein signal peptide is indicated by the bracket, the conserved core region by the bar and the L15 sequence is boxed.

All the 9 Lpls in USA300 shared highly similar core region, but the corresponding L15 sequences were not so similar (Fig. 3.9). Lp12, Lp14 and Lp17 showed more similarity to Lp1 with a percentage identity of 76%.

It should also be noted that the trypsin digestion of Lp1 (by ExPASy PeptideCutter tool) does not yield L13 or L15 (Gasteiger *et al.*, 2005). The peptides to our knowledge, do not inhibit the growth of bacteria, do not selectively affect any metabolic pathways in the latter and therefore might have a lower chance of resistance development.

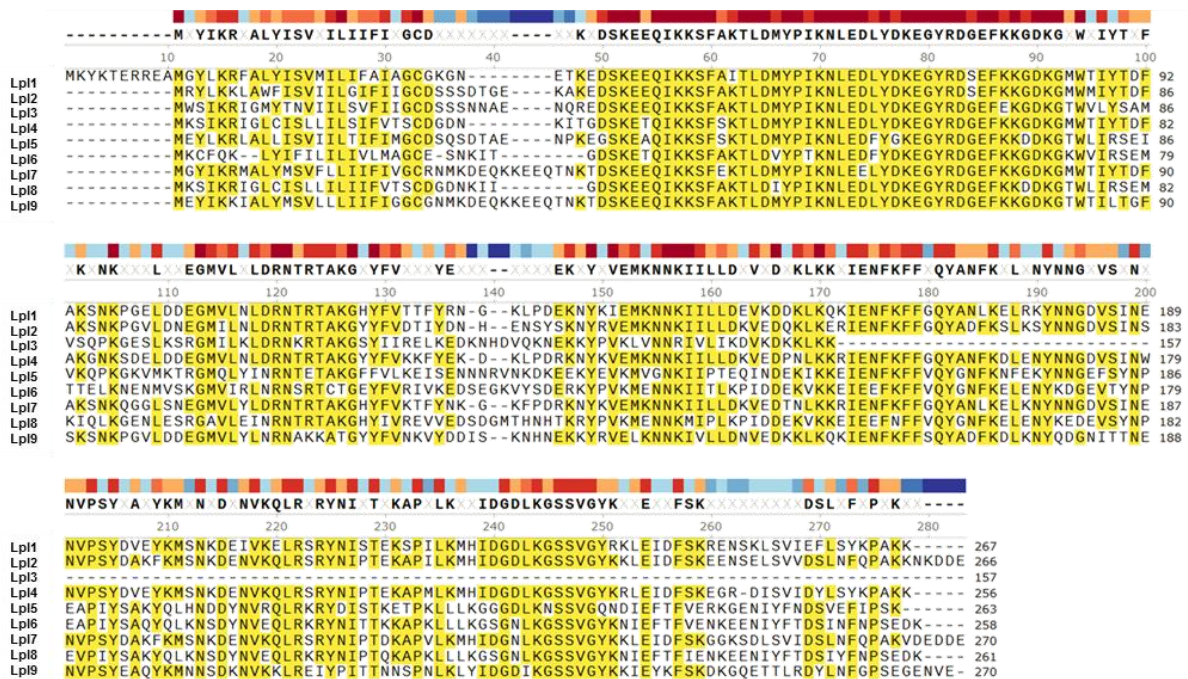


Figure 3.9. Multiple sequence alignments of Lp11 – Lp19.

L15/L13 couldn't rescue larvae from *E.coli* and *P. aeruginosa* infection

The sequence similarity of Lipoproteins in *E.coli* and *P. aeruginosa* prompted us to check whether L15 had any protective effect in infections caused by these pathogens. Unfortunately, the peptides failed to rescue the larvae from infective death.

Each larvae were infected with, 10^6 cfu of *E.coli* K12 after pre-treatment with $10\mu\text{l}$ of the peptides. L15 and L13 were not able to rescue the larvae from *E.coli* K12 infection (Fig. 10A). *E.coli* infection alone killed all the larvae by 5th day, whereas the larvae treated with L15 and L13 died by 4th and 3rd day respectively.

Similar protocol was followed for *P. aeruginosa* PA01 infection. 10^2 cfu of *P. aeruginosa* PA01 was injected into the larvae coelom preceded by L15/L13 injection. PA01 infected larvae died by 4th day whereas those pre-treated with L15 and L13 died on the 3rd day. L15 and L13 were unsuccessful in rescuing of Larvae from *P. aeruginosa* infection (Fig. 3.10B). This suggests that the peptides L13 and L15 have a narrow spectrum of activity and it can be used specifically against *S.aureus* strains.

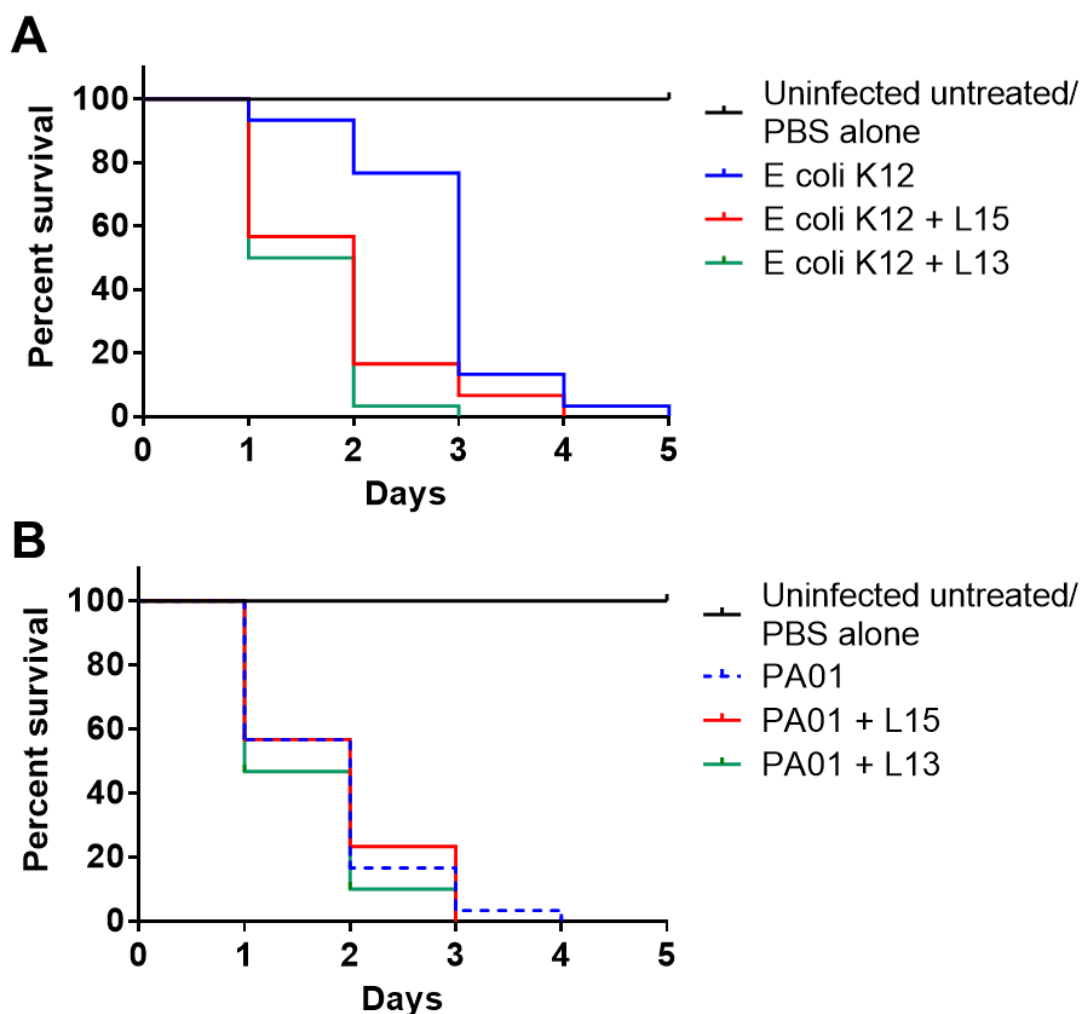


Figure 3.10. L15/L13 couldn't rescue larvae from (A) *E. coli* K12 and (B) *P. aeruginosa* PA01 infection. Ten *Galleria mellonella* larvae per group with weight average of 500mg/larvae were injected with bacteria and/or peptides on its last proleg using a BD insulin syringe. Each larvae were injected with 10 μ l of L15 (last left proleg) 1h before administration of bacteria. The larvae were maintained at 37 °C and observed for its mortality every day for the study period of 5 days. Total of 3 biological replicates are represented in the graph.

L15 didn't cause any immune stimulation in human PBMCs

Since L15 showed good results in mice model, we tested the immune stimulation activity of L15 in human PBMCs. Here, the buffy coat blood samples from healthy individuals (attained from Transfusion Blood Bank of the Medical Clinic Tübingen) were stimulated with L15 peptides to induce IL-6, IL-12p70, IL-23, and TNF α , IL-1 β , IL-1RA, and IP-12 for 20h. The secreted cytokines were then measured using the immunofluorescent bead-based immunoassay LEGENDplex® Human Macrophage/Microglia Panel (13-plex) and Data Analysis Software from BioLegend.

L15 was relatively inert with respect to cytokine inducing activity in PBMCs (Figure 3.11). Muramyl Dipeptide (MDP) which stimulates the NOD-2 receptors was employed as the positive control.

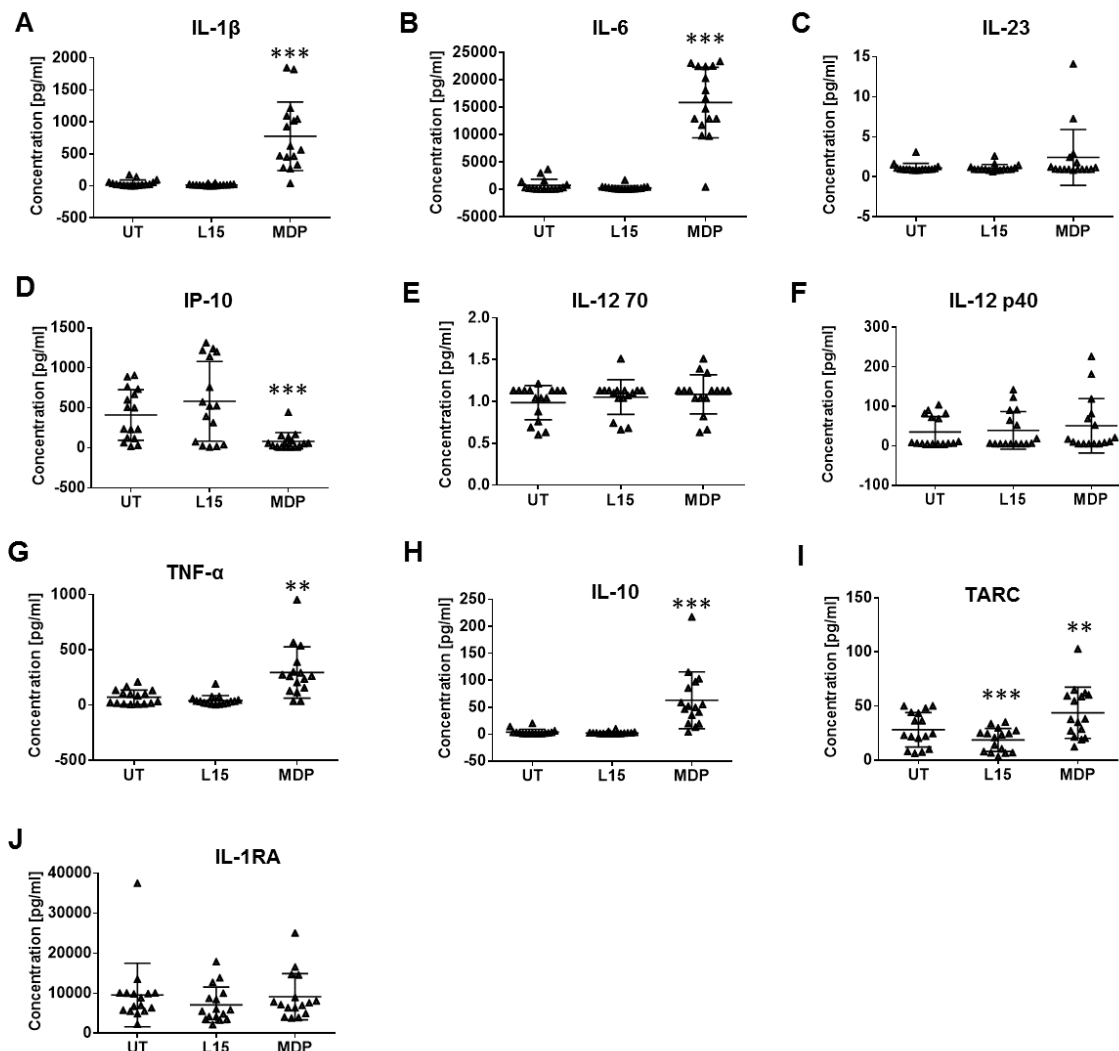


Figure 3.11. Cytokine quantification of PBMCs stimulated by L15, showed that the L15 didn't cause any immune stimulation at the tested concentration. Statistic significances were calculated between the peptide treated cells compared to control by using one-way ANOVA analysis with Tukey's multiple comparison test: *p < 0.05, **p < 0.01, ***p < 0.001, ns > 0.05.

Pretreatment with L15 and L13 reduced the phagocytosis of USA300 in CD14⁺ monocytes

Similarly like the keratinocytes, L15 and L13 could also reduce the phagocytosis of USA300 into monocytic cells (Figure 3.12A). The relative phagocytosed USA300 count

in monocytic cells were 0.77 ± 0.08 for L15, 0.38 ± 0.07 for L13 and 0.86 ± 0.17 for geldanamycin as compared to the untreated control (1.00 ± 0.0). Geldanamycin didn't significantly affect the phagocytosis of USA300 into the host cells (p value = 0.2).

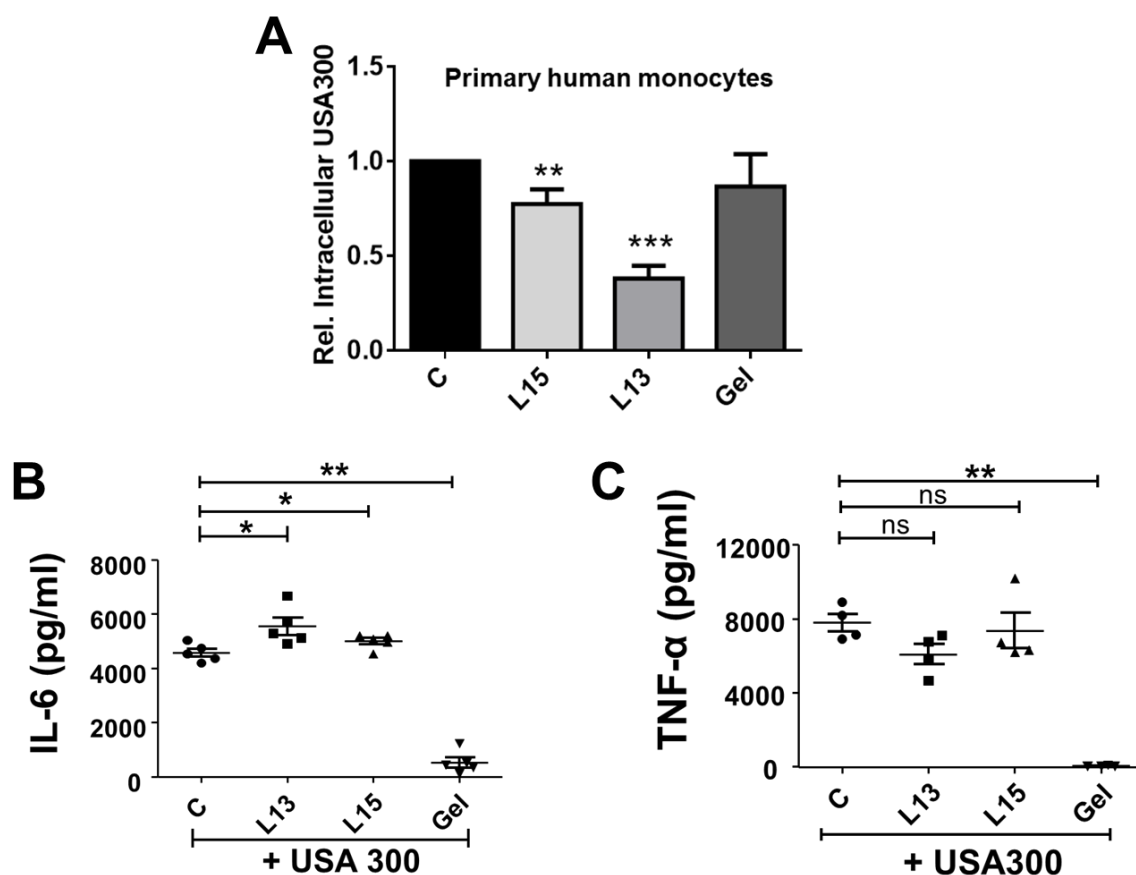


Figure 3.12. (A) Effect of L15 and L13 on *S. aureus* USA300 phagocytosis by primary human CD14⁺ monocytes. Influence of L13 and L15 on the response of host innate immune cells were tested. Release of (B) IL-6 and (C) TNF- α in the supernatant of *S. aureus*-infected PBMCs was assayed by ELISA 20 h after stimulation with L13 or L15 or geldanamycin. C indicates control cells without peptide pretreatment. Samples from 4 donors were carried out in triplicate. Samples from 4 donors were carried out in duplicate. Error bars represent SEM. Statistic significances were calculated between the peptide treated cells compared to control by using one-way ANOVA analysis with Tukey's multiple comparison test: * $p < 0.05$, ** $p < 0.01$, *** $p < 0.001$, ns > 0.05 .

The peptides effect the IL-6 immune response of PBMCs to *S.aureus* but not TNF- α response

We stimulated the PBMCs of 5 healthy donors with USA300 in combination with/without peptides. Both the peptides were able to significantly bring up the IL-6 cytokine production in PBMCs, but not TNF α production. Geldanamycin inhibited both IL-6 and TNF α release in infected PBMCs (Figure 3.12B, C).

L15 and L13 in combination with different TLR stimulants couldn't rescue larvae from USA300 infection

L15 and L13 was injected in combination with different TLR ligands in *S. aureus* infected larvae to see if their protective effect can be enhanced with the ligands. The ligands used were Muramyl di-peptide or MDP – ligand for TLR2/TLR4, Class A CpG oligonucleotide or CpG ligand for TLR9 and ssRNA for TLR7. Unfortunately, the combination treatment could not enhance the protective effect of L5 and L13 (Figure 3.13).

How the peptides rescue the larvae and mice from infection is not completely clear. It may be the case that the peptides are competing with the Lpl proteins on the surface of *S. aureus* for binding to the Hsp90 receptor. This could cause an indirect neutralization of the Lpl proteins, and in turn reduced pathogenicity. This is in consistence with our earlier data showing that deletion of the *lpl* genes markedly reduced the pathogenicity of *S. aureus* in a mouse kidney abscess model (Nguyen et al., 2015).

In summary, we have identified small peptides L15 and L13 that have huge potential against *S. aureus* infection which we have proved using *in vivo* models of *Galleria mellonella* and mice. *In vitro* studies indicated the peptides reduced invasion of *S. aureus* into keratinocytes by reducing the F-actin levels and possibly thereby reducing the endocytosis of the said bacteria. Future works will focus on understanding the mechanism of how these peptides protect the host from *S. aureus* infection.

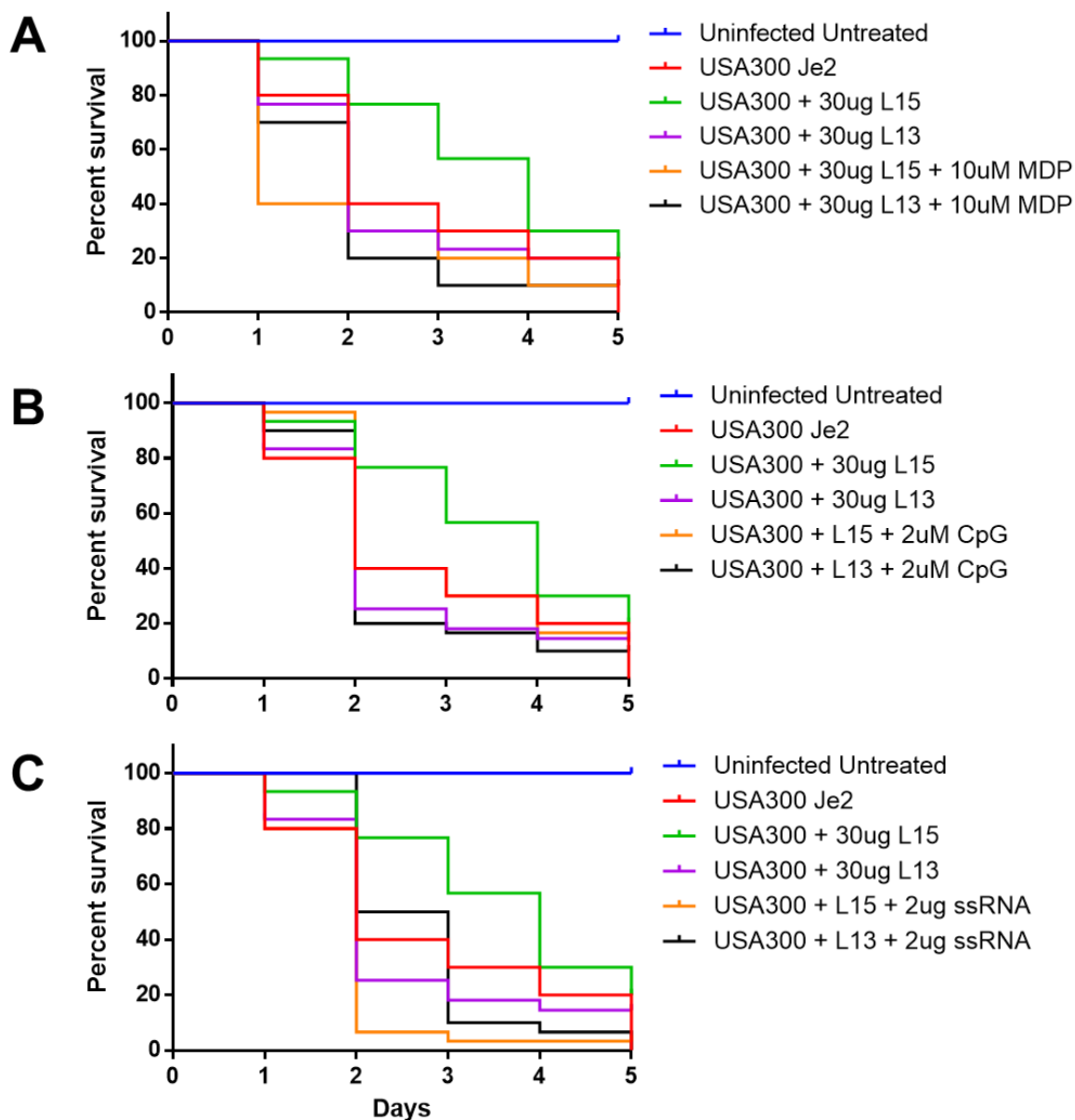


Figure 3.13. L15/L13 in combination with different TLR ligands (A) MDP, (B) CpG and (C) ssRNA couldn't rescue larvae from *S. aureus* infection. Ten *Galleria mellonella* larvae per group with weight average of 500mg/larvae were injected with bacteria and/or peptides on its last proleg using a BD insulin syringe. Each larva was injected with 10 μ l of L15 (last left proleg) 1h before administration of bacteria. The larvae were maintained at 37 °C and observed for its mortality every day for the study period of 5 days. Total of 3 biological replicates are represented in the graph.

Studies on Rhodomycortone

Potassium derivative of Rom, FH-54, is active against Rom resistant *S.aureus*

The MIC values of *S.aureus* HG001 and Rom^R strain against different Rom derivatives are listed in Table 2. The IC₅₀ values of the most promising Rom derivatives in HL60 cell lines were also determined by MTT assay. A derivative of Rom, called FH-54 was found to be active against even the Rom^R strain with MIC of 1 µg/mL. FH-54 was also found to be less cytotoxic to HL60 cell lines as compared to Rom.

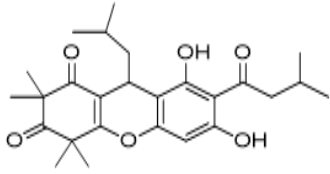
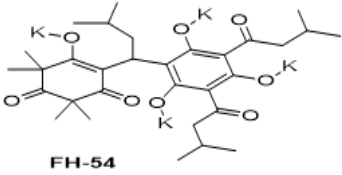
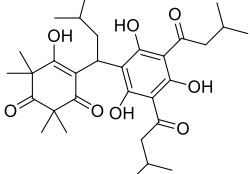
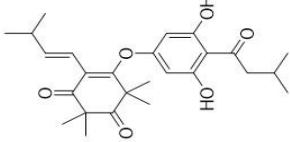
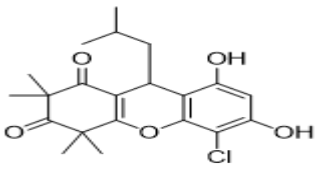
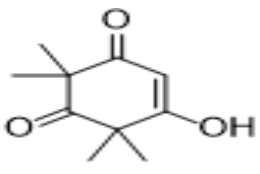
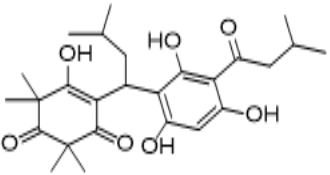
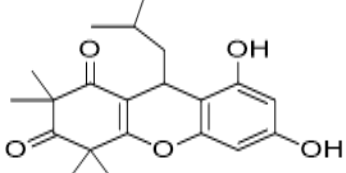
Rom resistance is facilitated by contact of PG with Rom, which nullifies its antibacterial activity

The deletion of *farE* in both wt HG001 and Rom^R made them supersensitive to Rom. The MIC of Rom in HG001 reduced to half (1 to 0.5 µg/ml) upon *farE* deletion, whereas the MIC went from >128 to 0.5 µg/ml in Rom^R strain after the same deletion. This gives us proof that *farE* is important for resistance in Rom^R strains.

Rom's antimicrobial activity could be neutralized by 2X concentrated Rom^R supernatant and 20X concentrated HG001 supernatant. This advocates that the elements causing Rom resistance are the present in both the parental strain and the Rom^R mutant but in different concentrations. This prompted us to conduct a lipidomic analysis on the supernatant and pellet wash of HG001 and Rom^R strain. The Rom^R strain released more PG and Lysl-PG as compared to HG001. The total amount of PG in supernatant of HG001 was 268 ng/OD and in Rom^R was 2244 ng/OD. Rom^R released more than 7 times Lysl-PG in comparison to HG001 (HG001: 268 ng/OD and Rom^R: 2244 ng/OD).

The deletion of *mprF* in Rom^R strain, didn't change its resistance towards Rom, disproving the hypothesis that *mprF* had any effect on Rom resistance. SLS/DLS experiment showed that Rom interacts with PG vesicles leading to an increase in the vesicle diameter (diameter changed from 100 nm to 200 nm). ITC studies revealed that the interaction of Rom and PG happens really fast with an enthalpy change (ΔH) of 6.10 kcal/mol, equilibrium binding constant of 2.30 ± 0.747 and a favorable (negative) entropy change. Moreover, resistance towards rom didn't cause any cross-resistance to known antibiotics.

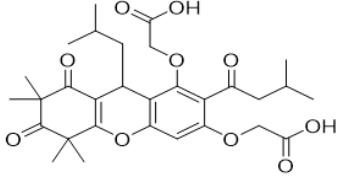
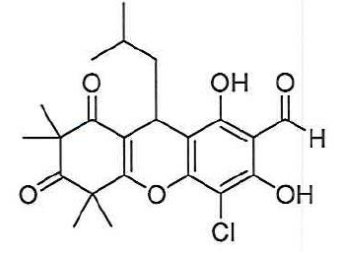
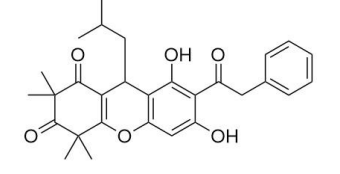
Table 2. MIC values of Rom and its derivatives towards *S.aureus* HG001 and its Rom^R strain.

Compounds	Structure	MIC ($\mu\text{g/mL}$)	
		HG001	Rom ^R
Rom HL60 IC ₅₀ (mg/ml) = 5		1	>64
FH-54 HL60 IC ₅₀ (mg/ml) = 44	 FH-54	1	1
2-152 HL60 IC ₅₀ (mg/ml) = 31		0.5	8
2-171 HL60 IC ₅₀ (mg/ml) = 4		0.5	1
MU_118		4	2-4
2-26 (Syncarpic acid)		> 32	> 32
2-27		16	64
2-151		16	16

Compounds	Structure	MIC ($\mu\text{g/mL}$)	
		HG001	Rom ^R
2-153		32	32
2-162 (Leptospermone)		>32	>32
2-175		>32	>32
2-181		>32	>32
2-182		>32	>32
2-185		>32	>32
2-187		>32	>32
2-189		>32	>32

Compounds	Structure	MIC ($\mu\text{g/mL}$)	
		HG001	Rom ^R
2-212		>32	>32
SR_01		>64	>64
MU_08_N1		64	>64
MU_08_N2		>64	>64
MU_15		2	>64
MU_19		16	>64
MU_20		32	32
MU_25		32	32

Compounds	Structure	MIC ($\mu\text{g/mL}$)	
		HG001	Rom ^R
MU_35		>64	>64
MU_77		>64	>64
MU_81		>64	>64
MU_96		8	>64
MU_98		8	>64
MU_99		>64	>64
MU_118 NP		16-32	16
MU_124		>64	>64

Compounds	Structure	MIC ($\mu\text{g/mL}$)	
		HG001	Rom ^R
MU_126		>64	>64
MU_124		>64	>64
MU_141		1	4

Rom is active against pathogenic Gram-positive gut anaerobes

The human gut harbors tons of microbes including bacteria, fungi, protozoa, and viruses, collectively known as the gut microbiota. These gut microbiota has established a symbiotic relationship with the host and help the host in metabolism, immune response and homeostasis as well as protection from pathogens. A dysbiosis or imbalance in the gut microbiota environment can cause esophageal or colorectal cancer, colitis and other gut disorders. Strategies to treat gut dysbiosis include fecal microbiota transplant, probiotics or a dietary intervention. Several studies show the potential of phytochemicals in improving this gut microbiota imbalance by selectively killing the pathogenic gut anaerobes and being harmless towards the commensal ones.

We tested the activity of Rom against different gut anaerobes. The MIC values of Rom against different anaerobic strains was done in collaboration with Dr. Lisa Maier from Universitätsklinikum Tübingen, an expert in anaerobic gut microbe research (Table 2). Rom was found to be very active against pathogenic gram positive gut anaerobe *Clostridium difficile* and *Clostridium perfringens* and 2 of the commensal gut anaerobes

Streptococcus parasanguinis and *Bifidobacterium adolescentis*. Rom was inactive against pathogenic gram negative bacteria. Rom was also inactive or very less active against most of the commensal gut anaerobes tested, suggesting its potential as a dietary supplement against gut dysbiosis.

Table 3. MIC of Rom against anaerobic microorganisms

	Strains	Rom MIC (μM)
Pathogenic G +ve gut anaerobe	<i>Clostridium difficile</i>	4
	<i>Clostridium perfringens</i>	4
Commensal gut anaerobe	<i>Streptococcus salivarius</i>	<2
	<i>Dorea formicigenerans</i>	22
	<i>Streptococcus parasanguinis</i>	4
	<i>Ruminococcus gnavus</i>	22
	<i>Clostridium ramosum</i>	22
	<i>Blautia obeum</i>	22
	<i>Roseburia intestinalis</i>	22
	<i>Coprococcus comes</i>	22
	<i>Collinsella aerofaciens</i>	22
	<i>Bifidobacterium adolescentis</i>	4
	<i>Parabacteroides distasonis</i>	>45
	<i>Eubacterium rectale</i>	>45
	<i>Lactobacillus paracasei</i>	22
	<i>Clostridium bolteae</i>	>45
	<i>Parabacteroides merdae</i>	22
	<i>Bifidobacterium longum</i> subsp. Longum	>45
	<i>Clostridium saccharolyticum</i>	>45
	<i>Prevotella copri</i>	>45
<i>Odoribacter splanchnicus</i>	>45	
<i>Fusobacterium nucleatum</i> subsp. Nucleatum	>45	
<i>Bilophila wadsworthia</i>	>45	

	<i>Bacteroides vulgatus</i>	>45
	<i>Bacteroides uniformis</i>	>45
	<i>Bacteroides thetaiotaomicron</i>	>45
	<i>Bacteroides fragilis</i> NT	>45
Pathogenic G -ve gut anaerobe	<i>Salmonella enterica</i> typhimurium ToIC	>45
	<i>Yersinia pseudotuberculosis</i>	>45
	<i>Yersinia enterocolitica</i> WA-314	>22
	<i>Vibrio cholerae</i>	>22
	<i>Shigella sonnei</i> 53G	>45
	<i>Shigella flexneri</i>	>45
	<i>Salmonella enterica</i> typhimurium LT2	>45
	<i>Salmonella enterica</i> typhimurium	>45
	<i>Escherichia coli</i> UTI89	>45

Studies on PPAP23 and PPAP53

Synthesis of the sodium salt of PPAP 22, named PPAP 53, has improved solubility

In this paper, we have mainly focused on the activities of PPAP 23, 22 and 53. PPAP 53 is the sodium salt of the newly synthesized PPAP 22. The structures of the three compounds are shown in Figure. 3.14. The difference between PPAP 23 and 22 is that in R2 and R2' of PPAP 23 there are prenyl-residues while in PPAP 22 there are allyl-residues (Guttruff *et al.*, 2017). We thought that the allyl residues in PPAP 22 would increase the solubility a little bit, however, the solubility of PPAP 22 was still comparatively low. Among the tested solvents in which PPAP 22 (5 mg/ml) was soluble were 100% DMSO, 100% ethanol, 80% methanol, 8.2% cyclodextrin/18% DMSO in PBS, and 0.4% Tween 80 / 18% DMSO in PBS. While too high concentrations of DMSO, ethanol and methanol, and beta-cyclodextrin are cytotoxic we have chosen 0.4% Tween 80 / 18% DMSO in PBS as a solvent. To increase the solubility of PPAP 22 its Na-salt, PPAP 53, was synthesized. Comparative *in vitro* determination of MIC values showed that the MIC of PPAP 22 and PPAP 53 was essentially the same for

the multidrug-resistant *S. aureus* USA300, namely $\sim 2 \mu\text{g/ml}$. For this reason, we used either PPAP 23 or PPAP 53 in our studies. We then moved from *in vitro* studies to *in vivo* studies.

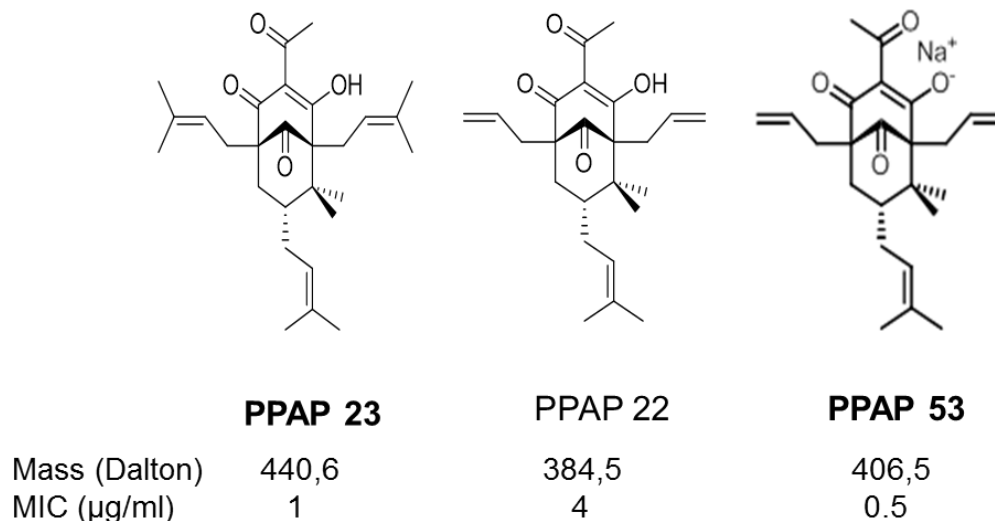


Figure 3.14. Structures of PPAP 23, 22 and 53 used in this work. The PPAPs have similar MIC values (1 to $2 \mu\text{g/ml}$) for the multi resistant *S. aureus* USA300. PPAP 53 is the Na salt of PPAP 22 and is therefore more water soluble. PPAP 23 was dissolved in DMSO.

PPAP 22 and PPAP 53 had no adverse effect on larvae but could not rescue larvae in an infection model

With PPAP 22 and PPAP 53 we carried out a *Galleria mellonella* larvae infection assays with *S. aureus* USA300. The used dose was 10 to 100 x MIC (20 mg/kg to 200 mg/kg). Without USA300, all larvae survived indicating that PPAP 23 and 53 are well-tolerated at this dose (Figure. 3.15A, B). However, if the larvae were infected with USA300 (10^6 CFU), all larvae died after about 3 days when treated with PPAP 23 (Figure. 3.15. A), and they also couldn't be rescued with the water-soluble PPAP 53 at a dose of 20 mg/kg (50 μM) (Figure. 3.15B). As a control we also tested vancomycin (Van) at a comparable dose 20 mg/kg Van (13 μM). Van could fully protect the USA300 infected larvae (Figure. 3.15C). Since *in vitro* PPAP 23 and PPAP 53 showed comparable good antimicrobial activity, the question arose why in the infection model the PPAPs were not effective.

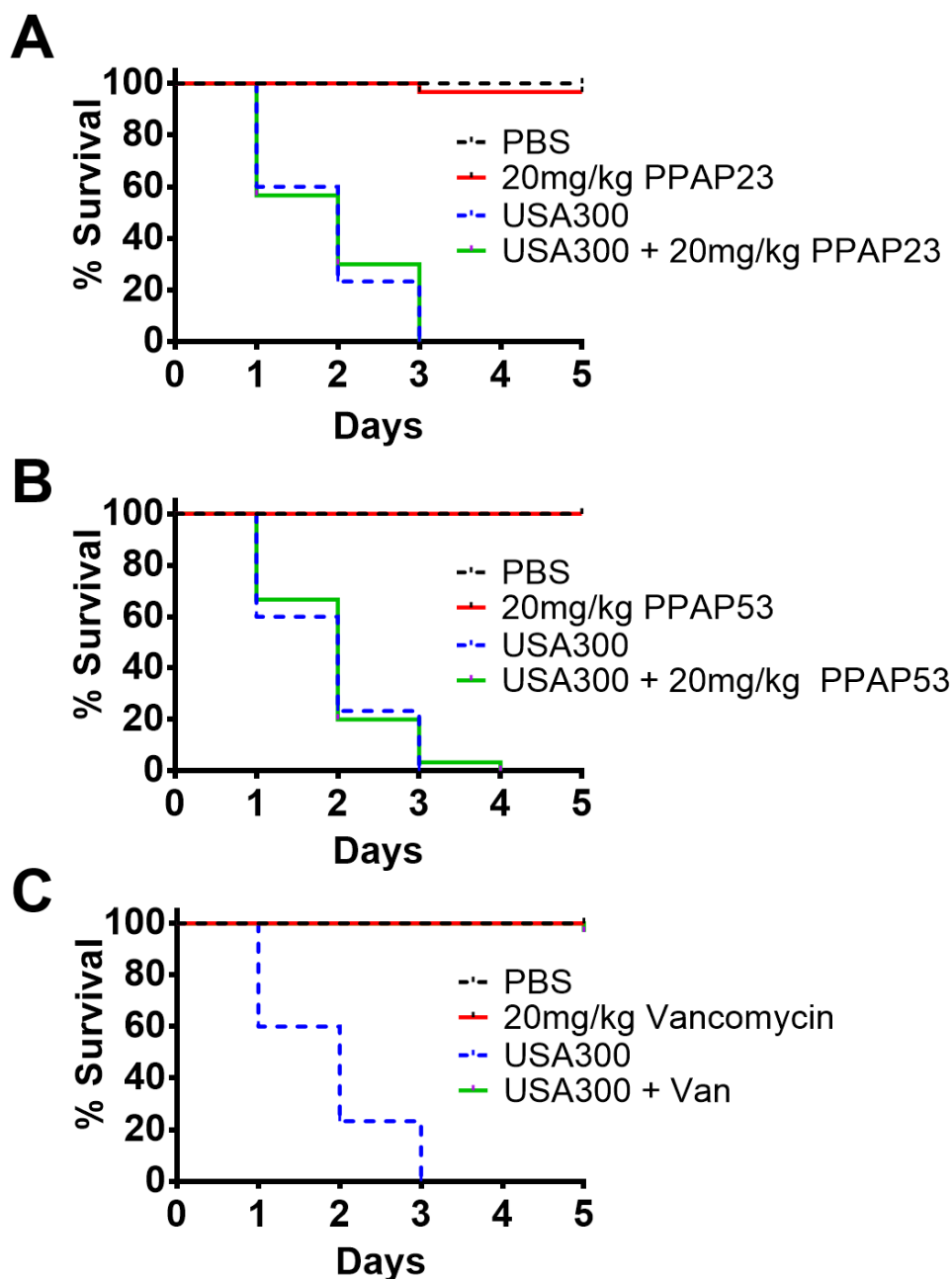


Figure 3.15. PPAP 23 and PPAP 53 are non-toxic to larvae, but failed to protect larvae from infection with *S. aureus* USA300. Ten *Galleria mellonella* larvae per group, with weight average of 500 mg/larvae, were either non-treated, injected with 10^6 colony forming units (cfu) *S. aureus* USA300 (last right proleg). 1 h after administration of bacteria larvae were treated with 20 mg/kg (45 μ M) PPAP 23 (**A**), or 20 mg/kg (50 μ M) PPAP 53 (**B**), or vancomycin (**C**) at a comparable dose (20 mg/kg, 13 μ M). Infected larvae without treatment were normally killed by *S. aureus* after 3 days. The larvae were maintained at 37 °C and observed for mortality every day over the course of 5 days. A total of three biological replicates are represented in the graph.

PPAP 23 showed a beneficial but not full protective effect on *S. aureus* septic arthritis mouse model

Since larval and mammalian models do not always give the same results, we investigated whether PPAP 23 has an effect in the mouse model of septic arthritis caused by *S. aureus* Newman. PPAP 23 was administered at a dose of 100 µg PPAP 23/mouse twice daily starting on day 2 after infection with *S. aureus*. Signs of septic arthritis appeared on day 2 post infection and continued to worsen through day 7. The clinical severity of septic arthritis was similar in PPAP 23-treated mice compared with control mice (Figure. 3.16A). Percent weight loss is a useful parameter for monitoring the severity of systemic staphylococcal infections. Mice treated with either vehicle (0.5% Tween 80 in PBS) or PPAP23 lost up to 25% of their body weight during the experimental period (Figure. 3.16B). No significant difference was observed between the PPAP23 group and controls. Interestingly, however, there were macroscopically more abscesses in the kidneys of mice receiving vehicle compared with PPAP 23-treated mice ($P < 0.05$; Figure. 3.16C). The abscess score and the actual bacterial load in the kidneys were significantly correlated ($r=0.95$; $P<0.001$), and control mice had >25-fold higher bacterial load in the kidneys than PPAP 23-treated mice ($P<0.05$; Figure. 3.16D). This suggests that PPAP 23 treatment had a beneficial effect on bacterial clearance in septic arthritis caused by *S. aureus*.

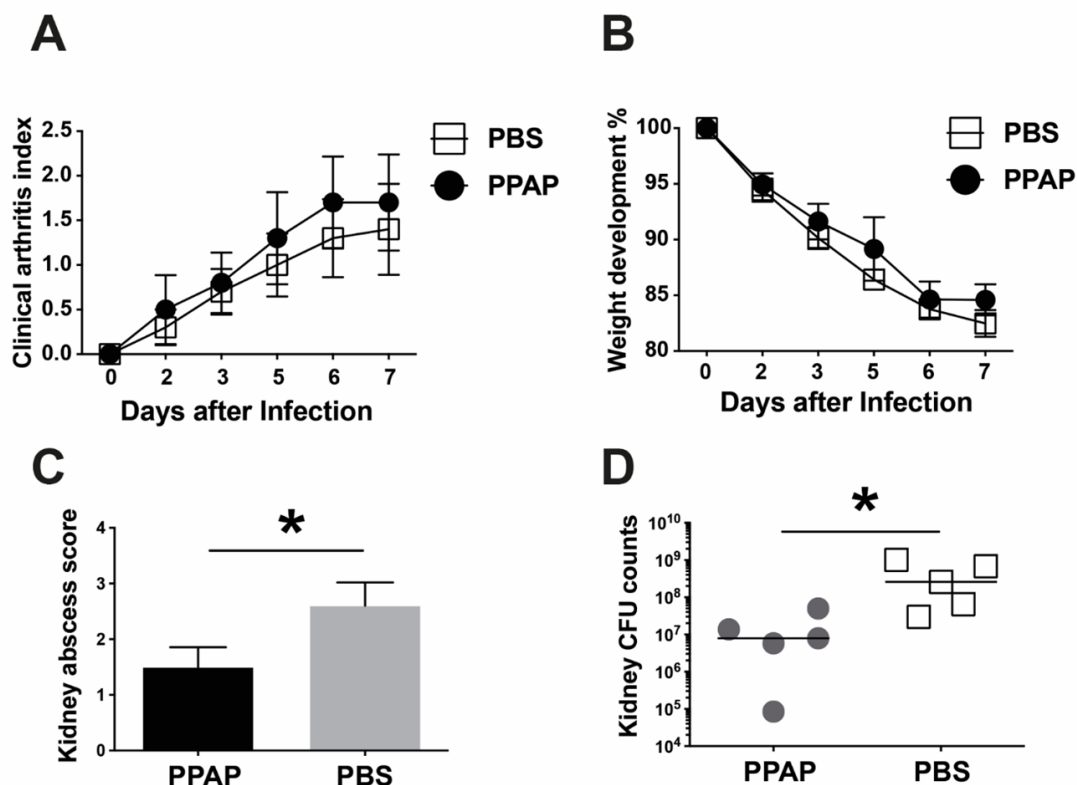


Figure 3.16. PPAP 23 treatment significantly reduced the abscess formation and bacterial load in kidneys in mice with *S. aureus* septic arthritis. NMRI mice inoculated with *S. aureus* Newman strain (4×10^6 colony-forming units/mouse) were treated with PPAP 23 dissolved in 0.5% tween 80 in PBS (100 μ g/mouse; $n = 5$) or same volume of 0.5% tween 80 in PBS ($n = 5$) twice a day starting on day 2 after inoculation with bacteria and continuing until the animals were euthanized on day 7. The severity of clinical arthritis (A) and the body weight development (B) in the mice were observed for 7 days after infection. Kidney abscess scores (C) and persistence of *S. aureus* in kidneys (D) from the mice euthanized 7 days after infection. Statistical evaluations were performed using the Mann–Whitney U test. Data are mean values \pm standard error of the mean. * $P < 0.05$.

The coelomic fluid of the larvae antagonized the activity of PPAP 53

We suspected that coelomic fluid abrogated the effect of PPAPs. Therefore, we examined the effect of coelomic fluid on PPAP 53 activity *in vitro*. To mimic the *in vivo* larval experiment, 100 μ l of filter-sterile coelomic fluid of larvae was incubated overnight with 20 mg/kg PPAP 53 and 10^6 CFU/ml *S. aureus* USA300. As a control, PBS was incubated with PPAP 53 and USA300. While PPAP 53 alone was able to kill *S. aureus* by 3 logs after 24 hours, PPAP 53 failed to kill *S. aureus* in the presence of coelomic fluid (Figure. 3.17A). This result indicates that components in the coelomic fluid have a neutralizing effect on PPAP 53. This result raises the question of whether

components of mammalian blood, like albumin, can also antagonize the activity of PPAP 53.

Bovine serum and albumin neutralized the activity of PPAP 53

Larvae contain hemolymph (coelomic fluid) that is analogous to mammalian blood (Fredrick & Ravichandran, 2012). Since coelomic fluid could antagonize the antimicrobial activity of PPAP 53, we wondered if mammalian serum would have the same effect on PPAP 53 activity. Therefore, the MIC of PPAP 53 was determined in the presence of fetal bovine serum (FBS). We found that 25% FBS decreased the antibacterial activity of PPAP 53 by 32-fold (Table 4). Albumin is the most abundant serum protein, accounting for 55% of all proteins ($\approx 35\text{-}50$ mg/ml), and the second most abundant proteins are immunoglobulins ($\approx 10\text{-}15$ mg/ml) (Anderson & Anderson, 2002, Schuster *et al.*, 2014). Therefore, we investigated whether albumin immunoglobulins can abrogate the antimicrobial activity of PPAP 53 against *S. aureus* USA300. Indeed, whole serum (FBS) and also BSA (50 mg/ml, as found in blood) significantly decreased the antimicrobial activity of PPAP 53 *in vitro* (Figure. 3.17B).

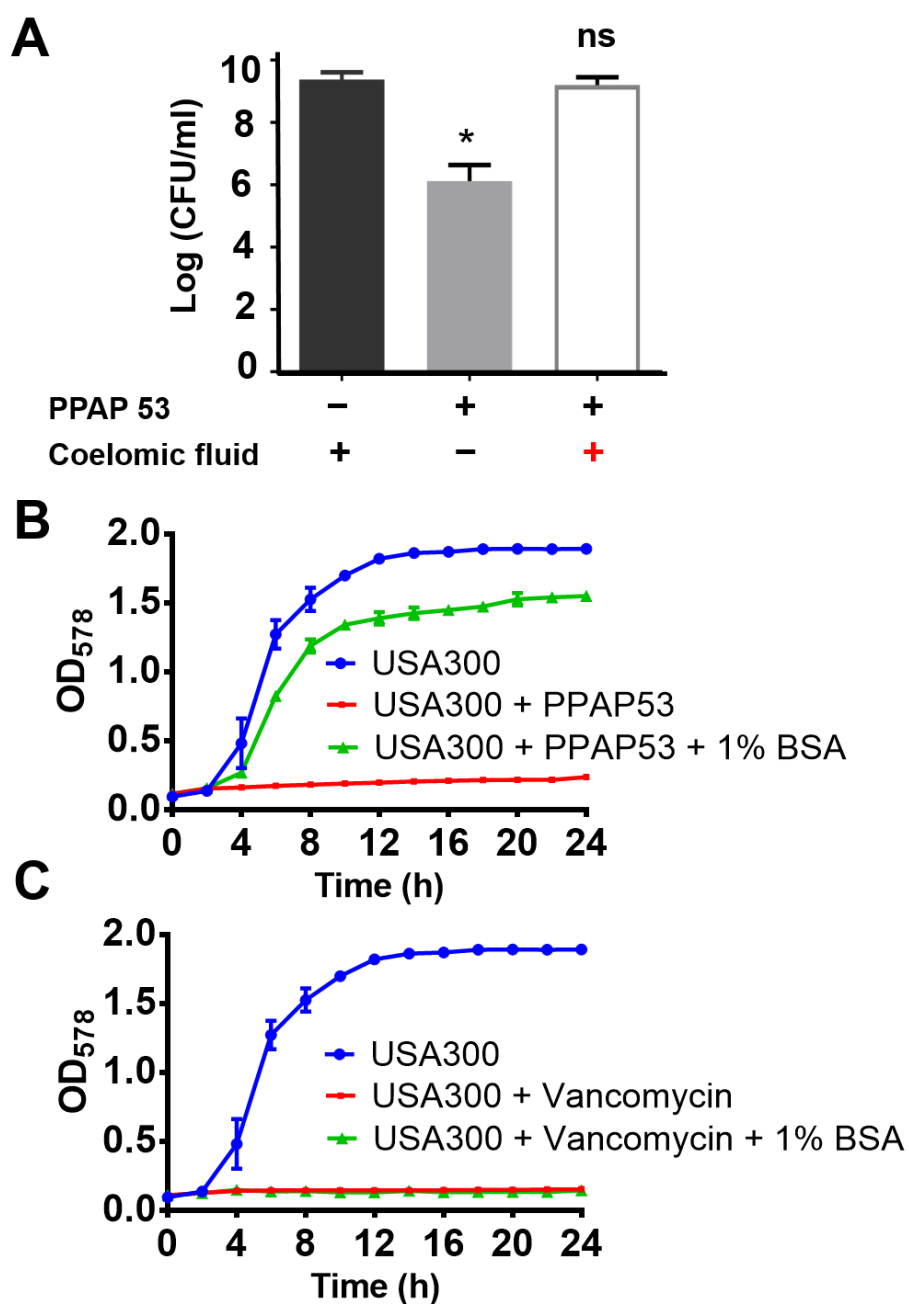


Figure 3.17. The bactericidal activity of PPAP53 is reversed by the larval coelomic fluid or 1% BSA. (A) To mimic *the in vivo* larva infection assay, the *ex vivo* killing assay was adopted. Bacterial inoculum of 10^5 CFU and $10 \mu\text{g}$ of PPAP was added to $100 \mu\text{l}$ of larva coelomic fluid as the treatment group. Untreated larval liquid and larval liquid treated with PBS were used as controls. The viability of bacteria in each group was determined by the drop plate method. The bactericidal effect of PPAP 53 on *S. aureus* is reversed by coelomic fluid. (B) The bactericidal effect of PPAP 53 (MIC: $0.5\text{-}1 \mu\text{g/ml}$) on *S. aureus* USA300 is reversed by 1% BSA whereas the effect of vancomycin remained unchanged.

Table 4. Impact of serum components on PPAP53 activity

Medium	MIC ($\mu\text{g/ml}$)	
	PPAP53	Vancomycin
MHB	1	1
MHB + 25% FBS	32	2
MHB + 0.5% BSA	4	1
MHB + 1% BSA	8	1
MHB + 2.5% BSA	16	1
MHB + 5% BSA	32	2
MHB + 1% IgG	1	1
MHB + 2.5% IgG	1	1
MHB + 1% Fg	1	1
MHB + 2.5% Fg	1	1

We also investigated the effect of immunoglobulins (IgG) and fibrinogen (Fg), other relatively abundant proteins in serum. However, these serum proteins at concentrations up to 25 mg/ml had no effect on the activity of PPAP 53 (Table 4). It appears that albumin is the major protein in serum that neutralizes the activity of PPAP 53. Studies on the growth kinetics of USA300 in combination with PPAP53 and/or 1% bovine serum albumin (BSA) showed that the bactericidal effect of PPAP 53 was already abolished by 1% BSA. While the bactericidal effect of vancomycin remained unchanged in the presence of 1% BSA (Figure. 3.17C).

***In silico* docking studies showed PPAP53 binds to the Heme binding pocket of BSA**

Serum albumin, the most abundant plasma protein ($\sim 640 \mu\text{M}$), can bind a wide variety of hydrophobic ligands including fatty acids, bilirubin, thyroxine or hemin (Zunszain *et al.*, 2003). If one knew whether the binding site of PPAP 53 overlapped with one of the known ligands, one could try to displace the binding of PPAP by the corresponding ligand. For this reason, we attempted to identify *in silico* the binding pocket for PPAP 53. A well-defined crystal structure of bovine serum albumin (BSA) was downloaded

from protein data bank (PDB ID: 3V03). The calcium and acetate ions attached to the crystal structure, as well as the water molecules used for crystallization were removed to get a clean structure of the BSA protein. From the 2D structure of PPAP 53 (Wang *et al.*, 2019), a 3D structure was prepared by Chem3D 16.0 and its geometry was optimised by energy minimisation.

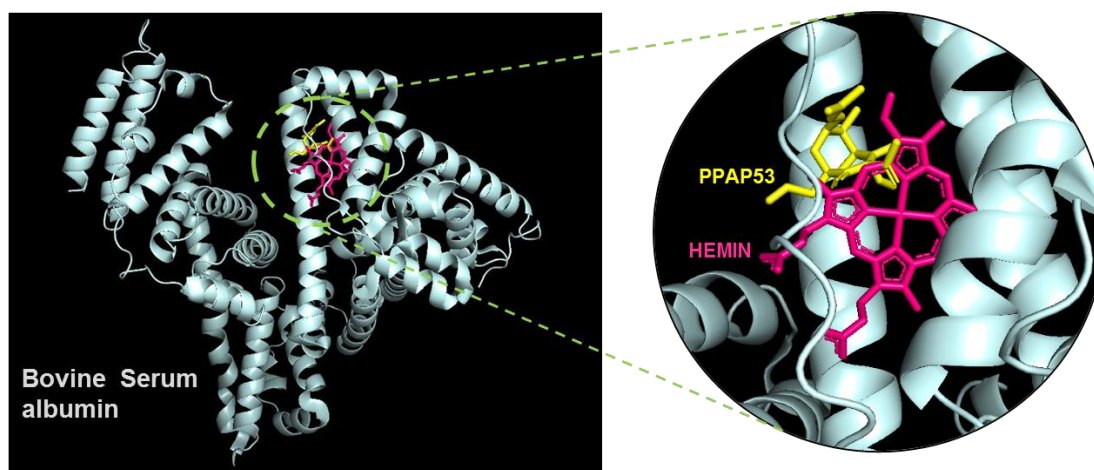


Figure 3.18. PPAP53 binds to the hemin binding pocket of BSA. *In silico* docking analysis by AutoDock vina showed that PPAP53 binds to FA1-IB pocket of BSA with a binding energy of -7.2 kcal/mol. This pocket represents the third main ligand (e.g., drug) binding pocket of BSA, the hemin being a prototypical ligand.

The structures were visualized and verified using PyMoL software. The PDBQT files of BSA and ligands were prepared using AutoDock Tools and blind docking was performed in AutoDock vina. During the preparation of PDBQT files polar hydrogens and Kollman charges are added for both the protein and ligand. BSA was considered as a rigid structure and PPAP 53 as the flexible one during docking. *In silico* docking analysis showed that PPAP 53 binds to the IB pocket of BSA with a binding energy of -7.2 kcal/mol (Figure. 3.18). This pocket represents the third main ligand (e.g., drug) binding pocket of BSA, the hemin being a prototypical ligand besides other compounds such as azapropazone, indomethacin and 3, 5-triiodobenzoic acid (Ghuman *et al.*, 2005).

Addition of known BSA ligands couldn't improve the *in vitro* bactericidal activity of PPAP53 in presence of BSA

Addition of known FDA approved drugs that binds to HSA, failed to restore the bactericidal activity of PPAP23. Different drugs/ligands used as well as their binding sites (Ghuman *et al.*, 2005) are given in Table 5. Even though, *in silico* studies showed the binding of PPAP53 at the IB site, same like that of hemin, the addition of hemin, didn't improve the *in vitro* bactericidal activity of PPAP53 (Figure. 3.19A). Figure 19, 20, and 21 shows the growth curve kinetics of USA300 in combination with 1% BSA and its different ligands. The addition of different ligands couldn't resuscitate the bactericidal activity of PPAP53.

Table 5. Tested ligands (FDA approved drugs) binding to HSA and their binding pockets

No.	Drugs tested	Binding pocket of HSA
1	Diffusinal	IIIA, IIA-IIB
2	Iodipamide	IIA, Cleft
3	Azapropazone	IIA, IB
4	Ibuprofen	IIIA, IIA-IIB
5	Diazepam	IIIA
6	Indomethacin	IIA, IB
7	Oxyphenbutazone	IIA, IIIB
8	Phenylbutazone	IIA
9	Warfarin	IIA
10	3,5 diidosalicylic acid	IIA
11	Hemin	IB

PPAP23 is active against pathogenic Gram-positive gut anaerobes

PPAP 23 is already known from our previous publication where we could show that it has good antimicrobial properties against aerobic and facultative aerobic Gram-positive bacteria (Wang *et al.*, 2019). What has not been studied, however, is its effect on anaerobic gut bacteria. Here we show that PPAP 23 is very active against Gram-

positive anaerobic pathogenic gut bacteria such as *Clostridium difficile* and *Clostridium perfringens*. It was also active against some of the commensal gut anaerobes like *Streptococcus salivarius*, *Ruminococcus gnavus*, *Clostridium ramosum*, *Blautia obeum* and *Parabacteroides distasonis*. But it was inactive or very less active against most of the commensal gut anaerobes tested (Table 6). As expected, it was inactive against Gram (-) gut bacteria. These results show that PPAP 23 has the potential to be used as a nutritional supplement in cases of intestinal dysbiosis by *Clostridium difficile*. PPAP 23 would have the advantage over conventional antibiotics that the entire intestinal flora would not be affected.

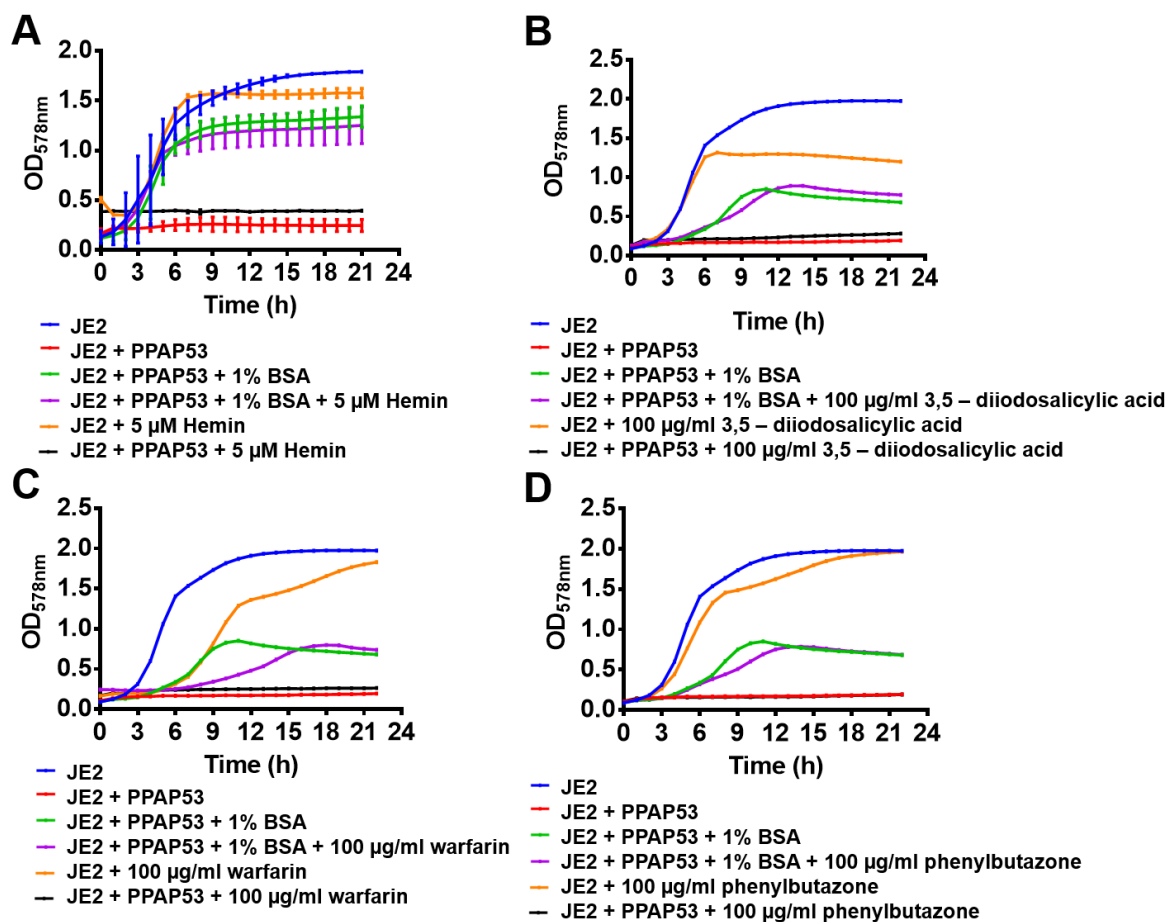


Figure 3.19. Addition of known BSA ligands couldn't improve the in vitro bactericidal activity of PPAP53 in presence of BSA. *S. aureus* precultured in TSB overnight were inoculated to OD=0.01 to a 48 well plate and 1X MIC PPAP53 and/or 1% BSA with or without ligands were added to study effect of peptides on bacterial growth using Varioskan LUX Multimode Microplate Reader. Here with this instrument, a kinetic measurement of optical density 578 nm was obtained every 1 h for a total of 24 hr, at 37°C with continuous shaking. Ligands tested were (A) Hemin, (B) 3,5 diiodosalicylic acid (C) warfarin and (D) phenylbutazone.

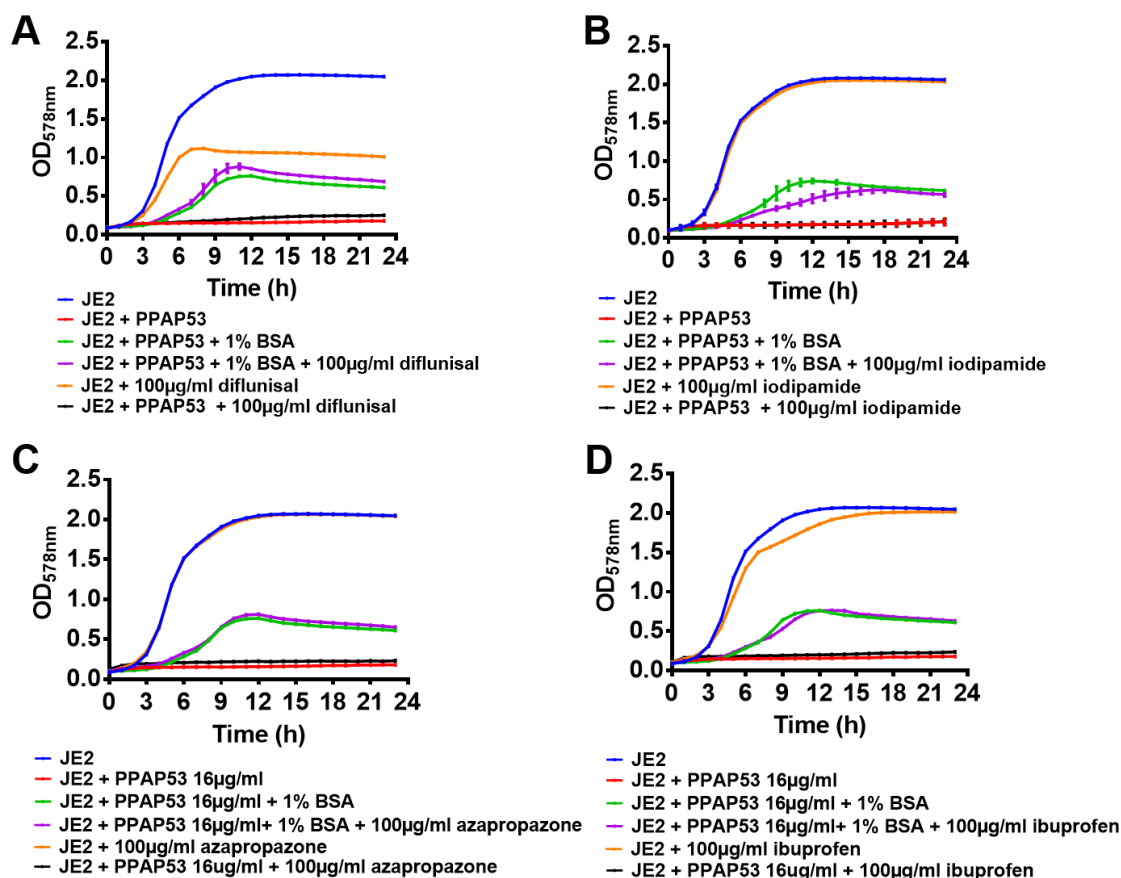


Figure 3.20. Addition of known BSA ligands couldn't improve the in vitro bactericidal activity of PPAP53 in presence of BSA. *S. aureus* precultured in TSB overnight were inoculated to OD=0.01 to a 48 well plate and 1X MIC PPAP53 and/or 1% BSA with or without ligands were added to study effect of peptides on bacterial growth using Varioskan LUX Multimode Microplate Reader. Here with this instrument, a kinetic measurement of optical density 578 nm was obtained every 1 h for a total of 24 hr, at 37°C with continuous shaking. Ligands tested were (A) diffunisal, (B) iodipamide (C) azapropazone and (D) ibuprofen.

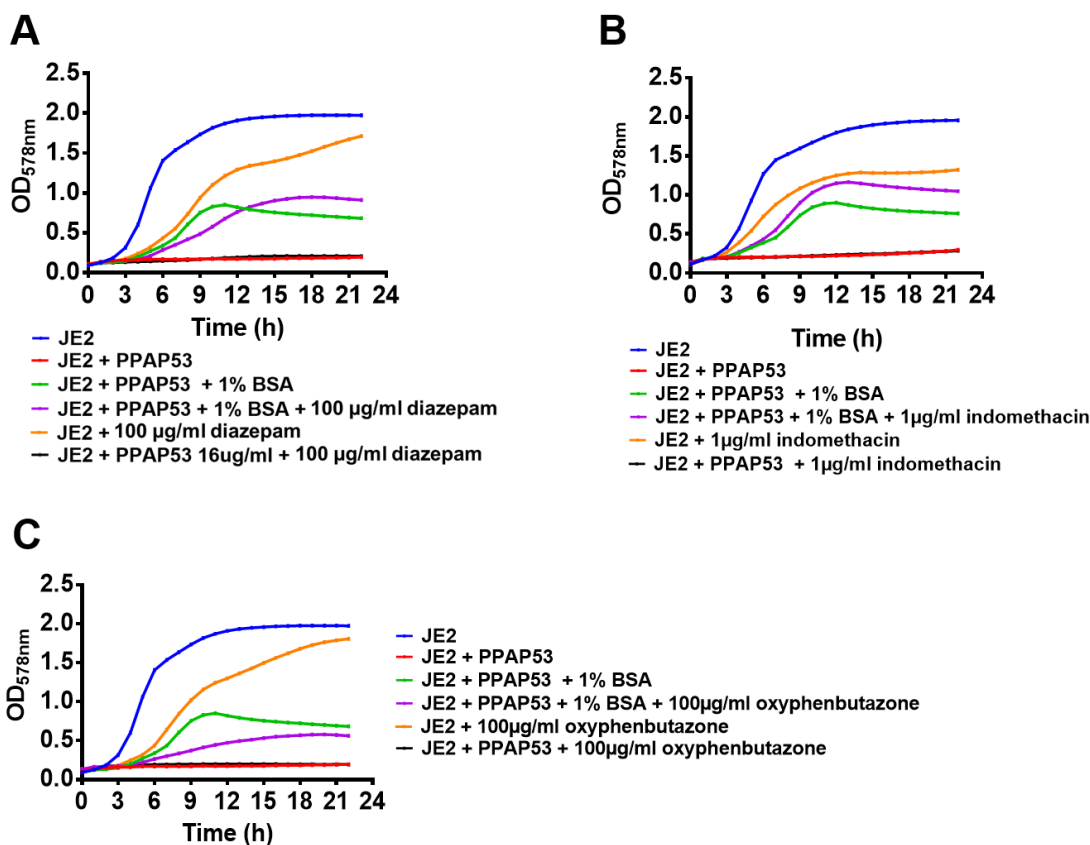


Figure 3.21. Addition of known BSA ligands couldn't improve the in vitro bactericidal activity of PPAP53 in presence of BSA. *S. aureus* precultured in TSB overnight were inoculated to OD=0.01 to a 48 well plate and 1X MIC PPAP53 and/or 1% BSA with or without ligands were added to study effect of peptides on bacterial growth using Varioskan LUX Multimode Microplate Reader. Here with this instrument, a kinetic measurement of optical density 578 nm was obtained every 1 h for a total of 24 hr, at 37°C with continuous shaking. Ligands tested were (A) diazepam (B) indomethacin (C) oxyphenbutazone.

Table 6. MIC values of PPAP23 against some of the anaerobic bacterial strains

	Strains	PPAP MIC (μM)
Pathogenic G +ve gut anaerobe	<i>Clostridium difficile</i>	<2
	<i>Clostridium perfringens</i>	4
Commensal gut anaerobe	<i>Streptococcus salivarius</i>	4
	<i>Dorea formicigenerans</i>	22
	<i>Streptococcus parasanguinis</i>	22
	<i>Ruminococcus gnavus</i>	4
	<i>Clostridium ramosum</i>	4
	<i>Blautia obeum</i>	4
	<i>Roseburia intestinalis</i>	22
	<i>Coprococcus comes</i>	22
	<i>Collinsella aerofaciens</i>	22
	<i>Bifidobacterium adolescentis</i>	45
	<i>Parabacteroides distasonis</i>	4
	<i>Eubacterium rectale</i>	22
	<i>Lactobacillus paracasei</i>	>45
	<i>Clostridium bolteae</i>	22
	<i>Parabacteroides merdae</i>	>45
	<i>Bifidobacterium longum</i> subsp. Longum	22
	<i>Clostridium saccharolyticum</i>	>45
	<i>Prevotella copri</i>	>45
	<i>Odoribacter splanchnicus</i>	>45
	<i>Fusobacterium nucleatum</i> subsp. Nucleatum	>45
	<i>Bilophila wadsworthia</i>	>45
	<i>Bacteroides vulgatus</i>	>45
<i>Bacteroides uniformis</i>	>45	
<i>Bacteroides thetaiotaomicron</i>	>45	
<i>Bacteroides fragilis</i> NT	>45	
Pathogenic G – ve gut anaerobe	<i>Salmonella enterica</i> typhimurium ToIC	>45
	<i>Yersinia pseudotuberculosis</i>	>22
	<i>Yersinia enterocolitica</i> WA-314	>45
	<i>Vibrio cholerae</i>	>45
	<i>Shigella sonnei</i> 53G	>45
	<i>Shigella flexneri</i>	>45
	<i>Salmonella enterica</i> typhimurium LT2	>45
	<i>Salmonella enterica</i> typhimurium	>45
	<i>Escherichia coli</i> UTI89	>45

Chapter 4

Discussion

Discussion

Hsp90 is a molecular chaperone that ensures cellular proteostasis by folding, stabilizing, activating and degrading over 400 client proteins (Hoter *et al.*, 2018). There exist two isoforms, Hsp90 α and β , however, because of the structural and functional similarity the name HSP90 is normally used for both (Hoter *et al.*, 2018). Normally, Hsp90 α localizes in the cytoplasm but it can be secreted under stress such as reactive oxygen species, heat, hypoxia, irradiation, or tissue injury (Jackson, 2013). The extracellular form, eHsp90 α , has been shown to enhance cell motility and support wound healing (Li *et al.*, 2012). Due to its ability to affect numerous client proteins, inhibition of Hsp90 is regarded as an attractive approach for cancer treatment (Sanchez *et al.*, 2020). Therefore, any new compound that interacts with and alters the activity of Hsp90 is regarded with great interest.

Geldanamycin for example inhibits the essential ATPase activity of Hsp90, resulting in the inactivation, destabilization and degradation of Hsp90 client proteins. Since these processes play an important role in the regulation of cell cycle, cell growth, cell survival, apoptosis and oncogenesis, geldanamycin inhibits the proliferation of cancer cells and shows anti-cancer activity in animal studies (Miyata, 2005). Nonetheless, its pharmaceutical application is limited by its high cytotoxicity (Blagosklonny, 2002, Miyata, 2005).

The well-studied geldanamycin and our L15 and L13 peptides have one thing in common, namely binding to Hsp90. This was the reason why we always included geldanamycin as a control in our studies. However, beyond the binding to Hsp90 the similarities become less pronounced. For example, Lp11 increased both the internalization of *S. aureus* by host cells and F-actin formation, whereas geldanamycin decreased the internalization and F-actin formation by about the same factor suggesting that they bind to different sites of Hsp90 (Tribelli *et al.*, 2020).

In the search for Lp11 domains that interacted with Hsp90 α , we found 2 peptides, L15 and L13, that interacted with Hsp90 α but, unlike parent protein Lp11, decreased the internalization of *S. aureus* into host cells, much like geldanamycin does. L15 and L13 are part of a β -sheet domain in Lp11. The previously described L27 peptide (38 aa long)

is localized in the C-terminal alpha-helical and loop structures part of Lp11 and activates, like the parent protein Lp11, the internalization of *S. aureus*. Hsp90 comprises three main conserved domains, the N-terminal domain (NTD), C-terminal domain (CTD), and middle domain (MD) each performing a specific function (Hoter *et al.*, 2018). While geldanamycin is known to bind to the N-terminal NTD domain thereby inhibiting the ATPase activity that is necessary to regulate Hsp90 conformation (Gorska *et al.*, 2012), we currently don't know with which Hsp90 domain L15 and L13 interact.

Owing to the significant roles of protein kinases and phosphatases in cellular regulation (Cheng *et al.*, 2011) we also investigated whether L15 or L13 exerted an effect on total ATPase activity in HaCaT cells. However, we could not detect any significant inhibition by L15 or L13 and assumed that Hsp90 ATPase activity is not significantly affected. Most likely the peptides bind to a different site on Hsp90 as geldanamycin.

Similarly to geldanamycin, L15 and L13 inhibit F-actin formation in host cells and *S. aureus* internalization (Figure. 3.3 and Table 1). Since geldanamycin shows a much higher cytotoxicity than L15 and L13 we took care of using it at the subinhibitory concentration of 5 μ M, while L15 and L13 were used at concentrations of 20 and 30 μ M, respectively. In both the insect model with *G. mellonella* and the mouse model, L13 and L15 reduced the lethality of *S. aureus*, by about 30% in the insect model and about 40% in the mouse model (Figure. 3.5 and 7). In the insect model the peptides were added immediately before application of *S. aureus*. In the mouse model, L15 was added one hour before the application of *S. aureus* and at daily time intervals, similar to classical antibiotic treatment. This positive effect, which was completely unexpected, shows that the peptides act not only at the cellular level but also on the entire organism.

In order to reduce the lethality of *S. aureus*, we speculated that a) L15 and L13 inhibited growth and expression of virulence factors of *S. aureus* or b) they strengthened the host defense or c) both.

At the concentrations used, L15 and L13 neither inhibit the viability of host cells (Figure. 3.2) nor the growth of *S. aureus* or its hemolytic activity (Figure. 3.2C, 3.6). We therefore believe that they probably strengthen host defenses through their interaction with Hsp90. However, there might be also a third mechanism. In the blood stream there

are abundant neutrophils who can sense, engulf, and kill the bacteria. The inhibitory effect of L15 on bacterial internalization in keratinocytes and monocytes may also apply to the endothelial cells. In the bacteremia model, less internalized bacteria upon L15 treatment may result in higher number of bacteria in the blood stream that are more susceptible to immune killing which may lead to less focal infection in the vital organs.

How the defense is strengthened is not completely clear. However, insects and mammals have one defense system in common, namely the innate immune system (Sheehan *et al.*, 2018). Both peptides are relatively inert with respect to cytokine inducing activity in PBMCs (Figure. 3.11). However, *S. aureus* infected PBMCs that were pretreated with L13 and L15 showed an increase in IL-6 production (Figure. 3.12B), and in primary human monocytes pretreatment with L13 or L15 decreased the *S. aureus* internalization (Figure. 3.12A). In the latter case, the peptides could compete with the Lpl proteins on the surface of *S. aureus* for binding to the Hsp90 receptor. This could lead to neutralization of the Lpl proteins, and this in turn could lead to reduced pathogenicity. This would be consistent with our previous results showing that deletion of the *lpl* genes significantly reduces the pathogenicity of *S. aureus* in a mouse kidney abscess model (Nguyen *et al.*, 2015, Nguyen *et al.*, 2015).

Hsp90 and related heat shock proteins are also involved in host defence (Calderwood *et al.*, 2016). Hsp90 induces the adaptive immunity by activation of antigen presenting cells and dendritic cells. And the related heat shock protein, GRP94 (gp96), shows the same domain structure as Hsp90 and also binds geldanamycin. It is the most abundant glycoprotein in the ER hence known as endoplasmic. The remarkable feature of GRP94 is that some of its client proteins are important components of the immune system such as TLR1, 2, 4 and MHC class II (Schaiff *et al.*, 1992, Randow & Seed, 2001, Staron *et al.*, 2010, Mesquita *et al.*, 2017). In fact, GRP94 (GP96) is the master chaperone for Toll-like receptors and is important in the innate function of macrophages (Yang *et al.*, 2007).

Polycyclic polyprenylated acylphloroglucinols (PPAPs) represent an important group of natural products that are extremely diversified and present in many plants (Ciochina & Grossman, 2006, Richard *et al.*, 2012, Yang *et al.*, 2018, Bailly & Vergoten, 2021). The PPAPs database includes > 850 structures, with molecules having extremely

diverse bioactivity profiles (Grossman). There are compounds that have anti-adipogenesis activities (Cao *et al.*, 2020), that modulate the major histocompatibility complex (MHC) expression (Coste *et al.*, 2020), that have antiparasitic activity (Fromentin *et al.*, 2015), and that have antidepressant and hepatoprotective activity (Ma *et al.*, 2021). Still other PPAPs have anti-cancer properties (Bailly & Vergoten, 2021) or can interfere with the heat shock protein HSPA8, a chaperone (Han *et al.*, 2020). The development of a seven-step synthetic approach for an iterative introduction of R(1) to R(4) facilitated the synthesis of a wide variety of structurally diverse trans-type B PPAPs (Biber *et al.*, 2011, Horeischi *et al.*, 2014).

In collaboration with the research group of Bernd Plietker (Organic Chemistry, University of Dresden), we are concerned with the antimicrobial properties of novel synthetic type B PPAP-derivatives. Here we compared two PPAP derivatives, PPAP 23 and PPAP 53, a more water-soluble sodium salt of PPAP22. We primarily used the multidrug-resistant *S. aureus* USA300 as the pathogenic test strain. The mode of action of PPAP 23 has been described already earlier (Guttruff *et al.*, 2017, Wang *et al.*, 2019). While in previous studies we were mainly concerned with the *in vitro* antimicrobial activity, we have focused here on the *in vivo* effect. Since PPAP 53 is a new compound, we first carried out comparative studies *in vitro*. Surprisingly, we found that the Na salt of PPAP 53 exhibited *in vitro* almost the same good antimicrobial properties (MIC ~ 2 µg/ml) as the less water-soluble PPAP 23. We then extended our studies to the wax moth model. Here, both compounds were found to be well tolerated at a dose up to 200 mg/kg (100 x MIC) and no larvae died in the 5-day period. Infecting the larvae with a dose 10⁶ CFU USA300 they died within 3 days. Neither PPAP 23 nor PPAP 53 at a dose of 10 x MIC (20 mg/kg) could save the larvae, but vancomycin at a comparable dose could.

Since one cannot necessarily infer the same results from an insect model in a mammalian model, we tested PPAP 23 in a septic arthritis mouse model. As common practice with antibiotics, PPAP23 was administered twice daily at a dose of 100 µg/mouse. The first treatment was given 2 days after infection with *S. aureus* Newman. PPAP23 failed to prevent the progression of septic arthritis. However, it caused a reduction in abscess formation in the kidneys and the bacterial load was also decreased (Figure. 3.16). From this we see that PPAP23 cannot stop an incipient

septic arthritis. It follows that PPAP23 cannot stop an incipient septic arthritis, but it can reduce the bacterial load somewhat most likely by its antibiotic effect.

What concerned us most, however, was the question why the two PPAPs worked so well *in vitro* but largely failed to work *in vivo*. The answer was that not only larval coelomic fluid but also bovine serum and albumin (BSA) neutralized the activity of PPAP 53 (Figure. 3.17). Other very common serum proteins such as immunoglobulins or fibrinogen had no neutralizing effect (Table 4).

Serum albumin (SA) is the most abundant protein in the blood plasma of all vertebrates with the concentration in human serum being 35–50 mg/mL. As mentioned by Theodore Peters Jr. albumin is best known for its ability to bind smaller molecules of many types interacting with a broad spectrum of compounds (Peters Jr, 1995). Most strongly bound are hydrophobic organic anions of medium size, 100 to 600 Da such as long-chain fatty acids, hematin, and bilirubin. Smaller and less hydrophobic compounds such as tryptophan and ascorbic acid are less well bound, but their binding can still be highly specific. Affinity for L-tryptophan exceeds that for the D-tryptophan by 100-fold. With their hydrophobic character and their size of around 400 Da PPAP 23 and PPAP 53 fall exactly into the group of compounds that are bound by albumin. Although PPAP 53 is more water-soluble than PPAP 23 it still is effectively neutralized by albumin, suggesting that both compounds are efficiently bound by albumin.

It has been reported that Hyperforin, a highly hydrophobic and poor water soluble prenylated acylphloroglucinol from St. John's Wort, also strongly binds to albumin which impairs its therapeutic value, namely, suppressing the formation of proinflammatory leukotrienes by inhibiting the key enzyme 5-lipoxygenase (5-LO) (Fuller *et al.*, 2018, Traeger *et al.*, 2020). To overcome this hurdle hyperforin was encapsulated into nanoparticles (NPs) consisting of acetalated dextran (AcDex) to avoid albumin binding, which improved inhibition of 5-LO activity in neutrophils in the presence of albumin because of effective uptake and circumvention of plasma protein binding (Traeger *et al.*, 2020).

We thought of a similar strategy namely to identify the binding site of PPAP to albumin by *in silico* docking and to suppress the binding of PPAP by ligands that bind to the

same site. We found that PPAP53 binds to the heme-binding pocket of BSA, which is also the binding site of several other compounds. However, all of the different ligands that we tested (Table 5) failed to restore the bactericidal activity of PPAP23. This could mean that PPAP 53 also binds to other sites of albumin, or that the binding of PPAP 53 to albumin is stronger than that of the other tested ligands. We assume that the latter is the case. These results show that PPAP 23 and PPAP 53 are of limited use in the treatment of septic infections because of the high albumin content in the blood.

However, could these PPAPs play a role in the treatment of gastrointestinal infections? An examination of plasma proteins in the faeces of healthy volunteers showed that the main plasma proteins, albumin and IgG, were detectable but only in traces. When albumin was added to the faeces, it was rapidly degraded within a few hours (Schmidt *et al.*, 1995). The albumin concentration in humans is 0.01-0.24 mg/g wet weight of faeces (Morrow *et al.*, 1990). At this low albumin concentration in the gastrointestinal tract (GIT), the antimicrobial activity of PPAP 23 and PPAP 53 is unlikely to be affected. Furthermore, in patients with inflammatory bowel disease (IBD), a chronic nonspecific inflammatory disease involving the intestine, which is comprised by two major disorders, Crohn's disease (CD) and ulcerative colitis the serum albumin is decreased (Su *et al.*, 2019, Wang *et al.*, 2022), suggesting that the albumin content in GIT might also be decreased.

Considering the possibility that PPAP 23 and PPAP 53 may have an effect in GIT infections, we investigated the antimicrobial activity of typical pathogenic and commensal anaerobic GIT bacteria. Interestingly, some of the most feared intestinal pathogenic bacteria are particularly susceptible to PPAP 53. These include *Clostridium difficile* and *Clostridium perfringens*, well-known intestinal pathogens the one causing colitis (Abt *et al.*, 2016) the other causes food poisoning and antibiotic-associated diarrhea (Eichner *et al.*, 2017). *Clostridium ramosum* is occasionally found to cause bacteraemia (Legaria *et al.*, 2020). *Parabacteroides distasonis* is an aerotolerant gut anaerobe with emerging antimicrobial resistance and pathogenic and probiotic roles in human health (Ezeji *et al.*, 2021). *Ruminococcus gnavus*, a member of the human gut microbiome associated with Crohn's disease, produces an inflammatory polysaccharide (Henke *et al.*, 2019). The majority of the commensal Gram-positive gut anaerobes and also Gram-negative bacteria are not affected by PPAP 53.

Conclusion

Any compound that interacts with Hsp90 and thereby exerts an effect on cellular physiology is of particular interest. The Lpl1-derived small peptides, L15 and L13, not only affect the cytoskeleton and the associated internalization of *S. aureus* by the host cells in vitro. They also exert a global effect on the entire organism in both insect and mammalian models by reducing the lethality of *S. aureus* infection. How this happens is still unclear. Currently, we see two scenarios: a) binding of the peptides to Hsp90 and related Hsp proteins engages the innate immune system in such a way that it responds faster or more strongly to *S. aureus* infection, or b) binding of the peptides to Hsp90 counteracts the binding of the membrane-anchored Lpl proteins of *S. aureus*. Both mechanisms may reduce the lethality of a *S. aureus* infection.

The lipidomic analysis gives us with a solid proof that in RomR strains, the antibacterial activity of Rom is nullified by the neutralising effect of phospholipids. We could see significantly higher amount of phospholipids excreted by the RomR strains in comparison to the wild type. In RomR strain, FarE, functioning as the efflux pump is overexpressed. This overexpression leads to high accumulation of phospholipids in the bacterial supernatant and cell envelope. These accumulated phospholipids neutralize rom in RomR strains. Additionally, potassium salt of Rom, FH-54 was found to be the best candidate among all the derivatives tested, considering it is active even against the RomR strains. Also, Rom was seen to be active against pathogenic gut anaerobes, which gives another potential applications for Rom.

Here we show that PPAP 23 and PPAP 53 are only conditionally suitable for therapeutic use in Gram-positive sepsis since the high albumin co-concentration in the blood abrogates their antimicrobial effect. However, a possible application in environments with low albumin content, such as in the gastrointestinal tract or topical application in skin infections, is conceivable. Neutralization by albumin seems to be a general problem of the hydrophobic PPAPs. Work should therefore be done to mitigate the hydrophobic character by introducing hydrophilic side groups. Neutralization by albumin seems to be a general problem of the hydrophobic PPAPs. Work should therefore be done to mitigate the hydrophobic character by introducing hydrophilic side groups. To what extent this will change the diverse activities remains to be seen.

References

- Abt MC, McKenney PT & Pamer EG (2016) Clostridium difficile colitis: pathogenesis and host defence. *Nat Rev Microbiol* **14**: 609-620.
- Agerer F, Lux S, Michel A, Rohde M, Ohlsen K & Hauck CR (2005) Cellular invasion by Staphylococcus aureus reveals a functional link between focal adhesion kinase and cortactin in integrin-mediated internalisation. *J Cell Sci* **118**: 2189-2200.
- Ali A, Welin A, Schwarze JC, et al. (2015) CTLA4 Immunoglobulin but Not Anti-Tumor Necrosis Factor Therapy Promotes Staphylococcal Septic Arthritis in Mice. *J Infect Dis* **212**: 1308-1316.
- Alnaseri H, Arsic B, Schneider JE, Kaiser JC, Scinocca ZC, Heinrichs DE & McGavin MJ (2015) Inducible Expression of a Resistance-Nodulation-Division-Type Efflux Pump in Staphylococcus aureus Provides Resistance to Linoleic and Arachidonic Acids. *J Bacteriol* **197**: 1893-1905.
- Alva-Murillo N, Lopez-Meza JE & Ochoa-Zarzosa A (2014) Nonprofessional phagocytic cell receptors involved in Staphylococcus aureus internalization. *Biomed Res Int* **2014**: 538546.
- Anantharaman V & Aravind L (2003) Evolutionary history, structural features and biochemical diversity of the NlpC/P60 superfamily of enzymes. *Genome Biol* **4**: R11.
- Anderson NL & Anderson NG (2002) The human plasma proteome: history, character, and diagnostic prospects. *Mol Cell Proteomics* **1**: 845-867.
- Bailly C & Vergoten G (2021) Anticancer Properties and Mechanism of Action of Oblongifolin C, Guttiferone K and Related Polyprenylated Acylphloroglucinols. *Nat Prod Bioprospect* **11**: 629-641.
- Barnes J, Anderson LA & Phillipson JD (2001) St John's wort (Hypericum perforatum L.): a review of its chemistry, pharmacology and clinical properties. *J Pharm Pharmacol* **53**: 583-600.
- Basavanna S, Chimalapati S, Maqbool A, et al. (2013) The effects of methionine acquisition and synthesis on Streptococcus pneumoniae growth and virulence. *PLoS One* **8**: e49638.
- Bayles KW, Wesson CA, Liou LE, Fox LK, Bohach GA & Trumble WR (1998) Intracellular Staphylococcus aureus escapes the endosome and induces apoptosis in epithelial cells. *Infect Immun* **66**: 336-342.
- Biber N, Mows K & Plietker B (2011) The total synthesis of hyperpapuanone, hyperibone L, epi-clusianone and oblongifolin A. *Nat Chem* **3**: 938-942.

- Biswas L, Biswas R, Nerz C, *et al.* (2009) Role of the twin-arginine translocation pathway in *Staphylococcus*. *J Bacteriol* **191**: 5921-5929.
- Blagosklonny MV (2002) Hsp-90-associated oncoproteins: multiple targets of geldanamycin and its analogs. *Leukemia* **16**: 455-462.
- Brochado AR, Telzerow A, Bobonis J, *et al.* (2018) Species-specific activity of antibacterial drug combinations. *Nature* **559**: 259-263.
- Brown SE, Howard A, Kasprzak AB, Gordon KH & East PD (2008) The discovery and analysis of a diverged family of novel antifungal moricin-like peptides in the wax moth *Galleria mellonella*. *Insect Biochem Mol Biol* **38**: 201-212.
- Brown SE, Howard A, Kasprzak AB, Gordon KH & East PD (2009) A peptidomics study reveals the impressive antimicrobial peptide arsenal of the wax moth *Galleria mellonella*. *Insect Biochem Mol Biol* **39**: 792-800.
- Calderwood SK, Gong J & Murshid A (2016) Extracellular HSPs: The Complicated Roles of Extracellular HSPs in Immunity. *Front Immunol* **7**: 159.
- Cao TW, Liu X, Yan S, Zhou HM, Liu DW, Xiong WY & Xu G (2020) Anti-adipogenic adamantane type polycyclic polyprenylated acylphloroglucinols from *Hypericum subsessile*. *Fitoterapia* **147**: 104755.
- Cheng HC, Qi RZ, Paudel H & Zhu HJ (2011) Regulation and function of protein kinases and phosphatases. *Enzyme Res* **2011**: 794089.
- Ciochina R & Grossman RB (2006) Polycyclic polyprenylated acylphloroglucinols. *Chem Rev* **106**: 3963-3986.
- Coste C, Gerard N, Dinh CP, Bruguiere A, Rouger C, Leong ST, Awang K, Richomme P, Derbre S & Charreau B (2020) Targeting MHC Regulation Using Polycyclic Polyprenylated Acylphloroglucinols Isolated from *Garcinia bancana*. *Biomolecules* **10**.
- Cueva C, Mingo S, Munoz-Gonzalez I, Bustos I, Requena T, del Campo R, Martin-Alvarez PJ, Bartolome B & Moreno-Arribas MV (2012) Antibacterial activity of wine phenolic compounds and oenological extracts against potential respiratory pathogens. *Lett Appl Microbiol* **54**: 557-563.
- Cushnie TP, Taylor PW, Nagaoka Y, Uesato S, Hara Y & Lamb AJ (2008) Investigation of the antibacterial activity of 3-O-octanoyl(-)-epicatechin. *J Appl Microbiol* **105**: 1461-1469.
- Cytrynska M, Mak P, Zdybicka-Barabas A, Suder P & Jakubowicz T (2007) Purification and characterization of eight peptides from *Galleria mellonella* immune hemolymph. *Peptides* **28**: 533-546.

- Dale SE, Sebulsky MT & Heinrichs DE (2004) Involvement of SirABC in iron-siderophore import in *Staphylococcus aureus*. *J Bacteriol* **186**: 8356-8362.
- Deurenberg RH & Stobberingh EE (2008) The evolution of *Staphylococcus aureus*. *Infect Genet Evol* **8**: 747-763.
- Dickson MA, Hahn WC, Ino Y, Ronfard V, Wu JY, Weinberg RA, Louis DN, Li FP & Rheinwald JG (2000) Human keratinocytes that express hTERT and also bypass a p16 INK4a -enforced mechanism that limits life span become immortal yet retain normal growth and differentiation characteristics. *Molecular and Cellular Biology* **20**: 1436-1447.
- Dunny GM & Leonard BA (1997) Cell-cell communication in gram-positive bacteria. *Annu Rev Microbiol* **51**: 527-564.
- Dziarski R & Gupta D (2006) The peptidoglycan recognition proteins (PGRPs). *Genome Biol* **7**: 232.
- Dziewanowska K, Patti JM, Deobald CF, Bayles KW, Trumble WR & Bohach GA (1999) Fibronectin binding protein and host cell tyrosine kinase are required for internalization of *Staphylococcus aureus* by epithelial cells. *Infect Immun* **67**: 4673-4678.
- Dziewanowska K, Carson AR, Patti JM, Deobald CF, Bayles KW & Bohach GA (2000) Staphylococcal fibronectin binding protein interacts with heat shock protein 60 and integrins: role in internalization by epithelial cells. *Infect Immun* **68**: 6321-6328.
- Eichner M, Augustin C, Fromm A, *et al.* (2017) In Colon Epithelia, *Clostridium perfringens* Enterotoxin Causes Focal Leaks by Targeting Claudins Which are Apically Accessible Due to Tight Junction Derangement. *J Infect Dis* **217**: 147-157.
- Ezeji JC, Sarikonda DK, Hopperton A, *et al.* (2021) *Parabacteroides distasonis*: intriguing aerotolerant gut anaerobe with emerging antimicrobial resistance and pathogenic and probiotic roles in human health. *Gut Microbes* **13**: 1922241.
- Flannagan SE & Clewell DB (2002) Identification and characterization of genes encoding sex pheromone cAM373 activity in *Enterococcus faecalis* and *Staphylococcus aureus*. *Mol Microbiol* **44**: 803-817.
- Fowler T, Wann ER, Joh D, Johansson S, Foster TJ & Hook M (2000) Cellular invasion by *Staphylococcus aureus* involves a fibronectin bridge between the bacterial fibronectin-binding MSCRAMMs and host cell beta1 integrins. *Eur J Cell Biol* **79**: 672-679.

- Fredrick WS & Ravichandran S (2012) Hemolymph proteins in marine crustaceans. *Asian Pac J Trop Biomed* **2**: 496-502.
- Fromentin Y, Cottet K, Kritsanida M, Michel S, Gaboriaud-Kolar N & Lallemand MC (2015) *Symphonia globulifera*, a widespread source of complex metabolites with potent biological activities. *Planta Med* **81**: 95-107.
- Fuller J, Kellner T, Gaid M, Beerhues L & Muller-Goymann CC (2018) Stabilization of hyperforin dicyclohexylammonium salt with dissolved albumin and albumin nanoparticles for studying hyperforin effects on 2D cultivation of keratinocytes in vitro. *Eur J Pharm Biopharm* **126**: 115-122.
- Gasteiger E, Hoogland C, Gattiker A, Duvaud Se, Wilkins MR, Appel RD & Bairoch A (2005) Protein Identification and Analysis Tools on the ExPASy Server. *The Proteomics Protocols Handbook*, (Walker JM, ed.) p. 571-607. Humana Press, Totowa, NJ.
- Geiger C, Korn SM, Hasler M, Peetz O, Martin J, Kotter P, Morgner N & Entian KD (2019) LanI-Mediated Lantibiotic Immunity in *Bacillus subtilis*: Functional Analysis. *Appl Environ Microbiol* **85**.
- Gemmell CG, Edwards DI, Fraise AP, Gould FK, Ridgway GL, Warren RE, Joint Working Party of the British Society for Joint Working Party of the British Society for Antimicrobial Chemotherapy HIS & Infection Control Nurses A (2006) Guidelines for the prophylaxis and treatment of methicillin-resistant *Staphylococcus aureus* (MRSA) infections in the UK. *J Antimicrob Chemother* **57**: 589-608.
- Ghuman J, Zunszain PA, Petitpas I, Bhattacharya AA, Otagiri M & Curry S (2005) Structural basis of the drug-binding specificity of human serum albumin. *J Mol Biol* **353**: 38-52.
- Gorska M, Popowska U, Sielicka-Dudzin A, Kuban-Jankowska A, Sawczuk W, Knap N, Cicero G & Wozniak F (2012) Geldanamycin and its derivatives as Hsp90 inhibitors. *Front Biosci (Landmark Ed)* **17**: 2269-2277.
- Gorwitz RJ, Kruszon-Moran D, McAllister SK, McQuillan G, McDougal LK, Fosheim GE, Jensen BJ, Killgore G, Tenover FC & Kuehnert MJ (2008) Changes in the prevalence of nasal colonization with *Staphylococcus aureus* in the United States, 2001-2004. *J Infect Dis* **197**: 1226-1234.
- Gothel SF & Marahiel MA (1999) Peptidyl-prolyl cis-trans isomerases, a superfamily of ubiquitous folding catalysts. *Cell Mol Life Sci* **55**: 423-436.

- Gotz F & Mayer S (2013) Both terminal oxidases contribute to fitness and virulence during organ-specific *Staphylococcus aureus* colonization. *mBio* **4**: e00976-00913.
- Grossman RB Table of PPAPs. <http://wwwchem.umd.edu/research/grossman/PPAPs>.
- Guo J, Chang C & Li W (2017) The role of secreted heat shock protein-90 (Hsp90) in wound healing - how could it shape future therapeutics? *Expert Rev Proteomics* **14**: 665-675.
- Guttruff C, Baykal A, Wang H, Popella P, Kraus F, Biber N, Krauss S, Gotz F & Plietker B (2017) Polycyclic Polyprenylated Acylphloroglucinols: An Emerging Class of Non-Peptide-Based MRSA- and VRE-Active Antibiotics. *Angew Chem Int Ed Engl* **56**: 15852-15856.
- Hacker C, Christ NA, Duchardt-Ferner E, *et al.* (2015) The Solution Structure of the Lantibiotic Immunity Protein NisI and Its Interactions with Nisin. *J Biol Chem* **290**: 28869-28886.
- Haggar A, Hussain M, Lonnie H, Herrmann M, Norrby-Teglund A & Flock JI (2003) Extracellular adherence protein from *Staphylococcus aureus* enhances internalization into eukaryotic cells. *Infect Immun* **71**: 2310-2317.
- Halwani AE, Niven DF & Dunphy GB (2000) Apolipoprotein III and the interactions of lipoteichoic acids with the immediate immune responses of *Galleria mellonella*. *J Invertebr Pathol* **76**: 233-241.
- Han L, Xu D, Xi Z, *et al.* (2020) The Natural Compound Oblongifolin C Exhibits Anticancer Activity by Inhibiting HSPA8 and Cathepsin B In Vitro. *Front Pharmacol* **11**: 564833.
- Hantke K & Braun V (1973) Covalent binding of lipid to protein. Diglyceride and amide-linked fatty acid at the N-terminal end of the murein-lipoprotein of the *Escherichia coli* outer membrane. *Eur J Biochem* **34**: 284-296.
- Henke MT, Kenny DJ, Cassilly CD, Vlamakis H, Xavier RJ & Clardy J (2019) *Ruminococcus gnavus*, a member of the human gut microbiome associated with Crohn's disease, produces an inflammatory polysaccharide. *Proc Natl Acad Sci U S A* **116**: 12672-12677.
- Herigstad B, Hamilton M & Heersink J (2001) How to optimize the drop plate method for enumerating bacteria. *J Microbiol Methods* **44**: 121-129.
- Hiron A, Borezee-Durant E, Piard JC & Juillard V (2007) Only one of four oligopeptide transport systems mediates nitrogen nutrition in *Staphylococcus aureus*. *J Bacteriol* **189**: 5119-5129.

- Hirschhausen N, Schlesier T, Schmidt MA, Gotz F, Peters G & Heilmann C (2010) A novel staphylococcal internalization mechanism involves the major autolysin Atl and heat shock cognate protein Hsc70 as host cell receptor. *Cell Microbiol* **12**: 1746-1764.
- Horeischi F, Biber N & Plietker B (2014) The total syntheses of guttiferone A and 6-epi-guttiferone A. *J Am Chem Soc* **136**: 4026-4030.
- Hoter A, El-Sabban ME & Naim HY (2018) The HSP90 Family: Structure, Regulation, Function, and Implications in Health and Disease. *Int J Mol Sci* **19**.
- Hudson MC, Ramp WK, Nicholson NC, Williams AS & Nousiainen MT (1995) Internalization of Staphylococcus aureus by cultured osteoblasts. *Microb Pathog* **19**: 409-419.
- Jackson SE (2013) Hsp90: structure and function. *Top Curr Chem* **328**: 155-240.
- Kawaoka S, Katsuma S, Daimon T, Isono R, Omuro N, Mita K & Shimada T (2008) Functional analysis of four Gloverin-like genes in the silkworm, Bombyx mori. *Arch Insect Biochem Physiol* **67**: 87-96.
- Khameneh B, Iranshahy M, Ghandadi M, Ghoochi Atashbeyk D, Fazly Bazzaz BS & Iranshahi M (2015) Investigation of the antibacterial activity and efflux pump inhibitory effect of co-loaded piperine and gentamicin nanoliposomes in methicillin-resistant Staphylococcus aureus. *Drug Dev Ind Pharm* **41**: 989-994.
- Khan IA, Mirza ZM, Kumar A, Verma V & Qazi GN (2006) Piperine, a phytochemical potentiator of ciprofloxacin against Staphylococcus aureus. *Antimicrob Agents Chemother* **50**: 810-812.
- Khare T, Anand U, Dey A, Assaraf YG, Chen ZS, Liu Z & Kumar V (2021) Exploring Phytochemicals for Combating Antibiotic Resistance in Microbial Pathogens. *Front Pharmacol* **12**: 720726.
- Kim CH, Lee JH, Kim I, Seo SJ, Son SM, Lee KY & Lee IH (2004) Purification and cDNA cloning of a cecropin-like peptide from the great wax moth, Galleria mellonella. *Mol Cells* **17**: 262-266.
- Kim CH, Shin YP, Noh MY, Jo YH, Han YS, Seong YS & Lee IH (2010) An insect multiligand recognition protein functions as an opsonin for the phagocytosis of microorganisms. *J Biol Chem* **285**: 25243-25250.
- Kluytmans J, van Belkum A & Verbrugh H (1997) Nasal carriage of Staphylococcus aureus: epidemiology, underlying mechanisms, and associated risks. *Clin Microbiol Rev* **10**: 505-520.

- Koide A & Hoch JA (1994) Identification of a second oligopeptide transport system in *Bacillus subtilis* and determination of its role in sporulation. *Mol Microbiol* **13**: 417-426.
- Kontinen VP & Sarvas M (1993) The PrsA lipoprotein is essential for protein secretion in *Bacillus subtilis* and sets a limit for high-level secretion. *Mol Microbiol* **8**: 727-737.
- Kovacs-Simon A, Titball RW & Michell SL (2011) Lipoproteins of bacterial pathogens. *Infect Immun* **79**: 548-561.
- Krismer B, Weidenmaier C, Zipperer A & Peschel A (2017) The commensal lifestyle of *Staphylococcus aureus* and its interactions with the nasal microbiota. *Nat Rev Microbiol* **15**: 675-687.
- Langen G, Imani J, Altincicek B, Kieseritzky G, Kogel KH & Vilcinskis A (2006) Transgenic expression of gallerimycin, a novel antifungal insect defensin from the greater wax moth *Galleria mellonella*, confers resistance to pathogenic fungi in tobacco. *Biol Chem* **387**: 549-557.
- Lazarevic V, Margot P, Soldo B & Karamata D (1992) Sequencing and analysis of the *Bacillus subtilis* lytRABC divergon: a regulatory unit encompassing the structural genes of the N-acetylmuramoyl-L-alanine amidase and its modifier. *J Gen Microbiol* **138**: 1949-1961.
- Legaria MC, Garcia SD, Tudanca V, Barberis C, Cipolla L, Cornet L, Famiglietti AMR, Stecher D & Vay CA (2020) *Clostridium ramosum* rapidly identified by MALDI-TOF MS. A rare gram-variable agent of bacteraemia. *Access Microbiol* **2**: acmi000137.
- Li W, Sahu D & Tsen F (2012) Secreted heat shock protein-90 (Hsp90) in wound healing and cancer. *Biochim Biophys Acta* **1823**: 730-741.
- Limsuwan S, Hesselting-Meinders A, Voravuthikunchai SP, van Dijk JM & Kayser O (2011) Potential antibiotic and anti-infective effects of rhodomyrtone from *Rhodomyrtus tomentosa* (Aiton) Hassk. on *Streptococcus pyogenes* as revealed by proteomics. *Phytomedicine* **18**: 934-940.
- Lugman A, Muttaqin MZ, Yulaipi S, Ebner P, Matsuo M, Zabel S, Tribelli PM, Nieselt K, Hidayati D & Götz F (2020) Trace amines produced by skin bacteria accelerate wound healing in mice. *Communications Biology* **3**: 1-10.
- Ma J, Zang YD, Zhang JJ, Li CJ, Li Y, Su YL, Wang AG & Zhang DM (2021) Nine prenylated acylphloroglucinols with potential anti-depressive and hepatoprotective activities from *Hypericum scabrum*. *Bioorg Chem* **107**: 104529.

- Mesquita FS, Brito C, Mazon Moya MJ, Pinheiro JC, Mostowy S, Cabanes D & Sousa S (2017) Endoplasmic reticulum chaperone Gp96 controls actomyosin dynamics and protects against pore-forming toxins. *EMBO Rep* **18**: 303-318.
- Miyata Y (2005) Hsp90 inhibitor geldanamycin and its derivatives as novel cancer chemotherapeutic agents. *Curr Pharm Des* **11**: 1131-1138.
- Mohammad M, Nguyen MT, Engdahl C, *et al.* (2019) The YIN and YANG of lipoproteins in developing and preventing infectious arthritis by *Staphylococcus aureus*. *PLoS Pathog* **15**: e1007877.
- Moran GJ, Krishnadasan A, Gorwitz RJ, Fosheim GE, McDougal LK, Carey RB, Talan DA & Group EMINS (2006) Methicillin-resistant *S. aureus* infections among patients in the emergency department. *N Engl J Med* **355**: 666-674.
- Morrow RJ, Lawson N, Hussaini SH & Asquith P (1990) The usefulness of faecal haemoglobin, albumin and alpha-1-antitrypsin in the detection of gastrointestinal bleeding. *Ann Clin Biochem* **27 (Pt 3)**: 208-212.
- Mowlds P, Coates C, Renwick J & Kavanagh K (2010) Dose-dependent cellular and humoral responses in *Galleria mellonella* larvae following beta-glucan inoculation. *Microbes Infect* **12**: 146-153.
- Nakayama H, Kurokawa K & Lee BL (2012) Lipoproteins in bacteria: structures and biosynthetic pathways. *FEBS J* **279**: 4247-4268.
- Naveed R, Hussain I, Tawab A, Tariq M, Rahman M, Hameed S, Mahmood MS, Siddique AB & Iqbal M (2013) Antimicrobial activity of the bioactive components of essential oils from Pakistani spices against *Salmonella* and other multi-drug resistant bacteria. *BMC Complement Altern Med* **13**: 265.
- Neubauer H, Pantel I, Lindgren PE & Gotz F (1999) Characterization of the molybdate transport system ModABC of *Staphylococcus carnosus*. *Arch Microbiol* **172**: 109-115.
- Nguyen MT, Matsuo M, Niemann S, Herrmann M & Gotz F (2020) Lipoproteins in Gram-Positive Bacteria: Abundance, Function, Fitness. *Front Microbiol* **11**: 582582.
- Nguyen MT, Kraft B, Yu W, *et al.* (2015) The vS α specific lipoprotein like cluster (lpl) of *S. aureus* USA300 contributes to immune stimulation and invasion in human cells. *PLoS Pathogens* **11**: 1004984.
- Nguyen MT, Kraft B, Yu W, *et al.* (2015) The vS α Specific Lipoprotein Like Cluster (lpl) of *S. aureus* USA300 Contributes to Immune Stimulation and Invasion in Human Cells. *PLoS Pathog* **11**: e1004984.

- Nguyen MT, Saising J, Tribelli PM, *et al.* (2019) Inactivation of farR Causes High Rhodomyrtone Resistance and Increased Pathogenicity in *Staphylococcus aureus*. *Front Microbiol* **10**: 1157.
- Nielsen JB & Lampen JO (1982) Glyceride-cysteine lipoproteins and secretion by Gram-positive bacteria. *J Bacteriol* **152**: 315-322.
- Peters Jr T (1995) *All About Albumin*. Elsevier.
- Popella P, Krauss S, Ebner P, Nega M, Deibert J & Gotz F (2016) VraH Is the Third Component of the *Staphylococcus aureus* VraDEH System Involved in Gallidermin and Daptomycin Resistance and Pathogenicity. *Antimicrob Agents Chemother* **60**: 2391-2401.
- Pratt CC & Weers PM (2004) Lipopolysaccharide binding of an exchangeable apolipoprotein, apolipoprotein III, from *Galleria mellonella*. *Biol Chem* **385**: 1113-1119.
- Randow F & Seed B (2001) Endoplasmic reticulum chaperone gp96 is required for innate immunity but not cell viability. *Nat Cell Biol* **3**: 891-896.
- Remy L, Carriere M, Derre-Bobillot A, Martini C, Sanguinetti M & Borezee-Durant E (2013) The *Staphylococcus aureus* Opp1 ABC transporter imports nickel and cobalt in zinc-depleted conditions and contributes to virulence. *Mol Microbiol* **87**: 730-743.
- Rennie RP, Turnbull L, Brosnikoff C & Cloke J (2012) First comprehensive evaluation of the M.I.C. evaluator device compared to Etest and CLSI reference dilution methods for antimicrobial susceptibility testing of clinical strains of anaerobes and other fastidious bacterial species. *J Clin Microbiol* **50**: 1153-1157.
- Richard JA, Powner RH & Chen DY (2012) The chemistry of the polycyclic polyprenylated acylphloroglucinols. *Angew Chem Int Ed Engl* **51**: 4536-4561.
- Saeloh D, Wenzel M, Rungrotmongkol T, Hamoen LW, Tipmanee V & Voravuthikunchai SP (2017) Effects of rhodomyrtone on Gram-positive bacterial tubulin homologue FtsZ. *PeerJ* **5**: e2962.
- Saising J & Voravuthikunchai SP (2012) Anti *Propionibacterium acnes* activity of rhodomyrtone, an effective compound from *Rhodomyrtus tomentosa* (Aiton) Hassk. leaves. *Anaerobe* **18**: 400-404.
- Saising J, Nguyen MT, Hartner T, *et al.* (2018) Rhodomyrtone (Rom) is a membrane-active compound. *Biochim Biophys Acta Biomembr* **1860**: 1114-1124.
- Saising J, Nguyen MT, Härtner T, *et al.* (2018) Rhodomyrtone (Rom) is a membrane-active compound. *Biochimica et Biophysica Acta - Biomembranes* **1860**: 1114-1124.

- Saleh M, Bartual SG, Abdullah MR, *et al.* (2013) Molecular architecture of *Streptococcus pneumoniae* surface thioredoxin-fold lipoproteins crucial for extracellular oxidative stress resistance and maintenance of virulence. *EMBO Mol Med* **5**: 1852-1870.
- Samuelson JC, Chen M, Jiang F, Moller I, Wiedmann M, Kuhn A, Phillips GJ & Dalbey RE (2000) YidC mediates membrane protein insertion in bacteria. *Nature* **406**: 637-641.
- Sanchez J, Carter TR, Cohen MS & Blagg BSJ (2020) Old and New Approaches to Target the Hsp90 Chaperone. *Curr Cancer Drug Targets* **20**: 253-270.
- Sauvageot N, Mokhtari A, Joyet P, *et al.* (2017) *Enterococcus faecalis* Uses a Phosphotransferase System Permease and a Host Colonization-Related ABC Transporter for Maltodextrin Uptake. *J Bacteriol* **199**.
- Schaiff WT, Hruska KA, Jr., McCourt DW, Green M & Schwartz BD (1992) HLA-DR associates with specific stress proteins and is retained in the endoplasmic reticulum in invariant chain negative cells. *J Exp Med* **176**: 657-666.
- Schmidt PN, Blirup-Jensen S, Svendsen PJ & Wandall JH (1995) Characterization and quantification of plasma proteins excreted in faeces from healthy humans. *Scand J Clin Lab Invest* **55**: 35-45.
- Schuster S, Yu W, Nega M, Chu YY, Zorn S, Zhang F, Gotz F & Schreiber F (2014) The role of serum proteins in *Staphylococcus aureus* adhesion to ethylene glycol coated surfaces. *Int J Med Microbiol* **304**: 949-957.
- Sebulsky MT, Hohnstein D, Hunter MD & Heinrichs DE (2000) Identification and characterization of a membrane permease involved in iron-hydroxamate transport in *Staphylococcus aureus*. *J Bacteriol* **182**: 4394-4400.
- Seitz V, Clermont A, Wedde M, Hummel M, Vilcinskas A, Schlatterer K & Podsiadlowski L (2003) Identification of immunorelevant genes from greater wax moth (*Galleria mellonella*) by a subtractive hybridization approach. *Dev Comp Immunol* **27**: 207-215.
- Shahmirzadi SV, Nguyen MT & Gotz F (2016) Evaluation of *Staphylococcus aureus* Lipoproteins: Role in Nutritional Acquisition and Pathogenicity. *Front Microbiol* **7**: 1404.
- Shaik HA & Sehnal F (2009) Hemolin expression in the silk glands of *Galleria mellonella* in response to bacterial challenge and prior to cell disintegration. *J Insect Physiol* **55**: 781-787.

- Sheehan G, Garvey A, Croke M & Kavanagh K (2018) Innate humoral immune defences in mammals and insects: The same, with differences? *Virulence* **9**: 1625-1639.
- Sinha B & Herrmann M (2005) Mechanism and consequences of invasion of endothelial cells by *Staphylococcus aureus*. *Thromb Haemost* **94**: 266-277.
- Sinha B, Francois PP, Nusse O, Foti M, Hartford OM, Vaudaux P, Foster TJ, Lew DP, Herrmann M & Krause KH (1999) Fibronectin-binding protein acts as *Staphylococcus aureus* invasin via fibronectin bridging to integrin $\alpha 5\beta 1$. *Cell Microbiol* **1**: 101-117.
- Smits JPH, Niehues H, Rikken G, Van Vlijmen-Willems IMJJ, Van De Zande GWHJF, Zeeuwen PLJM, Schalkwijk J & Van Den Bogaard EH (2017) Immortalized N/TERT keratinocytes as an alternative cell source in 3D human epidermal models. *Scientific Reports* **7**: 1-14.
- Sowa-Jasilek A, Zdybicka-Barabas A, Staczek S, Wydrych J, Mak P, Jakubowicz T & Cytrynska M (2014) Studies on the role of insect hemolymph polypeptides: *Galleria mellonella* anionic peptide 2 and lysozyme. *Peptides* **53**: 194-201.
- Staron M, Yang Y, Liu B, Li J, Shen Y, Zuniga-Pflucker JC, Aguila HL, Goldschneider I & Li Z (2010) gp96, an endoplasmic reticulum master chaperone for integrins and Toll-like receptors, selectively regulates early T and B lymphopoiesis. *Blood* **115**: 2380-2390.
- Su Q, Li X, Mo W & Yang Z (2019) Low serum bilirubin, albumin, and uric acid levels in patients with Crohn's disease. *Medicine (Baltimore)* **98**: e15664.
- Sun X, Ge R, Chiu JF, Sun H & He QY (2008) Lipoprotein MtsA of *MtsABC* in *Streptococcus pyogenes* primarily binds ferrous ion with bicarbonate as a synergistic anion. *FEBS Lett* **582**: 1351-1354.
- Sun X, Ge R, Zhang D, Sun H & He QY (2010) Iron-containing lipoprotein SiaA in *SiaABC*, the primary heme transporter of *Streptococcus pyogenes*. *J Biol Inorg Chem* **15**: 1265-1273.
- Taiyab A & Rao Ch M (2011) HSP90 modulates actin dynamics: inhibition of HSP90 leads to decreased cell motility and impairs invasion. *Biochim Biophys Acta* **1813**: 213-221.
- Tedde V, Rosini R & Galeotti CL (2016) Zn²⁺ Uptake in *Streptococcus pyogenes*: Characterization of *adcA* and *lmb* Null Mutants. *PLoS One* **11**: e0152835.

- The Lancet Infectious D (2017) Antibiotic research priorities: ready, set, now go. *Lancet Infect Dis* **17**: 349.
- Tong SY, Davis JS, Eichenberger E, Holland TL & Fowler VG, Jr. (2015) Staphylococcus aureus infections: epidemiology, pathophysiology, clinical manifestations, and management. *Clin Microbiol Rev* **28**: 603-661.
- Traeger A, Voelker S, Shkodra-Pula B, Kretzer C, Schubert S, Gottschaldt M, Schubert US & Werz O (2020) Improved Bioactivity of the Natural Product 5-Lipoxygenase Inhibitor Hyperforin by Encapsulation into Polymeric Nanoparticles. *Mol Pharm* **17**: 810-816.
- Tranchemontagne ZR, Camire RB, O'Donnell VJ, Baugh J & Burkholder KM (2016) Staphylococcus aureus Strain USA300 Perturbs Acquisition of Lysosomal Enzymes and Requires Phagosomal Acidification for Survival inside Macrophages. *Infect Immun* **84**: 241-253.
- Tribelli PM, Luqman A, Nguyen MT, et al. (2020) Staphylococcus aureus Lpl protein triggers human host cell invasion via activation of Hsp90 receptor. *Cell Microbiol* **22**: e13111.
- Tribelli PM, Luqman A, Nguyen MT, et al. (2020) Staphylococcus aureus Lpl protein triggers human host cell invasion via activation of Hsp90 receptor. *Cellular Microbiology* **22**: 13111.
- Tsai CJ, Loh JM & Proft T (2016) Galleria mellonella infection models for the study of bacterial diseases and for antimicrobial drug testing. *Virulence* **7**: 214-229.
- Vermassen A, Leroy S, Talon R, Provot C, Popowska M & Desvaux M (2019) Cell Wall Hydrolases in Bacteria: Insight on the Diversity of Cell Wall Amidases, Glycosidases and Peptidases Toward Peptidoglycan. *Front Microbiol* **10**: 331.
- Vesga O, Groeschel MC, Otten MF, Brar DW, Vann JM & Proctor RA (1996) Staphylococcus aureus small colony variants are induced by the endothelial cell intracellular milieu. *J Infect Dis* **173**: 739-742.
- Voravuthikunchai SP, Dolah S & Charennjiratrakul W (2010) Control of Bacillus cereus in foods by Rhodomyrtus tomentosa (Ait.) Hassk. Leaf extract and its purified compound. *J Food Prot* **73**: 1907-1912.
- Wang H, Kraus F, Popella P, Baykal A, Guttroff C, Francois P, Sass P, Plietker B & Gotz F (2019) The Polycyclic Polyprenylated Acylphloroglucinol Antibiotic PPAP 23 Targets the Membrane and Iron Metabolism in Staphylococcus aureus. *Front Microbiol* **10**: 14.

- Wang Y, Li C, Wang W, Wang J, Li J, Qian S, Cai C & Liu Y (2022) Serum Albumin to Globulin Ratio is Associated with the Presence and Severity of Inflammatory Bowel Disease. *J Inflamm Res* **15**: 1907-1920.
- Wertheim HF, Melles DC, Vos MC, van Leeuwen W, van Belkum A, Verbrugh HA & Nouwen JL (2005) The role of nasal carriage in *Staphylococcus aureus* infections. *Lancet Infect Dis* **5**: 751-762.
- Wiegand I, Hilpert K & Hancock RE (2008) Agar and broth dilution methods to determine the minimal inhibitory concentration (MIC) of antimicrobial substances. *Nat Protoc* **3**: 163-175.
- Wilburn KM, Fieweger RA & VanderVen BC (2018) Cholesterol and fatty acids grease the wheels of *Mycobacterium tuberculosis* pathogenesis. *Pathog Dis* **76**.
- Williams WA, Zhang RG, Zhou M, Joachimiak G, Gornicki P, Missiakas D & Joachimiak A (2004) The membrane-associated lipoprotein-9 GmpC from *Staphylococcus aureus* binds the dipeptide GlyMet via side chain interactions. *Biochemistry* **43**: 16193-16202.
- Wolschendorf F, Mahfoud M & Niederweis M (2007) Porins are required for uptake of phosphates by *Mycobacterium smegmatis*. *J Bacteriol* **189**: 2435-2442.
- Wunnoo S, Bilhman S, Amnuakit T, Ontong JC, Singh S, Auepemkiate S & Voravuthikunchai SP (2021) Rhodomyrtone as a New Natural Antibiotic Isolated from *Rhodomyrtus tomentosa* Leaf Extract: A Clinical Application in the Management of Acne Vulgaris. *Antibiotics (Basel)* **10**.
- Xu S, Andrews D & Hill BC (2015) The affinity of yeast and bacterial SCO proteins for CU(I) and CU(II). A capture and release strategy for copper transfer. *Biochem Biophys Rep* **4**: 10-19.
- Yang XW, Grossman RB & Xu G (2018) Research Progress of Polycyclic Polyprenylated Acylphloroglucinols. *Chem Rev* **118**: 3508-3558.
- Yang Y, Liu B, Dai J, Srivastava PK, Zammit DJ, Lefrancois L & Li Z (2007) Heat shock protein gp96 is a master chaperone for toll-like receptors and is important in the innate function of macrophages. *Immunity* **26**: 215-226.
- Yu Z, Tang J, Khare T & Kumar V (2020) The alarming antimicrobial resistance in ESKAPEE pathogens: Can essential oils come to the rescue? *Fitoterapia* **140**: 104433.
- Zapotoczna M, Jevnikar Z, Miajlovic H, Kos J & Foster TJ (2013) Iron-regulated surface determinant B (IsdB) promotes *Staphylococcus aureus* adherence to and internalization by non-phagocytic human cells. *Cell Microbiol* **15**: 1026-1041.

- Zdybicka-Barabas A, Staczek S, Mak P, Skrzypiec K, Mendyk E & Cytrynska M (2013) Synergistic action of *Galleria mellonella* apolipoprotein III and lysozyme against Gram-negative bacteria. *Biochim Biophys Acta* **1828**: 1449-1456.
- Zheng Z, Tharmalingam N, Liu Q, Jayamani E, Kim W, Fuchs BB, Zhang R, Vilcinskas A & Mylonakis E (2017) Synergistic efficacy of *Aedes aegypti* antimicrobial peptide cecropin A2 and tetracycline against *Pseudomonas aeruginosa*. *Antimicrobial Agents and Chemotherapy* **61**: 00686-00617.
- Zunzain PA, Ghuman J, Komatsu T, Tsuchida E & Curry S (2003) Crystal structural analysis of human serum albumin complexed with heme and fatty acid. *BMC Struct Biol* **3**: 6.

Appendix

Appendix A: Abbreviations

Ala	Alanine
AMPs	Antimicrobial Peptides
ApoL-III	Apolipoprotein III
Arg	Arginine
Atl	Autolysin
BSA	Bovine Serum Albumin
CDC	Centers For Disease Control and Prevention
Cys	Cysteine
Eap	Extracellular Adherence Protein
ECDC	The European Centre for Disease Prevention and Control
FA	Fatty Acid
FarR	Regulator of Fatty Acid Resistance
FDA	Food and Drug Administration
Fe	Iron
FnBPA	Fibronectin Binding Proteins A
FnBPB	Fibronectin Binding Proteins B
FtsZ	Filamenting Temperature Sensitive Mutant Z
Gly	Glycine
GmCP8	Cationic Protein 8
GTP	Guanosine Triphosphate
GTPase	Guanosine Triphosphatase
HaCaT	Human Keratinocyte Cells
HEK	Human Embryonic Kidney Cells
Hla	Human Leukocyte Antigens
Hsp90 α	Heat Shock Protein A
Hsp90 β	Heat Shock Protein B
HT-29	Human Colorectal Adenocarcinoma Cells
IsdB	Iron-Regulated Surface Determinant B
Leu	Leucine
Lgt	Lipoprotein Diacylglyceryl Transferase
Lnt	Lipoprotein N-Acyl Transferase
Lpl	Lipoprotein Like Lipoprotein
Lpp	Lipoproteins

Lsp	Lipoprotein Signal Peptidase
MDR	Multidrug Resistant
MM6	Human Monocytic Cell Line
Mn	Manganese
Mo	Molybdenum
MRSA	Methicillin-Resistant <i>Staphylococcus aureus</i>
MTT	3-(4,5-Dimethylthiazol-2-Yl)-2,5-Diphenyltetrazolium Bromide
Ni	Nickel
NlpC/P60	New Lipoprotein C/Protein Of 60-Kda
NPPCs	Non-Professional Phagocytic Cell
PBMC	Peripheral Blood Mononuclear Cell
PDR	Pandrug Resistant
PG	Phosphatidylglycerol
PGRPs	Peptidoglycan Recognition Proteins
PPAP	Polycyclic Polyprenylated Acylphloroglucinol
PrsA	Peptidylprolyl Isomerase
Psm β -1	Proteasome Subunit Beta Type 1
Rom	Rhodomyrtone
Rom ^R	Rhodomyrtone Resistance
ROS	Reactive Oxygen Species
SCO	Synthesis Of Cytochrome C Oxidase
Ser	Serine
Sp	Signal Peptide
TLR2	Toll-Like Receptor 2
VISA	Vancomycin Intermediate resistant <i>Staphylococcus Aureus</i>
XDR	Extensively Drug Resistant
Zn	Zinc

Symbols

Δ	Genetic deletion
$^{\circ}\text{C}$	Degree Celsius
%	Percentage
μ	Micro

Appendix B: List of figures

Figure 1.1. Biosynthesis of lipoprotein in bacteria. Adapted with Rightslink permission from (Nakayama *et al.*, 2012)

Figure 1.2. Proposed model of Lpl-Hsp90 interaction during USA300 invasion in keratinocyte cell. The C-terminal region of Lpl1 interacts with Hsp90. This interaction triggers F-actin formation and the bacteria is taken in by an endocytosis like process. G-actin: monomer of actin protein, F-actin: filamentous actin. Adapted from (Tribelli *et al.*, 2020).

Figure 1.3. (A) Structure of Rom drawn using ChemDraw Professional 16.0. (B) Mechanism of Rom resistance in Rom^R mutant facilitated by the FarE. Reprinted under the Creative Commons Attribution License (CC BY) from (Nguyen *et al.*, 2019).

Figure 1.4. Type A, B and C PPAPs. Adapted with permission from (Ciochina & Grossman, 2006). Copyright 2022 American Chemical Society.

Figure 1.5. Proposed antibacterial action of PPAP23. (A) PPAP 23 affects the membrane integrity by interacting with the lipophilic pocket of the membrane. Disintegrated membrane results in the diffusing out of ATP and diffusing in of iron to the bacterial cells. (B) PPAP 23 chelates iron from Fe–S cluster enzymes causing the inactivation of Fe–S cluster enzyme. This can disturb the cell respiration (through the enzymes involved) or DNA damage and cell death (due to iron overload). (C) PPAP 23's antimicrobial activity is lessened when it is iron bound. MQH2, menaquinol; MQ, menaquinone; CW, cell wall; CM, cytoplasmic membrane. Adapted with permission from (Wang *et al.*, 2019) with Creative Commons public licenses.

Figure 3.1. L15 and L13 hinders the invasion of *S.aureus* USA300 into (A) HaCaT and (B) N/TERT-1 cell lines upon pretreatment for 1.5h. Pretreatment of cells with geldanamycin, a well-known Hsp90 inhibitor or with α -Hsp90 α (Hsp90 α) antibody also inhibited USA300 invasion into the keratinocytes. Error bars show standard deviation of the mean of 3 biological replicates. P values were obtained by student's T-test. : * p < 0.05; ** p < 0.01; *** p < 0.001; and **** p < 0.0001.

Figure 3.2. L15, L13 and geldanamycin doesn't have any effect on cell lines (A) HaCaT and (B) N/TERT-1 during treatment time. (C) L13, L15 doesn't affect the USA300 growth in TSB at 37 °C.

Figure 3.3. L15, L13 and geldanamycin interaction with Hsp90 α effects the F-actin formation in (A) HaCaT and (B) N/TERT-1 cells. A significant reduction of F-actin levels were observed on treatment of keratinocytes with peptides and geldanamycin. Error bars show standard deviation of the mean of 3 biological replicates. P values were obtained by student's T-test. : * $p < 0.05$; ** $p < 0.01$; *** $p < 0.001$; and **** $p < 0.0001$

Figure 3.4. L13/L15 is non-toxic to (A) HaCaT, (B) HEK, (C) HT-29 and (D) MM6 cells *in vitro*. Error bars show standard deviation of the mean of 3 biological replicates. P values were obtained by student's T-test. : * $p < 0.05$; ** $p < 0.01$; *** $p < 0.001$; and **** $p < 0.0001$.

Figure 3.5. L15/L13 rescues larvae from *S.aureus* infection. Each group consists of 10 larvae with weight average of 500mg/larvae, and were administered with bacteria and/or peptides on its last proleg using a BD insulin syringe. Larvae were injected with different concentrations of (A) L15 and (B) L13 to find the optimum dosage against USA300 infection. Each larvae were injected with 10 μ l of L15 (last left proleg) 1h before injection of 10⁶ cfu *S. aureus* (last right proleg) (C) USA300 and (D) Newman. The larvae were maintained at 37 °C and checked for its mortality every day for the study period of 5 days. Total of 3 biological replicates are represented in the graph.

Figure 3.6. L13, L15 doesn't affect the hemolysin activity of USA300

Figure 3.7. L15 treatment reduces systemic *S. aureus* infection. NMRI mice infected intravenously with *S. aureus* Newman strain (2x10⁶ CFU/mouse) were treated with L15 intraperitoneally (10mg/kg) or PBS for control starting two hours before inoculation and continuing twice daily until animals were euthanized on day 7. (A) Weight development observed during 7 days. (B) Bacterial load in kidneys on day 7 post-infection. (C) Survival graph of mice infected with *S. aureus*.

Figure 3.8. Multiple sequence alignments of Lpl1 from *S. aureus* USA300 with other bacteria. These include *Staphylococcus epidermidis* SE62, *Staphylococcus hyicus* NCTC 8294, *Staphylococcus schweitzeri* NCTC 13712, *Staphylococcus argenteus* B3-

25B, *Listeria monocytogenes* ATCC 15313, *Ligilactobacillus ruminis* ATCC 27780, *Escherichia coli* NCTC 9001, *Klebsiella pneumoniae* NCTC 9633 and *Pseudomonas aeruginosa* PA216. The lipoprotein signal peptide is indicated by the bracket, the conserved core region by the bar and the L15 sequence is boxed.

Figure 3.9. Multiple sequence alignments of LpI1 – LpI9.

Figure 3.10. L15/L13 couldn't rescue larvae from (A) *E. coli* K12 and (B) *P. aeruginosa* PA01 infection. Ten *Galleria mellonella* larvae per group with weight average of 500mg/larvae were injected with bacteria and/or peptides on its last proleg using a BD insulin syringe. Each larva was injected with 10µl of L15 (last left proleg) 1h before administration of bacteria. The larvae were maintained at 37 °C and observed for its mortality every day for the study period of 5 days. Total of 3 biological replicates are represented in the graph.

Figure 3.11. Cytokine quantification of PBMCs stimulated by L15, showed that the L15 didn't cause any immune stimulation at the tested concentration. Statistic significances were calculated between the peptide treated cells compared to control by using one-way ANOVA analysis with Tukey's multiple comparison test: * $p < 0.05$, ** $p < 0.01$, *** $p < 0.001$, ns > 0.05 .

Figure 3.12. (A) Effect of L15 and L13 on *S. aureus* USA300 phagocytosis by primary human CD14+ monocytes. Influence of L13 and L15 on the response of host innate immune cells were tested. Release of (B) IL-6 and (C) TNF- α in the supernatant of *S. aureus*-infected PBMCs was assayed by ELISA 20 h after stimulation with L13 or L15 or geldanamycin. C indicates control cells without peptide pretreatment. Samples from 4 donors were carried out in triplicate. Samples from 4 donors were carried out in duplicate. Error bars represent SEM. Statistic significances were calculated between the peptide treated cells compared to control by using one-way ANOVA analysis with Tukey's multiple comparison test: * $p < 0.05$, ** $p < 0.01$, *** $p < 0.001$, ns > 0.05 .

Figure 3.13. L15/L13 in combination with different TLR ligands (A) MDP, (B) CpG and (C) ssRNA couldn't rescue larvae from *S. aureus* infection. Ten *Galleria mellonella* larvae per group with weight average of 500mg/larvae were injected with bacteria and/or peptides on its last proleg using a BD insulin syringe. Each larva was injected with 10µl of L15 (last left proleg) 1h before administration of bacteria. The larvae were

maintained at 37 °C and observed for its mortality every day for the study period of 5 days. Total of 3 biological replicates are represented in the graph.

Figure 3.14. Structures of PPAP 23, 22 and 53 used in this work. The PPAPs have similar MIC values (1 to 2 µg/ml) for the multi resistant *S. aureus* USA300. PPAP 53 is the Na salt of PPAP 22 and is therefore more water soluble. PPAP 23 was dissolved in DMSO.

Figure 3.15. PPAP 23 and PPAP 53 are non-toxic to larvae, but failed to protect larvae from infection with *S. aureus* USA300. Ten *Galleria mellonella* larvae per group, with weight average of 500 mg/larvae, were either non-treated, injected with 10⁶ colony forming units (cfu) *S. aureus* USA300 (last right proleg). 1 h after administration of bacteria larvae were treated with 20 mg/kg (45 µM) PPAP 23 (**A**), or 20 mg/kg (50 µM) PPAP 53 (**B**), or vancomycin (**C**) at a comparable dose (20 mg/kg, 13 µM). Infected larvae without treatment were normally killed by *S. aureus* after 3 days. The larvae were maintained at 37 °C and observed for mortality every day over the course of 5 days. A total of three biological replicates are represented in the graph.

Figure 3.16. PPAP 23 treatment significantly reduced the abscess formation and bacterial load in kidneys in mice with *S. aureus* septic arthritis. NMRI mice inoculated with *S. aureus* Newman strain (4 × 10⁶ colony-forming units/mouse) were treated with PPAP 23 dissolved in 0.5% tween 80 in PBS (100µg/mouse; n = 5) or same volume of 0.5% tween 80 in PBS (n = 5) twice a day starting on day 2 after inoculation with bacteria and continuing until the animals were euthanized on day 7. The severity of clinical arthritis (**A**) and the body weight development (**B**) in the mice were observed for 7 days after infection. Kidney abscess scores (**C**) and persistence of *S. aureus* in kidneys (**D**) from the mice euthanized 7 days after infection. Statistical evaluations were performed using the Mann–Whitney U test. Data are mean values ± standard error of the mean. *P < 0.05.

Figure 3.17. The bactericidal activity of PPAP53 is reversed by the larval coelomic fluid or 1% BSA. (A) To mimic *the in vivo* larva infection assay, the *ex vivo* killing assay was adopted. Bacterial inoculum of 10⁵ CFU and 10 µg of PPAP was added to 100 µl of larva coelomic fluid as the treatment group. Untreated larval liquid and larval liquid treated with PBS were used as controls. The viability of bacteria in each group was determined by the drop plate method. The bactericidal effect of PPAP 53 on *S. aureus*

is reversed by coelomic fluid. (B) The bactericidal effect of PPAP 53 (MIC: 0.5-1 µg/ml) on *S. aureus* USA300 is reversed by 1% BSA whereas the effect of vancomycin remained unchanged.

Figure 3.18. PPAP53 binds to the hemin binding pocket of BSA. *In silico* docking analysis by AutoDock vina showed that PPAP53 binds to FA1-IB pocket of BSA with a binding energy of -7.2 kcal/mol. This pocket represents the third main ligand (e.g., drug) binding pocket of BSA, the hemin being a prototypical ligand.

Figure 3.19. Addition of known BSA ligands couldn't improve the in vitro bactericidal activity of PPAP53 in presence of BSA. *S. aureus* precultured in TSB overnight were inoculated to OD=0.01 to a 48 well plate and 1X MIC PPAP53 and/or 1% BSA with or without ligands were added to study effect of peptides on bacterial growth using Varioskan LUX Multimode Microplate Reader. Here with this instrument, a kinetic measurement of optical density 578 nm was obtained every 1 h for a total of 24 hr, at 37°C with continuous shaking. Ligands tested were (A) Hemin, (B) 3,5 diidosalicylic acid (C) warfarin and (D) phenylbutazone.

Figure 3.20. Addition of known BSA ligands couldn't improve the in vitro bactericidal activity of PPAP53 in presence of BSA. *S. aureus* precultured in TSB overnight were inoculated to OD=0.01 to a 48 well plate and 1X MIC PPAP53 and/or 1% BSA with or without ligands were added to study effect of peptides on bacterial growth using Varioskan LUX Multimode Microplate Reader. Here with this instrument, a kinetic measurement of optical density 578 nm was obtained every 1 h for a total of 24 hr, at 37°C with continuous shaking. Ligands tested were (A) diffusinal, (B) iodipamide (C) azapropazone and (D) ibuprofen.

Figure 3.21. Addition of known BSA ligands couldn't improve the in vitro bactericidal activity of PPAP53 in presence of BSA. *S. aureus* precultured in TSB overnight were inoculated to OD=0.01 to a 48 well plate and 1X MIC PPAP53 and/or 1% BSA with or without ligands were added to study effect of peptides on bacterial growth using Varioskan LUX Multimode Microplate Reader. Here with this instrument, a kinetic measurement of optical density 578 nm was obtained every 1 h for a total of 24 hr, at 37°C with continuous shaking. Ligands tested were (A) diazepam (B) indomethacin (C) oxyphenbutazone.

Appendix C: List of tables

Table 1. Effect of tested Lpl1-derived peptides on their invasion potential, F-actin formation and binding to Hsp90 α

Table 2. MIC values of Rom and its derivatives towards *S.aureus* HG001 and its Rom^R strain.

Table 3. MIC of Rom against anaerobic microorganisms

Table 4. Impact of serum components on PPAP53 activity

Table 5. Tested ligands (FDA approved drugs) binding to HSA and their binding pockets

Table 6. MIC values of PPAP23 against some of the anaerobic bacterial strains

Appendix D: Publications and personal contributions to publications

Publications discussed in the thesis

a) Accepted publication

1. Li Huang*, Miki Matsuo*, Carlos Calderón*, Sook-Ha Fan, **Aparna Viswanathan Ammanath**, Xiaoqing Fu, Ningna Li, Arif Luqman, Marvin Ullrich, Florian Herrmann, Martin Maier, Anchun Cheng, Fajun Zhang, Filipp Oesterhelt, Michael Lämmerhofer, Friedrich Götz (2022). Molecular Basis of Rhodomyrtone Resistance in *Staphylococcus aureus*. *Mbio*, **13**: e03833-21.

*: Equal contribution

I performed some of the bacterial killing assays and helped in preparation of the manuscript.

2. From a Hsp90 - binding protein to a peptide drug

Aparna Viswanathan Ammanath, Anders Jarneborn, Minh-Thu Nguyen, Laura Wessling, Paula Tribelli, Mulugeta Nega, Christian Beck, Arif Luqman, Khaled A Selim, Hubert Kalbacher, Boris Macek, Sandra Beer Hammer, Tao Jin, Friedrich Götz (2022), From a Hsp90 - binding protein to a peptide drug, *microLife*, uqac023.

I planned and performed most of the experiments. I analyzed all the experimental data and wrote the manuscript under the guidance of Prof. Friedrich Götz.

Publications not discussed in the current thesis

a) Research articles

3. Huang, Li, Mafeng Liu, **Aparna Viswanathan Ammanath**, Dekang Zhu, Renyong Jia, Shun Chen, Xinxin Zhao, Qiao Yang, Ying Wu, Shaqiu Zhang, Juan Huang, Xumin Ou, Sai Mao, Qun Gao, Di Sun, Bin Tian, Friedrich Götz, Mingshu Wang, Anchun Cheng (2021). Identification of the Natural

Transformation Genes in *Riemerella anatipestifer* by Random Transposon Mutagenesis. *Frontiers in microbiology* **12**: 712198.

I performed *in silico* protein structure determination and docking studies, supported the writing and improvements of the article and did critical proofreading of the manuscript

4. Fredrick, R., Podder, A., **Viswanathan, A.**, Bhuniya, S (2019). Synthesis and characterization of polysaccharide hydrogel based on hydrophobic interactions. *Journal of Applied Polymer Science*, **136**: 47665.

I performed the cytotoxicity and haemolysis experiments.

5. Ruth Bright Chirayath, **Aparna Viswanathan A**, R. Jayakumar, Raja Biswas, Lakshmi Sumitra Vijayachandran (2019). Development of *Mangifera indica* leaf extract incorporated carbopol hydrogel and its antibacterial efficacy against *Staphylococcus aureus*. *Colloids and Surfaces B: Biointerfaces* **178**: 377-384.

I co-performed most of the experiments and helped in manuscript preparation.

b) Review

6. Sankaran Sathianarayanan, **Aparna Viswanathan Ammanath**, Raja Biswas, Anita B, Sunitha Sukumar, Baskar Venkidasamy (2022). A new approach against *Helicobacter pylori* using plants and its constituents: A review study. *Microbial Pathogenesis* **168**: 105594.

I co-wrote the review with other authors.

c) Book chapters

7. **Viswanathan, Aparna**, Jayakumar Rangasamy, Raja Biswas (2019). Functionalized antibacterial nanoparticles for controlling biofilm and intracellular infections. In *Surface Modification of Nanoparticles for Targeted Drug Delivery*, Springer, Cham, 183-206.

This book chapter was written by myself with assistance of Jayakumar Rangasamy, and Raja Biswas

8. **Aparna Viswanathan A.**, Raja Biswas, R. Jayakumar (2019). Targeted nanoparticles for treating infectious diseases. In *Biomimetic Nanoengineered Materials for Advanced Drug Delivery*, Elsevier, 169-185.

This book chapter was written by myself with assistance of Jayakumar Rangasamy, and Raja Biswas

9. *In press*: **Aparna Viswanathan Ammanath**, Jolly Thomas, Anjana Jayasree. Hyaluronic Acid in Tissue engineering. In *Natural Biopolymers in Drug Delivery & Tissue Engineering*, Elsevier.

I co-authored this book chapter with other authors.

Appendix E: RightsLink Permission

7/20/22, 3:42 PM

RightsLink Printable License

JOHN WILEY AND SONS LICENSE TERMS AND CONDITIONS

Jul 20, 2022

This Agreement between Centre for Nanosciences and Molecular Medicine -- Aparna Viswanathan Ammanath ("You") and John Wiley and Sons ("John Wiley and Sons") consists of your license details and the terms and conditions provided by John Wiley and Sons and Copyright Clearance Center.

License Number	5353081206522
License date	Jul 20, 2022
Licensed Content Publisher	John Wiley and Sons
Licensed Content Publication	FEBS Journal
Licensed Content Title	Lipoproteins in bacteria: structures and biosynthetic pathways
Licensed Content Author	Hiroshi Nakayama, Kenji Kurokawa, Bok Luel Lee
Licensed Content Date	Nov 7, 2012
Licensed Content Volume	279
Licensed Content Issue	23
Licensed Content Pages	22
Type of use	Dissertation/Thesis
Requestor type	Author of this Wiley article
Format	Print and electronic
Portion	Figure/table

<https://s100.copyright.com/AppDispatchServlet>

1/6

7/20/22, 3:42 PM

RightsLink Printable License

Number of figures/tables	1
Will you be translating?	No
Title	New anti-infective and anti-microbial compounds
Institution name	University of Tuebingen, Germany
Expected presentation date	Mar 2023
Order reference number	20072022-2
Portions	Fig 1 The canonical biosynthetic pathway of bacterial lipoproteins.
Requestor Location	Centre for Nanosciences and Molecular Medicine Amrita Institute of Medical Sciences Ponekkara Cochin, Cochin 682041 India Attn: Centre for Nanosciences and Molecular Medicine
Publisher Tax ID	EU826007151
Total	0.00 EUR
Terms and Conditions	

TERMS AND CONDITIONS

This copyrighted material is owned by or exclusively licensed to John Wiley & Sons, Inc. or one of its group companies (each a "Wiley Company") or handled on behalf of a society with which a Wiley Company has exclusive publishing rights in relation to a particular work (collectively "WILEY"). By clicking "accept" in connection with completing this licensing transaction, you agree that the following terms and conditions apply to this transaction (along with the billing and payment terms and conditions established by the Copyright Clearance Center Inc., ("CCC's Billing and Payment terms and conditions"), at the time that you opened your RightsLink account (these are available at any time at <http://myaccount.copyright.com>).

Terms and Conditions

- The materials you have requested permission to reproduce or reuse (the "Wiley Materials") are protected by copyright.

<https://s100.copyright.com/AppDispatchServlet>

2/5

- You are hereby granted a personal, non-exclusive, non-sub licensable (on a stand-alone basis), non-transferable, worldwide, limited license to reproduce the Wiley Materials for the purpose specified in the licensing process. This license, and any CONTENT (PDF or image file) purchased as part of your order, is for a one-time use only and limited to any maximum distribution number specified in the license. The first instance of republication or reuse granted by this license must be completed within two years of the date of the grant of this license (although copies prepared before the end date may be distributed thereafter). The Wiley Materials shall not be used in any other manner or for any other purpose, beyond what is granted in the license. Permission is granted subject to an appropriate acknowledgement given to the author, title of the material/book/journal and the publisher. You shall also duplicate the copyright notice that appears in the Wiley publication in your use of the Wiley Material. Permission is also granted on the understanding that nowhere in the text is a previously published source acknowledged for all or part of this Wiley Material. Any third party content is expressly excluded from this permission.
- With respect to the Wiley Materials, all rights are reserved. Except as expressly granted by the terms of the license, no part of the Wiley Materials may be copied, modified, adapted (except for minor reformatting required by the new Publication), translated, reproduced, transferred or distributed, in any form or by any means, and no derivative works may be made based on the Wiley Materials without the prior permission of the respective copyright owner. For STM Signatory Publishers clearing permission under the terms of the [STM Permissions Guidelines](#) only, the terms of the license are extended to include subsequent editions and for editions in other languages, provided such editions are for the work as a whole in situ and does not involve the separate exploitation of the permitted figures or extracts. You may not alter, remove or suppress in any manner any copyright, trademark or other notices displayed by the Wiley Materials. You may not license, rent, sell, loan, lease, pledge, offer as security, transfer or assign the Wiley Materials on a stand-alone basis, or any of the rights granted to you hereunder to any other person.
- The Wiley Materials and all of the intellectual property rights therein shall at all times remain the exclusive property of John Wiley & Sons Inc, the Wiley Companies, or their respective licensors, and your interest therein is only that of having possession of and the right to reproduce the Wiley Materials pursuant to Section 2 herein during the continuance of this Agreement. You agree that you own no right, title or interest in or to the Wiley Materials or any of the intellectual property rights therein. You shall have no rights hereunder other than the license as provided for above in Section 2. No right, license or interest to any trademark, trade name, service mark or other branding ("Marks") of WILEY or its licensors is granted hereunder, and you agree that you shall not assert any such right, license or interest with respect thereto
- NEITHER WILEY NOR ITS LICENSORS MAKES ANY WARRANTY OR REPRESENTATION OF ANY KIND TO YOU OR ANY THIRD PARTY, EXPRESS, IMPLIED OR STATUTORY, WITH RESPECT TO THE MATERIALS OR THE ACCURACY OF ANY INFORMATION CONTAINED IN THE MATERIALS, INCLUDING, WITHOUT LIMITATION, ANY IMPLIED WARRANTY OF MERCHANTABILITY, ACCURACY, SATISFACTORY QUALITY, FITNESS FOR A PARTICULAR PURPOSE, USABILITY, INTEGRATION OR NON-INFRINGEMENT AND ALL SUCH WARRANTIES ARE HEREBY EXCLUDED BY WILEY AND ITS LICENSORS AND WAIVED BY YOU.
- WILEY shall have the right to terminate this Agreement immediately upon breach of this Agreement by you.

7/20/22, 3:42 PM

RightsLink Printable License

- You shall indemnify, defend and hold harmless WILEY, its Licensors and their respective directors, officers, agents and employees, from and against any actual or threatened claims, demands, causes of action or proceedings arising from any breach of this Agreement by you.
- IN NO EVENT SHALL WILEY OR ITS LICENSORS BE LIABLE TO YOU OR ANY OTHER PARTY OR ANY OTHER PERSON OR ENTITY FOR ANY SPECIAL, CONSEQUENTIAL, INCIDENTAL, INDIRECT, EXEMPLARY OR PUNITIVE DAMAGES, HOWEVER CAUSED, ARISING OUT OF OR IN CONNECTION WITH THE DOWNLOADING, PROVISIONING, VIEWING OR USE OF THE MATERIALS REGARDLESS OF THE FORM OF ACTION, WHETHER FOR BREACH OF CONTRACT, BREACH OF WARRANTY, TORT, NEGLIGENCE, INFRINGEMENT OR OTHERWISE (INCLUDING, WITHOUT LIMITATION, DAMAGES BASED ON LOSS OF PROFITS, DATA, FILES, USE, BUSINESS OPPORTUNITY OR CLAIMS OF THIRD PARTIES), AND WHETHER OR NOT THE PARTY HAS BEEN ADVISED OF THE POSSIBILITY OF SUCH DAMAGES. THIS LIMITATION SHALL APPLY NOTWITHSTANDING ANY FAILURE OF ESSENTIAL PURPOSE OF ANY LIMITED REMEDY PROVIDED HEREIN.
- Should any provision of this Agreement be held by a court of competent jurisdiction to be illegal, invalid, or unenforceable, that provision shall be deemed amended to achieve as nearly as possible the same economic effect as the original provision, and the legality, validity and enforceability of the remaining provisions of this Agreement shall not be affected or impaired thereby.
- The failure of either party to enforce any term or condition of this Agreement shall not constitute a waiver of either party's right to enforce each and every term and condition of this Agreement. No breach under this agreement shall be deemed waived or excused by either party unless such waiver or consent is in writing signed by the party granting such waiver or consent. The waiver by or consent of a party to a breach of any provision of this Agreement shall not operate or be construed as a waiver of or consent to any other or subsequent breach by such other party.
- This Agreement may not be assigned (including by operation of law or otherwise) by you without WILEY's prior written consent.
- Any fee required for this permission shall be non-refundable after thirty (30) days from receipt by the CCC.
- These terms and conditions together with CCC's Billing and Payment terms and conditions (which are incorporated herein) form the entire agreement between you and WILEY concerning this licensing transaction and (in the absence of fraud) supersedes all prior agreements and representations of the parties, oral or written. This Agreement may not be amended except in writing signed by both parties. This Agreement shall be binding upon and inure to the benefit of the parties' successors, legal representatives, and authorized assigns.
- In the event of any conflict between your obligations established by these terms and conditions and those established by CCC's Billing and Payment terms and conditions, these terms and conditions shall prevail.
- WILEY expressly reserves all rights not specifically granted in the combination of (i) the license details provided by you and accepted in the course of this licensing transaction, (ii) these terms and conditions and (iii) CCC's Billing and Payment terms and conditions.

<https://s100.copyright.com/AppDispatchServlet>

4/6

7/20/22, 3:42 PM

RightsLink Printable License

- This Agreement will be void if the Type of Use, Format, Circulation, or Requestor Type was misrepresented during the licensing process.
- This Agreement shall be governed by and construed in accordance with the laws of the State of New York, USA, without regards to such state's conflict of law rules. Any legal action, suit or proceeding arising out of or relating to these Terms and Conditions or the breach thereof shall be instituted in a court of competent jurisdiction in New York County in the State of New York in the United States of America and each party hereby consents and submits to the personal jurisdiction of such court, waives any objection to venue in such court and consents to service of process by registered or certified mail, return receipt requested, at the last known address of such party.

WILEY OPEN ACCESS TERMS AND CONDITIONS

Wiley Publishes Open Access Articles in fully Open Access Journals and in Subscription journals offering Online Open. Although most of the fully Open Access journals publish open access articles under the terms of the Creative Commons Attribution (CC BY) License only, the subscription journals and a few of the Open Access Journals offer a choice of Creative Commons Licenses. The license type is clearly identified on the article.

The Creative Commons Attribution License

The [Creative Commons Attribution License \(CC-BY\)](#), allows users to copy, distribute and transmit an article, adapt the article and make commercial use of the article. The CC-BY license permits commercial and non-

Creative Commons Attribution Non-Commercial License

The [Creative Commons Attribution Non-Commercial \(CC-BY-NC\) License](#) permits use, distribution and reproduction in any medium, provided the original work is properly cited and is not used for commercial purposes.(see below)

Creative Commons Attribution-Non-Commercial-NoDerivs License

The [Creative Commons Attribution Non-Commercial-NoDerivs License \(CC-BY-NC-ND\)](#) permits use, distribution and reproduction in any medium, provided the original work is properly cited, is not used for commercial purposes and no modifications or adaptations are made. (see below)

Use by commercial "for-profit" organizations

Use of Wiley Open Access articles for commercial, promotional, or marketing purposes requires further explicit permission from Wiley and will be subject to a fee.

Further details can be found on Wiley Online Library
<http://olabout.wiley.com/WileyCDA/Section/id-410895.html>

Other Terms and Conditions:

v1.10 Last updated September 2015

Questions? customercare@copyright.com or +1-855-239-3415 (toll free in the US) or

<https://s100.copyright.com/AppDispatchServlet>

5/6

7/20/22, 3:42 PM
+1-978-646-2777.

RightsLink Printable License

